Lawrence Berkeley National Laboratory

Eastern Interconnection Situational Awareness Monitoring System (ESAMS) Demonstration Project

Joseph H. Eto
Lawrence Berkeley National Laboratory

Neeraj Nayak, Simon Mo, Ken Martin, Song Xue, Horacio Silva-Saravia, Jay Chen
Electric Power Group

Jim Follum, Nicholas Betzsold, Shuchismita Biswas, Tianzhixi Yin
Pacific Northwest National Laboratory

September 2022

This work was supported by the U.S. Department of Energy's Office of Electricity, Transmission Reliability and Renewables Integration Program under Lawrence Berkeley National Laboratory Contract No. DE-AC02-05CH11231.

DISCLAIMER

This document was prepared as an account of work sponsored by the United States Government. While this document is believed to contain correct information, neither the United States Government nor any agency thereof, nor The Regents of the University of California, nor any of their employees, makes any warranty, express or implied, or assumes any legal responsibility for the accuracy, completeness, or usefulness of any information, apparatus, product, or process disclosed, or represents that its use would not infringe privately owned rights. Reference herein to any specific commercial product, process, or service by its trade name, trademark, manufacturer, or otherwise, does not necessarily constitute or imply its endorsement, recommendation, or favoring by the United States Government or any agency thereof, or The Regents of the University of California. The views and opinions of authors expressed herein do not necessarily state or reflect those of the United States Government or any agency thereof, or The Regents of the University of California.

Ernest Orlando Lawrence Berkeley National Laboratory is an equal opportunity employer.

COPYRIGHT NOTICE

This manuscript has been authored by an author at Lawrence Berkeley National Laboratory under Contract No. DE-AC02-05CH11231 with the U.S. Department of Energy. The U.S. Government retains, and the publisher, by accepting the article for publication, acknowledges, that the U.S. Government retains a non-exclusive, paid-up, irrevocable, worldwide license to publish or reproduce the published form of this manuscript, or allow others to do so, for U.S. Government purposes.

Eastern Interconnection Situational Awareness Monitoring System (ESAMS) Demonstration Project

Prepared for the

Transmission Reliability and Renewables Integration Program
Office of Electricity
U.S. Department of Energy

Prepared by

Joseph H. Eto
Lawrence Berkeley National Laboratory

Neeraj Nayak, Simon Mo, Ken Martin, Song Xue, Horacio Silva-Saravia, Jay Chen
Electric Power Group

Jim Follum, Nicholas Betzsold, Shuchismita Biswas, Tianzhixi Yin
Pacific Northwest National Laboratory

Ernest Orlando Lawrence Berkeley National Laboratory
1 Cyclotron Road, MS 90R4000
Berkeley CA 94720-8136

September 2022

The work described in this study was funded by the U.S. Department of Energy's Office of Electricity under Lawrence Berkeley National Laboratory Contract No. DE-AC02-05CH11231.

Acknowledgements

The work described in this study was conducted at Lawrence Berkeley National Laboratory for the U.S. Department of Energy under Contract No. DE-AC02-05CH11231. The authors are grateful to Sandra Jenkins and Phil Overholt of the Office of Electricity, Transmission Reliability and Renewables Integration program for their support of this project.

The authors thank PJM Interconnection for hosting the ESAMS demonstration and staff members: Hamed Golestani, Christopher Callaghan, David Hislop, and Subbarao Eedupuganti for their support throughout the demonstration. The authors also thank Shaun Murphy, who since has left the organization, but who supported the early phases of the demonstration.

The authors thank Eastern Interconnection partners for participating in the ESAMS demonstration project:
ISO New England–Frankie Zhang, Slava Maslennikov, Xiaochuan Luo
Midcontinent Independent System Operator–Keith Mitchell
New York Independent System Operator–Emily Fernandez, Shubhrajit Bhattacharajee
Southern Company–Clifton Black, Shih-Min Hsu, James Viikinsalo, Chris Wakefield, Mark Newman, Michael Breuhl, John Pope
Southwest Power Pool–Cody Parker, William Holden, Daniel Baker
Tennessee Valley Authority–Tim Fritch, Gary Kobet, Phillip Crittenden, Jonathan Sides

The authors also acknowledge Dr. Brett Amidan, now at Brigham Young University–Idaho, who, as a researcher at Pacific Northwest National Laboratory, participated in the early phases of this project.

Finally, the authors thank the following experts for reviewing an early draft of this report:
Asher Steed, BC Hydro
Dan Trudnowski, Montana Tech
Daniel Goodrich, Bonneville Power Administration
John Pierre, University of Wyoming
Urmila Agrawal, California ISO
Yilu Liu, University of Tennessee, Knoxville

Table of Contents

List of Figures

List of Tables

Acronyms and Abbreviations

BPS	Bulk power system
DOE	Department of Energy
EIDSN	Eastern Interconnect Data Sharing Network
EMS	Energy management system
EPG	Electric Power Group
ESAMS	Eastern Interconnection Situational Awareness Monitoring System
Hz	Hertz
ISNE	ISO New England (reliability coordination region)
ISO NE	ISO New England
LBNL	Lawrence Berkeley National Laboratory
MISO	Midcontinent System Operator
MVAr	Megavolt-Ampere Reactive
MW	Megawatt
NASPI	North American Synchrophasor Initiative
NERC	North American Electric Reliability Corporation
NYIS	New York Independent System Operator (reliability coordination region)
NYISO	New York Independent System Operator
PDC	Phasor Data Concentrator
PJM	PJM Interconnection
PMU	Phasor Measurement Unit
PNNL	Pacific Northwest National Laboratory
PT	Power transducer
RC	Reliability Coordinator
RTDMS	Real Time Dynamics Monitoring System
SCADA	Supervisory control and data acquisition
SE	State estimator
SOCO	Southern Company (reliability coordination region)
Southern	Southern Company
SPP	Southwest Power Pool
TVA	Tennessee Valley Authority
TRRI	Transmission Reliability and Renewables Integration

Executive Summary

The demonstration of the Eastern Interconnection Situational Awareness Monitoring System (ESAMS) represents an important step toward realizing the wide-area situational awareness capabilities of synchrophasors for the Eastern Interconnection. The project demonstrated the feasibility of continuously collecting and integrating synchrophasor measurements from throughout the interconnection in real time to produce heretofore unavailable visibility of grid phenomena that affect the interconnection as a whole. More importantly, the project demonstrated that the synchrophasor systems currently operating in the Eastern Interconnection are capable of supporting real-time notification of forced oscillations, the primary example of critical grid phenomena.

The ESAMS project demonstrated applications that highlight the wide-area grid visibility only synchrophasors can provide. First, all the applications relied on the collection, integration, and analysis of synchrophasor data from multiple operating entities. None of the applications could be supported by synchrophasor data collected from within only a single grid operating region. Second, all the applications relied solely on synchrophasor data, incorporating none of the supplementary information that can be collected using conventional supervisory control and data acquisition (SCADA) systems and energy management systems (EMS).

Importantly, the applications demonstrated through the ESAMS project are intended to complement—not duplicate or replace—grid operators' situational awareness of local conditions, already available through their SCADA/EMS and synchrophasor-based, local monitoring. ESAMS applications produced results that were advisory only. The applications and their results do not suggest or indicate, much less direct, specific actions. Instead, results provided heretofore unavailable information on wide-area conditions that a single grid operator cannot see. They enable grid operators to communicate with one another more efficiently regarding appropriate actions. Such actions, in turn, are to be supported by each grid operator's internal SCADA/EMS and synchrophasor-based monitoring systems.

The ESAMS demonstration was timely because grid operators in the Eastern Interconnection have become keenly aware that forced oscillations within a grid occur frequently and, more importantly, that some warrant real-time communication and coordination among Reliability Coordinators (RCs). The ESAMS project demonstrated robust and standardized analysis of interconnection-wide events that can be reported on and delivered to RCs in real time.

The ESAMS demonstration project also confirmed the usefulness of routinely tracking and analyzing interconnection-wide grid phenomena, not solely through one-time studies. For example, data related to the two dominant natural oscillatory modes of the Eastern Interconnection were collected throughout the nine-month demonstration period. Analysis of those data not only confirmed prior findings, it extended them in several ways. First, the analysis greatly improved the characterization of the shapes of the two modes, which increases our understanding of how forced oscillations at those frequencies will propagate and be observable in other regions within the interconnection. Second, the

analysis identified heretofore unrecognized diurnal patterns in the two modes' frequencies and damping ratios. Third, project findings demonstrated that the characteristics of the two modes could be monitored and distinguished consistently even though their frequencies overlap from time to time.

The ESAMS demonstration project laid the groundwork for a potential means of monitoring grid stress throughout the interconnection based, in part, on synchrophasor data. The project confirmed that using synchrophasors to monitor phase angles provides a way to observe the effects of grid events or actions on power flows within broad regions of the grid. This finding is significant because it means that grid operators both adjacent to and distant from the location of an event or action can recognize the occurrence without communicating with the RC of the region where the event or action is occurring. Although this prospect is promising, significant additional work is required to pair information on phase angles with broader regional analyses (e.g., contingency analysis conducted by considering multiple operating regions simultaneously) in order to convert the information into guidance grid operators can use.

Finally, the demonstration project confirmed the growing maturity of synchrophasor-based monitoring systems in the Eastern Interconnection. At the technical level, the project produced and shared daily reports on the availability and quality of data received from project participants. The ESAMS application algorithms were hardened to detect and correct for signals created by features of synchrophasor measurements that initially seemed anomalous but became clear-cut. The project team carried out an independent investigation that confirmed the usefulness of interconnection-wide coordination regarding signal-naming conventions. The team's investigations also confirmed the validity of the measurements of very large phase angles, which formerly would have been discounted or deemed spurious.

At the institutional level, the ESAMS project prompted the demonstration partners and project team members to engage in regular discussion, information-sharing, and learning about synchrophasor technologies, applications, and systems. ESAMS project findings were shared widely with industry audiences in the North American Electric Reliability Corporation's (NERC's) Synchronized Measurement Working Group and at meetings of the North American Synchrophasor Initiative.

In summary, the ESAMS demonstration project confirmed the legitimacy of the promise synchrophasors make to provide real-time, wide-area situational awareness of grid phenomena. Although much work remains to be done to integrate and incorporate that promise into grid operations, an important next step has been taken.

1. Introduction

The high-voltage electric power systems of the United States and Canada are managed on a decentralized basis by independent grid operators, each of whom has responsibility for managing their region of the grid in accordance with mandatory reliability rules. In support of those responsibilities, each grid operator employs monitoring systems that provide continuous visibility of reliability-threatening events that might occur in their region. That visibility is a core element of the situational awareness operators rely on to manage their systems reliably.

The 2003 U.S.–Canada blackout was a dramatic reminder that the electric grid is an interconnected system. The blackout was triggered by events that originated within one region of the grid but then grew rapidly and uncontrollably to overwhelm unsuspecting grid operators in neighboring regions of the grid. Ultimately, 50 million electricity users in eight U.S. states and Canada's most populated province lost electric service. It was the largest blackout in the history of the North American electric power industry. Its economic impact has been estimated at $5 billion to $10 billion.[1]

The joint US-Canada investigation found that inadequate situational awareness was a principal cause of the blackout. Grid operators responsible for the region where the blackout started did not recognize the threats to reliability that were emerging in their systems. Grid operators in adjacent regions were unaware of the deteriorating state of their neighbor's system.

The investigation also found that newly available, although not widely deployed, time-synchronized, high-speed grid-monitoring technologies (called synchrophasors) could have provided the wide-area situational awareness that would have alerted grid operators of adjacent systems to the worsening conditions in their neighbor's system.[2] It generally is agreed that this information, had it been available, could have prompted defensive actions that would have limited the blackout to northern Ohio.

In order to prevent future large-scale blackouts, the American Recovery and Reinvestment Act of 2010 directed the U.S. Department of Energy (DOE) to launch a major initiative to accelerate the deployment of synchrophasors.[3] DOE invested $155 million, which was more than matched by $203 million from industry, to install nearly 1,400 synchrophasor devices, known as phasor measurement units (PMUs),

---

[1] U.S.-Canada Power System Outage Task Force. Final Report on the August 14, 2003, Blackout in the United States and Canada: Causes and Recommendations. April 2004. https://www.energy.gov/sites/default/files/oeprod/DocumentsandMedia/BlackoutFinal-Web.pdf [Last accessed June 21, 2022.]

[2] Time-synchronization enables measurements collected throughout the interconnection to be aligned so as to create a coherent picture of the entire interconnection. Measurements from current grid-monitoring systems are not time-synchronized; they must be combined using manual methods that can produce only an approximate picture of the entire interconnection. High-speed measurements (e.g., 30 to 120 samples per second) also make visible reliability-threatening events that otherwise cannot be seen. Measurements from current grid-monitoring systems are too slow (once every 2 to 5 seconds) to identify such events.

[3] Oak Ridge National Laboratory. Advancement of Synchrophasor Technology in Projects Funded by the American Recovery and Reinvestment Act of 2009. March 2016. https://www.energy.gov/sites/prod/files/2016/03/f30/Advancement%20of%20Sychrophasor%20Technology%20Report%20March%202016.pdf [Last accessed June 21, 2022.]

along with supporting technologies such as communication systems and analysis applications. The initiative was highly successfully in catalyzing the deployment of PMUs nationally. By 2022, several thousand networked PMUs were operating throughout the country.

Synchrophasors initially were used to meet local reliability needs through offline applications, such as for validating models and performing forensic investigations of past events. Such uses represented a logical and practical first step when introducing the new monitoring technology. The approach enabled grid operators to gain familiarity with and confidence in using the technology at a pace determined by local needs and circumstances. The next step, which was to monitor local conditions in real time, enabled operators to learn about characteristics and behaviors of the grid that cannot be observed using conventional monitoring technologies.[4] More recently, grid operators in the Eastern Interconnection have taken the next logical step by sharing synchrophasor data with one another in real time. As a result, the time is ripe to lay the groundwork for fulfilling one of the technology's original promises: wide-area situational awareness.

The Eastern Interconnection Situational Awareness Monitoring System (ESAMS) demonstration project was an important step toward realizing the operational benefits offered by the wide-area situational awareness capabilities of synchrophasors. The ESAMS project sought to demonstrate the feasibility of collecting and integrating synchrophasor measurements from throughout the interconnection in real time to produce heretofore unavailable visibility of grid phenomena that affect the interconnection as a whole. The project also aimed to confirm the usefulness of tracking and analyzing grid phenomena on an ongoing basis, not solely through one-time studies, as has been the practice. Finally, the project documented the issues surrounding inter-firm coordination and data quality management that must be addressed in order to develop the reliable capability to provide real-time visibility and analysis in production-grade environments.

This is the final report on the DOE's ESAMS demonstration project. Following this introduction, the report consists of four additional sections and three appendices. Section 2 provides an overview of the project, its origins, its primary tasks, and the organizations involved. Section 3 describes the applications of wide-area situational awareness that the project demonstrated. The section also describes the data quality review and remediation procedures required to run the applications in real time. Section 4 presents the principal findings from the demonstration. Section 5 summarizes the project's accomplishments.

[4] These efforts benefited greatly from prior, long-standing synchrophasor analysis practices pioneered in the Western Interconnection. See examples of these practices in NERC. Recommended Oscillation Analysis for Monitoring and Mitigation Reference Document. Synchronized Measurement Working Group. November 2021. https://www.nerc.com/comm/RSTC_Reliability_Guidelines/Oscillation_Analysis_for_Monitoring_And_Mitigation_TRD.pdf [Last accessed September 25, 2022.]

2. Project Overview

This section describes the origins of, the organizations involved in, and the primary activities of the ESAMS demonstration project. It also describes the locations of the PMUs that streamed synchrophasor data into the ESAMS applications and the architecture of the ESAMS demonstration platform, which was hosted by PJM Interconnection (PJM).

2.1 Background

The ESAMS demonstration project was sponsored by the DOE's Office of Electricity, Transmission Reliability and Renewables Integration (TRRI) program.

Between 2014 and 2017, the TRRI program sponsored an inaugural research activity called the Eastern Interconnection Baseline Project, which led to formation of the ESAMS project.[5] The initial project involved offline analysis of synchrophasor measurements provided by four industry partners: ISO New England (ISO-NE), Midcontinent Independent System Operator (MISO), New York Independent System Operator (NYISO), and PJM. The focus was on identifying pairs of wide-area phase angles that spanned the grid areas the four partners oversaw. After the pairs were identified, the measurements were analyzed by establishing baseline or reference values for each angle pair. In addition, sophisticated, statistically based algorithms were applied to identify unusual or atypical combinations of phase-angle measurements. At the conclusion of the project, the industry partners' principal recommendation was to shift the focus from offline analysis of historic information to continuous, real-time data collection and analysis, including regular dissemination of findings to grid operators.

The ESAMS project team consisted of researchers at the Electric Power Group (EPG), Pacific Northwest National Laboratory (PNNL), and Lawrence Berkeley National Laboratory (LBNL). EPG staff developed and managed the application software on a daily basis. EPG also contributed algorithms for several ESAMS applications and participated in reviewing and analyzing information in ESAMS reports. PNNL staff developed algorithms and code for ESAMS applications and also participated in reviewing and analyzing information in ESAMS reports. LBNL provided overall project management.

PJM hosted the ESAMS demonstration software. PJM received real-time synchrophasor data from the demonstration partners, combined those data with synchrophasor data collected from within its own system, and ported the data into the ESAMS software. PJM also supported the data links that distributed reports and notifications to the demonstration partners and the project team.

[5] That initial research identified wide-area phase angles, thereby prompting the ESAMS project, which was intended to monitor wide-area phase angles in real time. See Consortium for Electric Reliability Technology Solutions (CERTS) projects described at https://certs.lbl.gov/project/synchrophasor-system-data-baselining-and.html and https://certs.lbl.gov/project/baseline-studies-and-analysis.html [Both last accessed June 21, 2022.]

In addition to the four partners identified above, ESAMS demonstration partners were Southern Company (Southern), Southwest Power Pool (SPP), and Tennessee Valley Authority (TVA). In addition to streaming their synchrophasor data to PJM, the demonstration partners helped identify project priorities, contributed information on the PMUs to be used, followed up on data issues the project team identified, and conducted independent investigations to corroborate and extend ESAMS findings.

2.2 Summary of Project Activities

The ESAMS demonstration project began in 2017. The demonstration itself took place between June 2021 and March 2022.

The start-up phase of the project consisted of two parallel activities. The first, led by PJM, involved negotiating data-sharing agreements with the demonstration partners and the researchers. Negotiations began soon after the project was initiated and were completed in two stages. The first stage, which involved the researchers and the four original demonstration partners (ISO-NE, MISO, NYISO, and PJM), was completed in 2019. The second stage, which incorporated additional demonstration partners (Southern, SPP, and TVA), was completed in 2021.

The second start-up activity involved developing and testing the ESAMS software and data systems. In general, the basic algorithms underlying each of the ESAMS applications had been developed through previous research. Nevertheless, the algorithms required significant customization in order to process synchrophasor data continuously in real time. In June 2020, field testing of the core application algorithms in the ESAMS began at the PJM hosting environment.

As discussed in detail later in this report, significant effort was directed toward managing data quality. The start of the demonstration was pushed back six months to develop and test new methods of addressing data quality issues that were uncovered when real-time, streaming synchrophasor data were brought into the ESAMS.[6]

The demonstration began in June 2021, when reports of ESAMS findings began being generated and emailed to each demonstration partner shortly before 8 AM Eastern time each day (the daily report). The daily report consisted of a summary page listing every significant event or finding detected by the ESAMS applications during the previous day. See Figure 1. Each significant event or finding was accompanied by one or more pages that provided details. Section 3 presents examples of the additional pages, along with technical descriptions of the applications that generated them.

Throughout the demonstration period, the project team organized bi-weekly meetings with the demonstration partners to review and discuss recent findings. The meetings proved invaluable to the evolution of the project and to the confirmation and interpretation of its findings.

[6] These methods are described in Section 3.3.2

Summary (Eastern Daylight Time, 24-Hour Format)

Event Type	Event Time (EDT)	Additional Information
Dominant Natural Oscillation Baselining *PNNL Oscillation Engine*		Daily Report on Natural Oscillations
Forced Oscillation Detection & Source Location *EPG RTDMS®-Oscillation Detection algorithm PNNL periodogram-based sinusoid detector*		No forced oscillation event detected
Wide Area Disturbance Detection *EPG method-Control chart analysis*	**05:31** *Time for event with the most angle pairs participating*	**1 disturbance event(s) detected** Key info for event with the most angle pairs participating: • Number of Angle Pairs participating: 4 • Most sensitive angle pair during the event: [redacted]
Ringdown Detection *PNNL Oscillation Tool-Advanced spectral analysis*	**06:59-07:07** *Time for event with the earliest event time*	**3 ringdown event(s) detected** List of angle pair(s) for event with the earliest time: [redacted]
System Stress Detection *EPG method-Statistical analysis*	**11:00-11:59** *Time for event with the longest time under stress*	**1 stressed angle pair(s) detected** Angle pair with the longest time under stress: • Angle Pair: [redacted]
Anomaly Detection *PNNL tool-Multivariate analysis*	**04:47** *Time for event with the most angle pairs participating*	**5 atypicality event(s) detected** List of angle pair(s) contributed most to the event with the most angle pairs participating: [redacted]
PMU Data Quality *EPG DataNXT® -Six modules approach*		Daily Report on PMU Data Quality

Figure 1. First Page of an ESAMS Daily Summary Report

Early in the project, the demonstration partners requested two major enhancements to the ESAMS. First, they asked to include synchrophasor data from Southern, SPP, and TVA to support the application that identified source locations for forced oscillations. The three partners were added in September 2021. Second, the demonstration partners requested that the ESAMS be modified to send notifications of major forced oscillations in real time, a capability that was enabled at the start of January 2022.

The demonstration partners contributed generously to the confirmation and interpretation of project findings. They often shared their independent analyses based on the much larger set of synchrophasor data their systems collected. Those analyses both corroborated and extended the ESAMS findings. The partners proved invaluable in helping the project team further validate the ESAMS applications, especially regarding the robustness of the information obtained and the soundness of the logic underlying the applications.

2.3 Synchrophasors Used by the ESAMS

ESAMS applications were driven by synchrophasor data streamed continuously from PMUs that were either owned by or available to each of the demonstration partners: PJM, ISO-NE, MISO, NYISO, Southern, SPP, and TVA. For the demonstration, the ESAMS applications relied on synchrophasor data provided by only a small fraction of the thousands of PMUs operating in the Eastern Interconnection.

Synchrophasor measurements were selected according to requirements of the ESAMS applications. Table 1 lists the ESAMS applications and the number of synchrophasors from each demonstration partner that were used to support each application. Note that the applications both for detecting forced oscillations and for locating the region containing their sources used data from some of the same synchrophasors.

Table 1. Synchrophasors Categorized by ESAMS Application and Data Provider

Data Provider	Detection of Forced Oscillations (Only)	Detection of Forced Oscillations and Region Location (Both)	Region Location (Only)	Phase-Angle Pairs (Stress, Disturbance, Atypicality, Ringdown, Natural Modes)	Total Number of PMUs
ISO-NE	1	2	1	1	5
MISO	13	5	1	3	22
NYISO	1	1	2	2	5
PJM	31	10	54	16	106[7]
Southern	1	3	0	1	5
SPP	0	10	1	0	11
TVA	0	4	11	0	15
Total	**47**	**35**	**70**	**23**	**169**

Figure 2 shows the approximate locations of the PMUs that provided synchrophasor data used in the ESAMS applications. The figure depicts only those PMU locations used in the graphical displays that the ESAMS produced (that is, not all the PMU locations that provided synchrophasor data). Note also that in several locations, PMUs provided multiple synchrophasor signals.

[7] Note that some of the synchrophasors that provided data for applications related to phase-angle pairs also provided data for the applications developed to either detect forced oscillations and/or detect region locations.

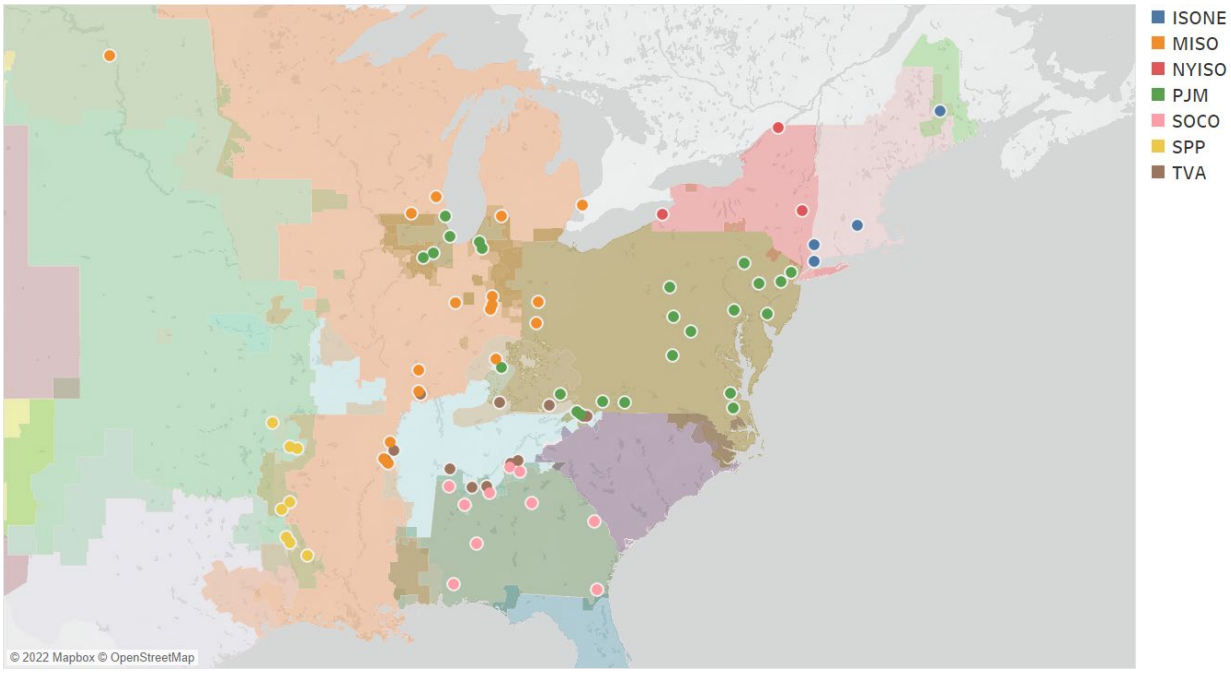

Figure 2. Locations of PMUs Used in ESAMS Graphical Displays

2.4 ESAMS System Architecture

Figure 3 illustrates the overall layout of the ESAMS demonstration software systems and the data flows among them. PJM received synchrophasor data continuously in real time via Eastern Interconnect Data Sharing Network's (EIDSN's) Electric Information network.[8] The received data were assembled by PJM's Phasor Data Concentrator (PDC) and then checked first by a series of data quality procedures embedded in the Real Time Dynamic Monitoring System (RTDMS).[9]

After the RTDMS performed initial processing, the ESAMS applications analyzed the data. As described in Section 3, the ESAMS applications can analyze data related to both oscillations and wide-area phase angles. The ESAMS also contains specialized data quality and data-processing algorithms (termed ESAMS data services).

The results from the application analyses were collected and distributed to demonstration partners in a daily report disseminated via email. In addition, analytical results related to identifying the source regions for any detected forced oscillation were distributed to demonstration partners via email in real time. The ESAMS stored results briefly (for approximately 2 weeks) to support offline follow-up analysis of unusual events or findings.

[8] Eastern Interconnect Data Sharing Network's Electric Information network. https://eidsn.org/. [Last accessed 06/22/2022.]
[9] RTDMS is a real-time platform developed by the Electric Power Group (EPG). https://www.electricpowergroup.com/rtdms.html [Last accessed 06/22/2022.]

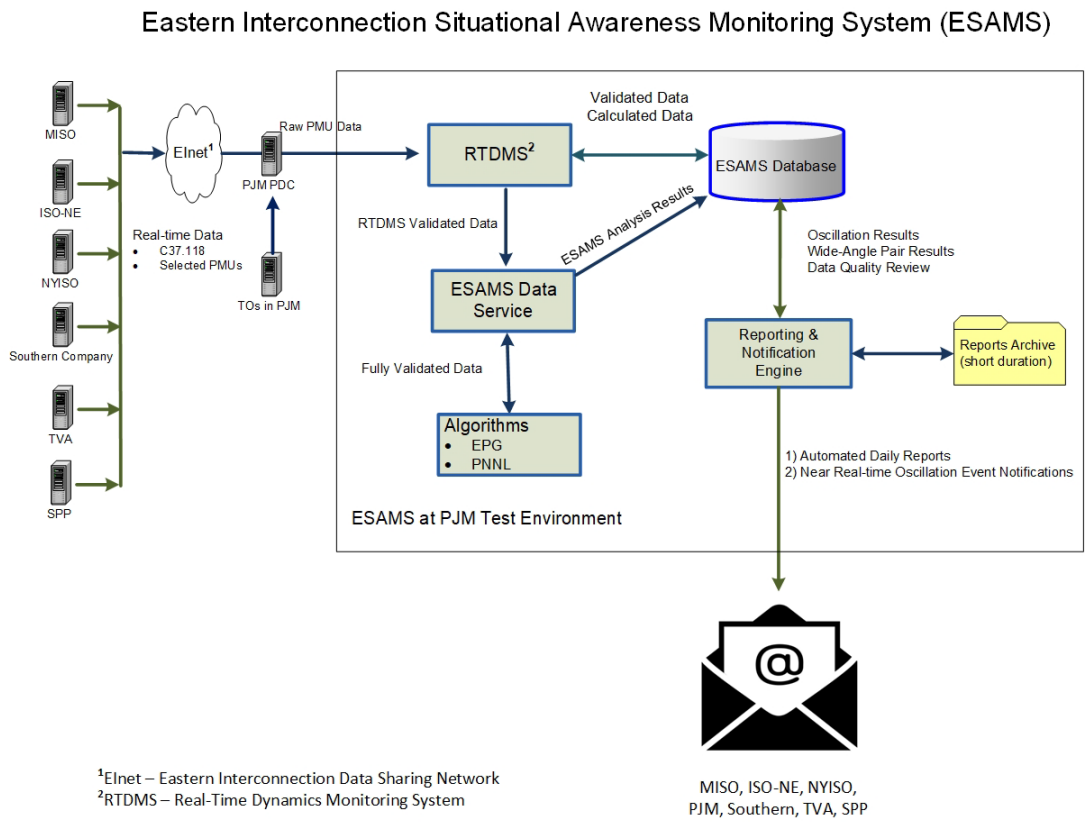

Figure 3. ESAMS System Architecture

3. ESAMS Applications for Wide-Area Situational Awareness

This section describes the two groups of applications that supported the wide-area situational awareness that the ESAMS project demonstrated. Each group of applications provided situational awareness of a distinct class of grid behaviors that are known to be precursors to, or potential indicators of, a major blackout. The first group monitored aspects of the oscillatory behavior of the Eastern Interconnection. The second group monitored phase angles in broad areas of the Eastern Interconnection.

This section first reviews the issues related to preventing the blackouts that both groups of applications were designed to address. Then the technical concepts underlying the two groups are summarized. Next, the individual applications are described. A final subsection describes the data quality and handling procedures, in particular those developed specifically to support the ESAMS applications.

The applications demonstrated in the ESAMS provided the wide-area grid visibility that is enabled uniquely by synchrophasors. First, all the applications rely on the collection, integration, and analysis of synchrophasor data from multiple operating entities. No application can be supported by synchrophasor data collected from within a single grid. Second, all the applications rely solely on synchrophasor data; none relies on supplementary information that can be collected using conventional SCADA systems and EMS.[10]

Importantly, the applications the ESAMS demonstrated are intended to complement—not duplicate or replace—grid operators' situational awareness of local conditions. That awareness already is available through their SCADA/EMS and synchrophasor-based, local monitoring. The applications demonstrated in the ESAMS are advisory only. They provide heretofore unavailable information on wide-area conditions that cannot be seen by a single grid operator. But they do not suggest or indicate, much less direct, specific actions. They are intended solely to enable grid operators to communicate with one another more efficiently regarding appropriate actions. Such actions, in turn, are expected to be supported by grid operators' internal SCADA/EMS and synchrophasor-based monitoring systems.

3.1 Applications Related to Oscillations

The first group of applications described here monitored aspects of the oscillatory behavior of the Eastern Interconnection. Synchrophasors are well suited to oscillation analysis because their high reporting rate (typically at least 30 measurements per second in a 60 Hz system) enables observability of the frequency range of bulk power system (BPS) oscillations. In contrast, conventional SCADA systems typically report measurements every several seconds. In addition, SCADA measurements are not synchronized, a feature that is critical when analyzing wide-area oscillations.

[10] Section 4 notes that the value of the information provided by synchrophasor measurements, especially as related to phase angles measured over wide areas, can be enhanced by incorporating information from conventional EMS.

Oscillations within bulk power systems (BPSs) can be divided into two general types, both of which ESAMS algorithms were designed to monitor. The first type, modal oscillations, are a natural property of interconnected power systems; they are always present. The ESAMS demonstration continuously monitored the natural oscillatory modes of the Eastern Interconnection. The second type of oscillations, forced oscillations, are caused by malfunctioning or poorly operating equipment that injects a periodic signal (either power, current, or voltage) into the power system. When such oscillations originate from certain locations within an interconnection and when they oscillate at frequencies that resonate with a natural system mode, forced oscillations can be observed throughout the interconnection. The ESAMS detected forced oscillations in real time and identified the regions from which they originated.

Before describing the ESAMS applications that monitored and analyzed oscillations (in subsection 3.1.2), the following subsection provides some background on BPS oscillations. Readers who are familiar with those concepts can skip this section.

3.1.1 Background on Power System Oscillations

Large interconnections are characterized by generators located relatively closely (electrically) to one another that self-organize to form groups that naturally oscillate against similarly self-organized groups in other regions of the interconnection. When the oscillations are poorly damped, a grid disturbance can cause them to become unstable, which can lead to a cascading blackout, such as occurred in the western United States on August 10, 1996. Poorly damped oscillations were confirmed as a direct contributor to this blackout, which left 7.5 million people in 14 states, 2 Canadian provinces, and the northernmost state of Mexico without power for periods ranging from a few minutes to 9 hours.[11]

Figure 4 shows synchrophasor measurements made during the 15 minutes immediately preceding the blackout of August 10, 1996. Analysis of the measurements confirms that approximately 7 minutes before the blackout began, there were clear indications that the grid was in a poorly damped state.[12] Industry members and researchers have postulated that had operators been aware of the dangerous condition, they may have been able to prevent the blackout.

[11] Western Systems Coordinating Council. Disturbance Report for the Power System Outage that Occurred on the Western Interconnection August 10, 1996, at 1548 PAST. October 1996.

[12] D. Trudnowski, J. Pierre, N. Zhou, J. Hauer, M. Parashar. "Performance of Three Mode-Meter Block-Processing Algorithms for Automated Dynamic Stability Assessment," *IEEE Transactions on Power Systems*, vol. 23, no. 2, pp. 680-690. May 2008. DOI: 10.1109/TPWRS.2008.919415.

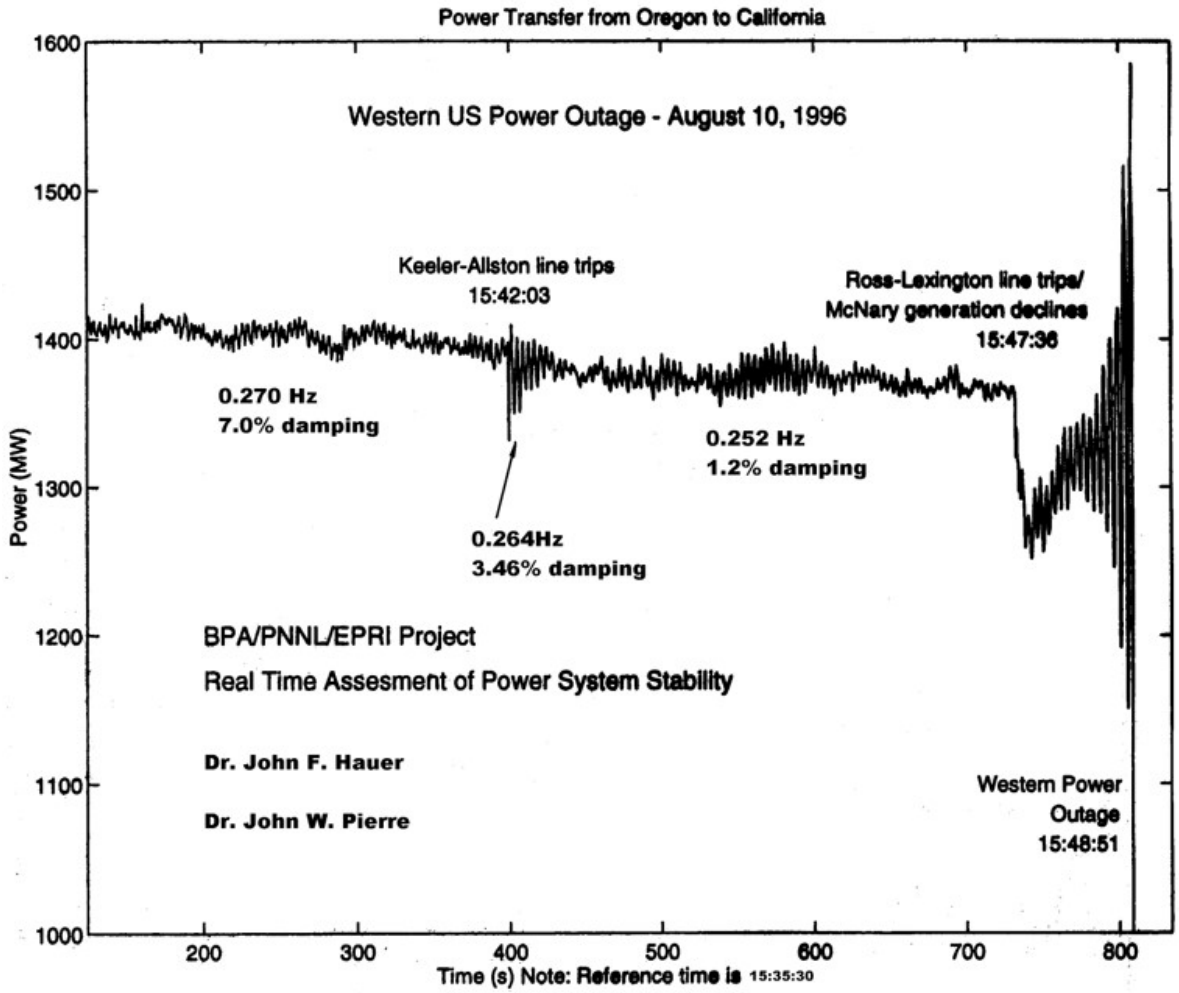

Figure 4. Western Interconnection Power Outage, August 10, 1996

Source: Trudnowski et al., 2008; see footnote 11.

Several related aspects of power system oscillations must be considered in order to assess their overall effect on reliability: (1) the frequency of natural system oscillations, which is called its mode; (2) the damping ratio of the mode*;* and (3) the shape of the mode.

As noted, groups of generators within a given region of an interconnection have a natural tendency to self-organize and operate synchronously in nearly exact harmony with one another. Such coherent groups, each in a different region of an interconnection and generally separated by long distances, also will naturally operate very slightly out of synchronism with one another. The slight differences between two such groups will create natural system oscillations at frequencies that typically range from 0.1 to 1.0 Hz. Those natural system oscillations are always present.

A large interconnection will contain more than one natural system oscillatory *mode*. Each mode is characterized by a narrow range of frequencies at which it is observable. Changes in the composition and loading of the generators in the two groups of generators oscillating against one another will cause

the frequency identified with each mode to drift slightly over time (typically less than about +/-0.1 Hz around a central dominant frequency).

Natural oscillatory modes generally are well damped. Well damped means that, when a grid disturbance produces a sudden increase in the amplitude of the oscillation at one mode, that amplitude will decrease monotonically and rapidly (within a few seconds) to its lower ambient amplitude. The capacity of this natural tendency of an interconnection to reduce or dampen oscillation amplitudes differs according to grid conditions and control system status. If the strength of this natural tendency has weakened, the amplitudes of an oscillation take longer to smooth out. If the grid enters a severely weakened state, a grid disturbance may cause it to enter an undamped state. An undamped state is dangerous because the oscillation will continue to grow until system protective devices engage, at which point a cascading blackout is likely.

The strength of the natural tendency for oscillation amplitudes to dampen is measured by a mode's *damping ratio*. When the damping ratio of all modes exceeds 10%, the system is considered well damped. When the damping ratio falls below 3% to 5%, the system is considered poorly damped. Estimates have indicated that the damping ratio was close to 1% when the comparatively minor disturbance in the Pacific Northwest initiated the chain of events that culminated in the August 10, 1996, blackout. See Figure 4.

Mode shape refers to the groupings of generators that oscillate swing against each other as part of a natural mode of oscillation. The two groups of generators commonly are located at opposite ends of an interconnection. The variation in a mode's shape (i.e., in the composition of generators that form each end of the shape) tends to be minimal, making the shape of a mode a key identifying characteristic.

Information about the generators that form a mode shape is important for assessing the potential effect on reliability of grid disturbances such as forced oscillations (to be discussed next). Disturbances occurring close to one end of a mode's shape can be magnified and pose a reliability threat at the opposite end of the interconnection, far from the original disturbance.

Forced oscillations are caused by malfunctioning or poorly operating equipment that injects a periodic signal into the power system. A forced oscillation is a concern for reliability when its amplitude is large (e.g., hundreds of MW from peak-to-peak); its frequency is at or near a natural system oscillatory mode; it originates at one end of its mode shape; and system damping of the mode is low. Under those conditions (or a subset of them), one can observe a forced oscillation within the entire interconnection because the oscillation's signal is amplified through resonance with the natural oscillatory mode of the system. The reliability of the interconnection is threatened when forced oscillations are large enough to overwhelm the tie-lines that connect regions to one another.

Given the potential danger that forced oscillations pose, grid operators seek to rapidly identify their source and assess the reliability risks. This task is complicated because, although multiple grid operators may observe a forced oscillation, an operator can determine only whether it is originating from within

their region. Some grid operators do not yet possess even this capability. Thus, RCs may be confused regarding the exact location of the source and hence which RC has lead responsibility for managing the situation.

Forced oscillations have become an area of growing concern for the Eastern Interconnection. On January 11, 2019, the controller on the steam turbine unit of a combined-cycle unit in Florida began mis-operating.[13] The mis-operation caused the turbine's output to oscillate 200 MW from peak to peak. Of particular significance, the oscillations were centered at 0.25 Hz, which is close to one of the major modes of the Eastern Interconnection. As a result, the oscillations were observable throughout the entire interconnection. Grid operators in New England reported oscillations of 50 MW peak-to-peak at their interface with New York.

Grid operators began contacting one another seeking information about the source of the forced oscillation. The NERC's investigation into the incident revealed confusion among grid operators, because only some had systems that were capable of observing the oscillations. Meanwhile, some grid operators contemplated taking operational actions. Fortunately, the operator of the source plant noticed the mis-operating equipment and took it offline after 18 minutes. The NERC investigation recommended, among other things, that "*RCs should improve communications with neighboring RCs in the event of widespread oscillation disturbances on the BPS*" and that "*RCs should jointly consider developing interconnection-wide oscillation detection and source location applications using interconnection-wide PMU and SCADA data*."

3.1.2 The ESAMS's Four Oscillation Applications

The ESAMS demonstrated four closely-related applications that analyzed oscillations. The first application detected the onset of a forced oscillation[14] and then identified the region from which it originated. The second application was used to baseline the frequencies of natural oscillations. This baselining information helped implement the third application. The third application continuously monitored the frequencies and damping ratios of the two most important Eastern Interconnection oscillatory modes. The fourth application identified grid disturbances leading to short-lived but highly visible oscillations, which proved useful for offline analysis of the system's modes.

[13] North American Electric Reliability Corporation (NERC). Eastern Interconnection Oscillation Disturbance: January 11, 2019, Forced Oscillation Event. December 2019.
https://www.nerc.com/pa/rrm/ea/Documents/January_11_Oscillation_Event_Report.pdf [Last accessed June 22, 2022.]

[14] The primary oscillation detection algorithm used in ESAMS is specifically designed to detect forced oscillations, rather than modal (natural) oscillations. Based on this design, along with the recognition that forced oscillations are much more common than wide-area sustained modal oscillations, all sustained oscillations detected by ESAMS were reported as forced oscillations. Details and additional references for the algorithm can be found in:
J. Follum, F. Tuffner and U. Agrawal, "Applications of a new nonparametric estimator of ambient power system spectra for measurements containing forced oscillations," 2017 IEEE Power & Energy Society General Meeting, 2017, pp. 1-5, doi: 10.1109/PESGM.2017.

3.1.2.1 Detecting Forced Oscillations and Identifying Source Regions

The application that detected forced oscillations and identified their source regions ran in real time. The application sent notifications in real-time when it detected a forced oscillation in the frequency range of 0.1-4 Hz that exceeded stipulated thresholds for amplitude. Notifications identified the RC region within the Eastern Interconnection that contained the source of the forced oscillation, the frequency of the oscillation, and the locations within the interconnection that were experiencing oscillations having the highest amplitudes.

The purpose of the application was to help RCs quickly identify which RC had lead responsibility for addressing a forced oscillation. Rapid identification of the source region can reduce confusion and the potentially conflicting information that may arise from independent observations made in the various areas of the interconnection. Although individual RCs may conclude that their region is not the source, they may not have the information needed to identify the region that is the source. Because the ESAMS provided a unified and integrated picture of the entire interconnection, the missing information was visible.

The ESAMS assessed each oscillation using a modification[15] of the dissipating energy flow method, [16] which has been shown to be the most reliable method for identifying the source of forced oscillations.[17] The method relies on measuring the flows of oscillation energy that are created by the source of a forced oscillation. Tracing those flows back to a particular generator requires nearly complete observability of the flows over all transmission lines that are connected to the source. Although it is feasible for an individual grid operator to achieve such observability within the part of the grid they manage, there are two reasons the ESAMS could not provide overall observability by relying on the signals available to the demonstration partners.

First, the purpose of the ESAMS was to identify the region containing the source of a forced oscillation, rather than the actual source. Thus, the dissipating energy flow method the ESAMS used relies on measurements made at the boundaries between regions (rather than around the perimeter of the generator that is the source). The topology of the Eastern Interconnection sometimes resulted in the ESAMS finding that dissipating energy was flowing across and through multiple regional boundaries.

Second, the ESAMS implementation of the dissipating energy flow method did not include measurements taken at every boundary between regions, because synchrophasor measurements are not yet available on all the tie-lines that connect regions of the interconnection. Because sometimes the ESAMS could not observe much of the dissipating energy flows at tie-line boundaries, findings could be inconclusive or even misleading.

---

[15] J. Follum. "Statistical Evaluation of New Estimators used in Forced Oscillation Source Localization," *Hawaii International Conference on System Sciences (HICSS-53)*. January 7-10, 2020. doi: http://hdl.handle.net/10125/64111.

[16] S. Maslennikov , E. Litvinov. "ISO New England Experience in Locating the Source of Oscillations Online," in *IEEE Transactions on Power Systems*, vol. 36, no. 1, pp. 495-503. January 2021. DOI: 10.1109/TPWRS.2020.3006625

[17] J. Follum, S. Maslennikov, E. Farantatos. IEEE/NASPI Oscillation Source Location Contest, NASPI Work Group Virtual Meeting and Vendor Show, October 5-7, 2021. PNNL-SA-167027. https://www.naspi.org/sites/default/files/2021-10/D3S8_01_follum_pnnl_20211007.pdf [Last accessed 06/22/2022.]

In addition, as with any application based on measured quantities, data availability and quality affected the ability of the ESAMS's analytical techniques to determine the source region of a forced oscillation. Given the first two considerations and the project team's early experience with the quality of the data available to support the demonstration, the team developed additional procedures for assessing the strength of the evidence available for identifying source regions.[18]

The team's assessment tool considers the number of regions that may be exporting (and/or importing) flows of dissipating energy. The tool also considers the coverage and availability of good data regarding the flows between regions. And finally, the tool evaluates a finding's robustness based on the number of signals upon which the source region was identified. Each of the three factors contributes a separate numerical score that is summed to produce a composite score that assigns an overall confidence level to the identified source location. Appendix A describes in more detail the assessment and scoring procedure, including suggested future enhancements identified during the demonstration.

Figure 5 shows the first page of a report the application generated about the source location for a forced oscillation. In this example, the highest-amplitude oscillations were observed in ISNE[19]; the source of the forced oscillation was identified as MISO, but with low confidence; and the oscillation frequency was outside the range of the two principal inter-area modes of the Eastern Interconnection.

The first page of the report has four sections. The first section provides a written summary of the event:

- the location where the highest amplitude was measured (which may be far from the source);
- the RC region showing the highest net export of oscillation energy, which likely was the region that contained the source; and
- the confidence with which the preliminary determination was made.

The second section of the report presents a schematic map of the RC regions in the Eastern Interconnection. The map is populated with information on both the source and the effects of the forced oscillation. The arrows on the map show the directions of dissipating energy flows across the tie-lines between regions that are monitored by synchrophasors. The color intensity of the arrows indicates the magnitude of the dissipating energy flow on a scale that is normalized to range from 0 to 1. The grey lines indicate the absence of synchrophasor data due to, for example, unacceptable data quality or data unavailability. The green numbered circles on the map rank the locations at which the five highest-amplitude oscillations were observed. Finally, the green cup shape on the right just below the map indicates the range of frequencies within which the forced oscillation was observed.
The third section of the report begins with a summary of the general features of the forced oscillation: date/time, frequency, and type (local or wide area). Below the summary is a table listing the locations where the highest-amplitude oscillations were detected. The locations in the table correspond to the

[18] J. Follum, J. Eto. "Confidence Metrics for Regional Forced Oscillation Source Localization," *The 2022 International Conference on Smart Grid Synchronized Measurements and Analytics (SGSMA),* May 24-26, 2022. Split, Croatia.
[19] The RC region for ISO-NE is designated "ISNE."

green numbered circles on the map. The fourth section provides a trace of the measurements recorded at the location of the highest-amplitude oscillation (Rank 1 in the table and 1 in the green circle on the map).

Forced Oscillation observed for 01/23/2022

Forced Oscillation event was detected by signal [redacted], 01/23/2022 09:16 ET - 01/23/2022 10:04 ET,
RC Region with Highest net oscillation energy export: MISO **Confidence Level:** Low
Doesn't appear to be localized only to MISO

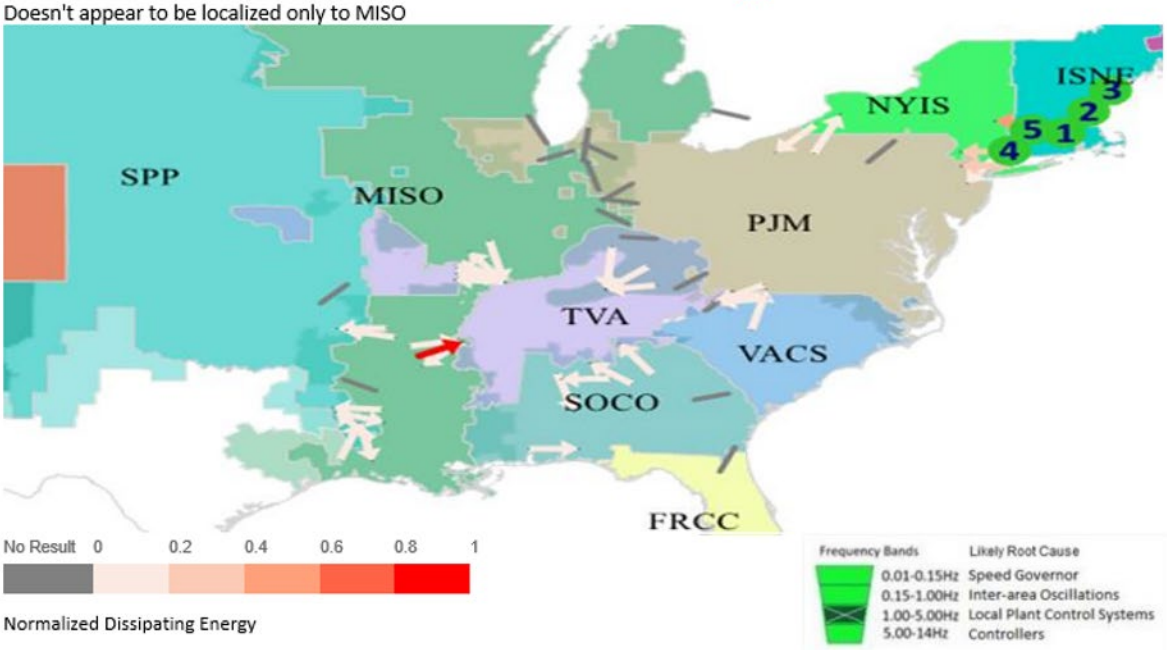

Time (EST): 09:16 - 10:04; Frequency: 1.18 Hz; Oscillation Type: Local Plant Control Systems

Rank	Oscillation Detected at	Peak to Peak Amplitude	Oscillation Band RMS Energy
1	[redacted]	8 MW	3 MW
2	[redacted]	5 MW	2 MW
3	[redacted]	5 MW	2 MW
4	[redacted]	3 MW	2 MW
5	[redacted]	2 MW	1 MW

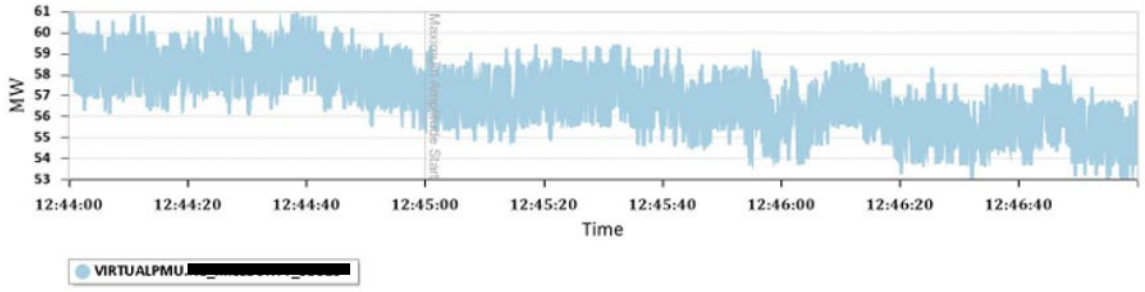

Figure 5. ESAMS Report on Forced Oscillation

Figure 6 presents the second page of the report on the forced oscillation depicted in Figure 5. This page provides additional information regarding the identification of the source location and the scoring factors that established the confidence level of the identification. The top part of the page presents a schematic line diagram illustrating the direction and magnitude of the net oscillation energy flows among affected regions. As noted above, the region having the highest total net energy flow is identified initially as the likely source of the forced oscillation.

The bottom part of the page lists the ESAMS findings that contributed to the confidence level assigned to the location identification. The example presents the following findings.

- First, although the ESAMS found that the net or sum total of oscillation energy flows was positive from MISO, the application also found that some of the measurements showed imports of oscillation energy into MISO. This finding did not increase confidence in the identification of MISO as the likely source.
- Second, the ESAMS found that, in addition to MISO, three regions also exported oscillation energy. This finding reduced confidence in the identification of MISO as the likely source.
- Third, the ESAMS found that even if nearly half the measurements showing the highest oscillation energy flows were removed, MISO still showed the highest net export of oscillation energy. This finding increased confidence in the identification of MISO as the likely source.
- Fourth, the ESAMS confirmed that data from all of the synchrophasors at the interface between MISO and adjacent regions were available and used in the analysis. This finding increased confidence in the identification of MISO as the likely source.
- Fifth, the ESAMS nevertheless found that, overall, only two-thirds of the total number of synchrophasors used by the application provided data or data of sufficient quality to support the analysis. This finding reduced confidence in the identification of MISO as the likely source.

Energy Flow Diagram:

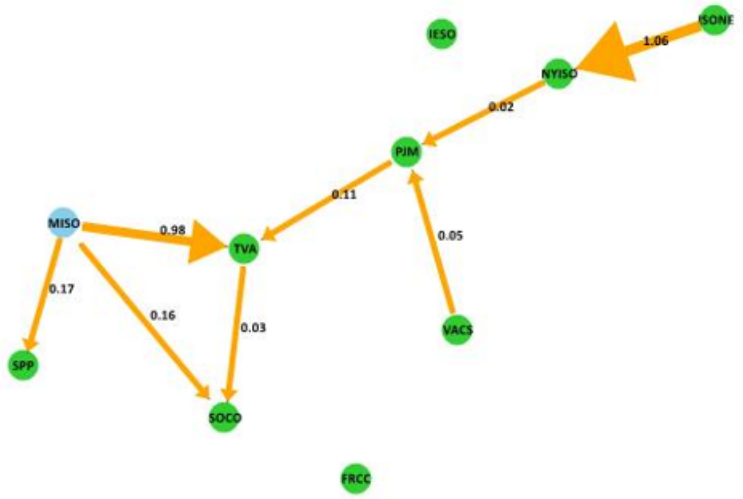

Confidence Level Scoring:

FO Source Identification	Region	Confidence Level	Criteria
REGION WITH HIGHEST POSITIVE NET ENERGY FLOW	MISO	Low (0)	*High:>2* *Medium:2* *Low:< 2*
Supporting Information	**Finding**	**Confidence Scoring Elements**	**Scoring Algorithm**
DOES THIS REGION ALSO HAVE IMPORTS?	Yes	0	*No = +* *Yes = 0*
OTHER REGIONS WITH POSITIVE NET ENERGY FLOW?	3	-	*None = +* *1 = 0* *2 or more = -*
ROBUSTNESS OF FINDING	47.06%	+	*<80% = +* *>80% And ≤90% = 0* *>90% = -*
SOURCE REGION'S DATA QUALITY/AVAILABILITY	100%	+	*>90% = +* *>80% And ≤90% = 0* *<80% = -*
OVERALL MEASURE OF DATA QUALITY/AVAILABILITY	66.67%	-	

Figure 6. Assessment of Confidence in Identifying Source of Forced Oscillation

3.1.2.2 Natural Oscillation Baselining

Rather than detecting distinct events, the natural oscillation baselining application uses ambient measurements to analyze the power system's modal frequencies throughout the day. The application is driven by the pairs of wide-area phase angles discussed in greater detail in subsection 3.2. At the end of each day, the application uses an unsupervised clustering analysis[20] to summarize the results and identify how well the various oscillatory modes in the Eastern Interconnection were observed by each angle pair. Figure 7 presents an example of a daily report from the application that provided natural oscillation baselining.

The daily report lists the angle pairs and oscillatory mode frequencies that were observed. When a single angle pair was observed having more than one frequency, the relative strength of each observation was indicated by the "dominant" observability of one frequency over the other.

The information collected for natural oscillation baselining can be used to identify the angle pairs that are best suited to support continuous observation of natural oscillatory modes via mode meters. The results generated by the ESAMS application that develops natural oscillation baselining provided evidence that modes near 0.2 Hz were consistently enough observable to enable the continual monitoring described in the next section.

[20] J. Follum, T. Yin, B. Amidan. "A New Spectral Estimator for Identifying Dominant Modes and Detecting Events in Power Systems," *2018 Probabilistic Methods Applied to Power Systems (PMAPS) Conference*, June 24-28, 2018, pp. 1-6. Boise, ID. Available online: https://doi.org/10.1109/PMAPS.2018.8440203. [Last accessed 06/23/2022.]

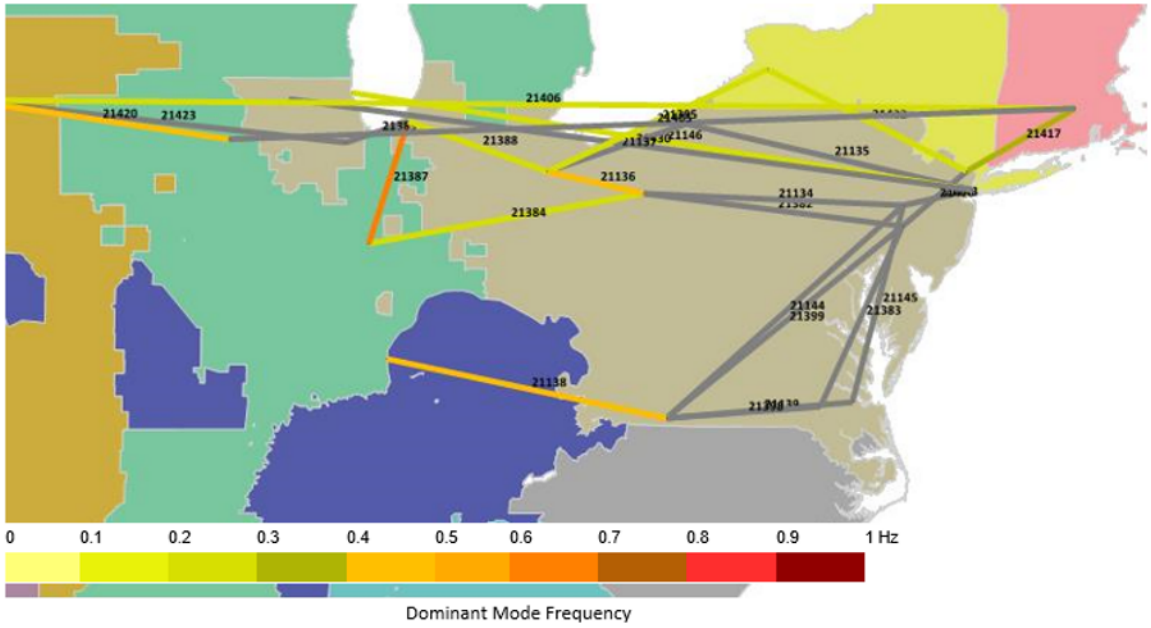

Dominant Natural Oscillation Observed in 11 Angle Pairs.

ID	Angle Pair/Path(top 15)	Dominant Mode		Secondary Mode	
		Freq (Hz)	Dominance	Freq (Hz)	Dominance
21384	[redacted]	0.215	0.953	0.785	0.047
21387	[redacted]	0.690	1.000	0.000	0.000
21388	[redacted]	0.225	0.836	0.860	0.164
21136	[redacted]	0.410	1.000	0.000	0.000
21395	[redacted]	0.215	1.000	0.000	0.000
21138	[redacted]	0.400	1.000	0.000	0.000
21406	[redacted]	0.220	1.000	0.000	0.000
21417	[redacted]	0.345	1.000	0.000	0.000
21420	[redacted]	0.445	1.000	0.000	0.000
21422	[redacted]	0.295	1.000	0.000	0.000

Figure 7. ESAMS Report on Dominant Natural Oscillation Baseline

3.1.2.3 Using Mode Meters to Monitor Natural Oscillations

Previous offline studies of a small set of disturbance recordings identified several system modes in the Eastern Interconnection. The work the ESAMS project team conducted to enable continuous tracking using mode meters greatly improved understanding of the two most important modes.

Every 15 seconds a mode meter generated an estimate of the frequency and damping ratio of the two primary natural oscillation modes of the Eastern Interconnection. The ESAMS's continuous monitoring of those modes was an important complement to past studies, which were based solely on analysis of snapshots made at various times in the past.

Monitoring each mode separately was important because their shapes reflect different parts of the interconnection. One mode, which involved the northeast part of the interconnection swinging against the midwest, is known as the NE-MW mode. This mode's shape is depicted in Figure 8. The other mode, which was characterized by the northeast part of the interconnection swinging against the south, is known as the NE-S mode. Its shape is displayed in Figure 9. In both figures, blue and red circles indicate the two groups swinging against each other; gray dots indicate low participation. Knowing which mode, along with its shape and damping ratio, was involved in a forced oscillation supports interpretation and understanding of the magnitude of oscillation measurements that should be observable (or not observable) by various regions within the interconnection

Although the frequencies of the two modes were close and sometimes overlapping, the ESAMS was capable of tracking each separately. Separate tracking was made possible using results from the application that performed natural oscillation baselining, which identified the voltage pairs that provided the greatest visibility of each mode.

The ESAMS utilized the commercially available mode meter in the EPG's RTDMS. That mode meter relies on the Yule-Walker algorithm, which the literature has evaluated and confirmed as a reliable means for estimating oscillation frequency and system damping ratio.[21] Examples of the output from the mode meters are presented and discussed in Section 4.

[21] Synchronized Measurement Working Group. Recommended Oscillation Analysis for Monitoring and Mitigation Reference Document, NERC. November 2021.
https://www.nerc.com/comm/RSTC_Reliability_Guidelines/Oscillation_Analysis_for_Monitoring_And_Mitigation_TRD.pdf
[Last accessed 06/23/2022.]
See also footnote 11.

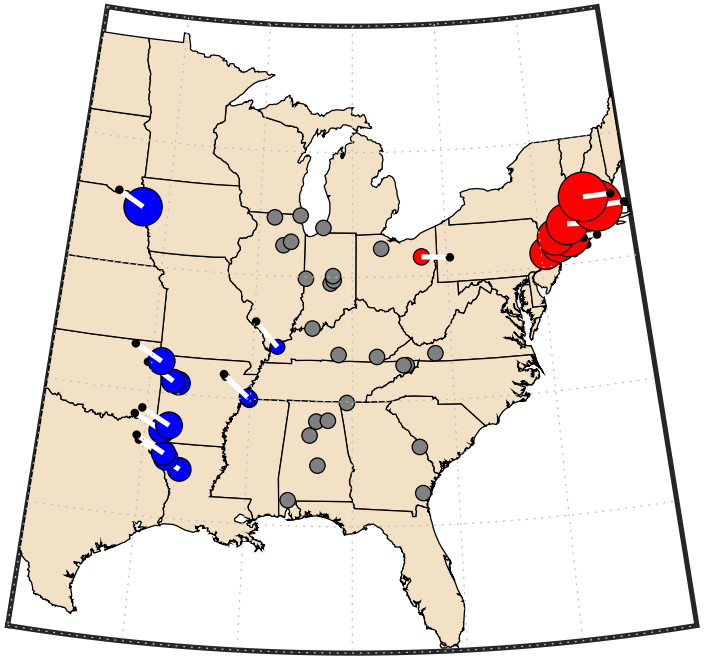

Figure 8. Shape of the NE-MW mode.

Source: Follum, J., N. Nayak, J. Eto. 2023.

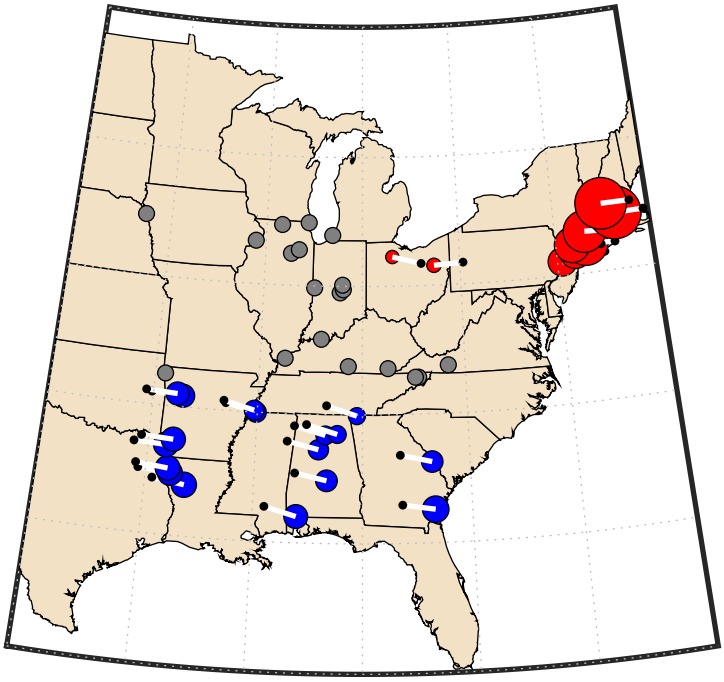

Figure 9. Shape of the NE-S mode.

Source: Follum, J., N. Nayak, J. Eto. 2023

3.1.2.4 Estimating Post-Event System Damping—Ringdown Analysis

The ringdown application has both an online and an offline element. The online element involves recording synchrophasor information from system events that might warrant a ringdown analysis. The offline element is a subsequent manual assessment of the data to identify the system oscillatory modes that were excited by the disturbance and the capacity of the grid to dampen those oscillations.

Manual post-event analysis of individual events enables estimating the system damping ratio more precisely than is feasible using mode meter data in real time. Thus, the offline analyses were important for corroborating findings from the mode meters and, when appropriate, further calibrating them.

Figure 10 shows the daily report for an event that underwent a subsequent ringdown analysis. The format follows the one used in presenting results from other ESAMS applications. The top of the page gives the date and time of the event and the number of phase-angle pairs that detected it. The map shows the locations of the phase-angle pairs in red. The table lists the phase-angle pairs and their locations. The final plot presents the ringdown information.

1) Ringdown event was detected by 8 angle pairs 01/23/2022 18:59 - 01/23/2022 18:59

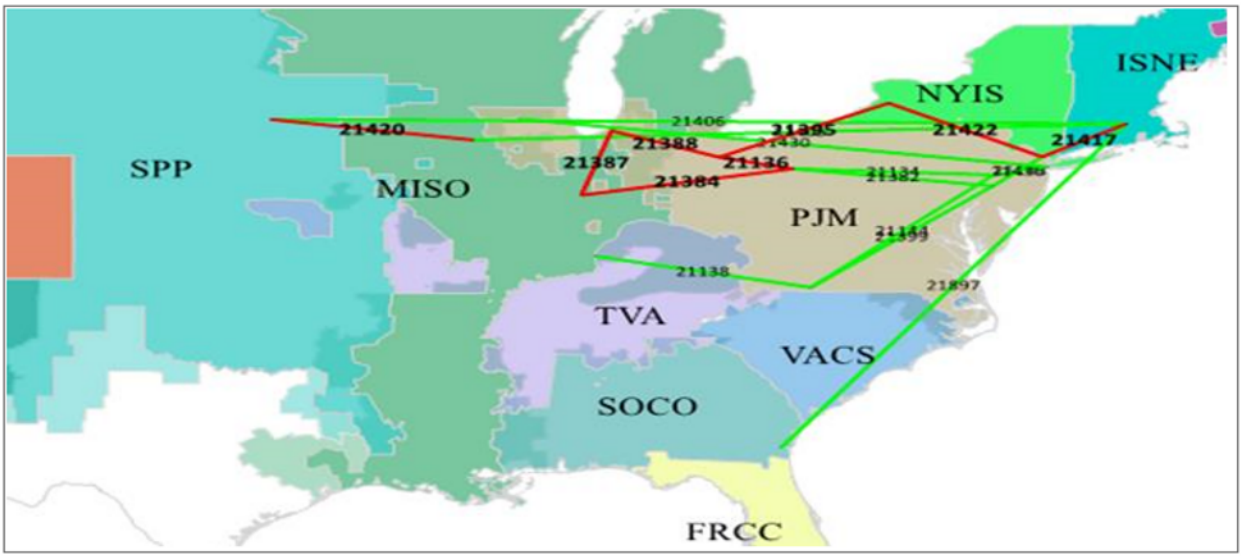

Angle Pairs showing ringdown event

Time (EST)	ID	Angle Pair	Stations
18:59 - 18:59	21136	[redacted]	[redacted]
	21384	[redacted]	[redacted]
	21387	[redacted]	[redacted]
	21388	[redacted]	[redacted]
	21395	[redacted]	[redacted]
	21417	[redacted]	[redacted]
	21420	[redacted]	[redacted]
	21422	[redacted]	[redacted]

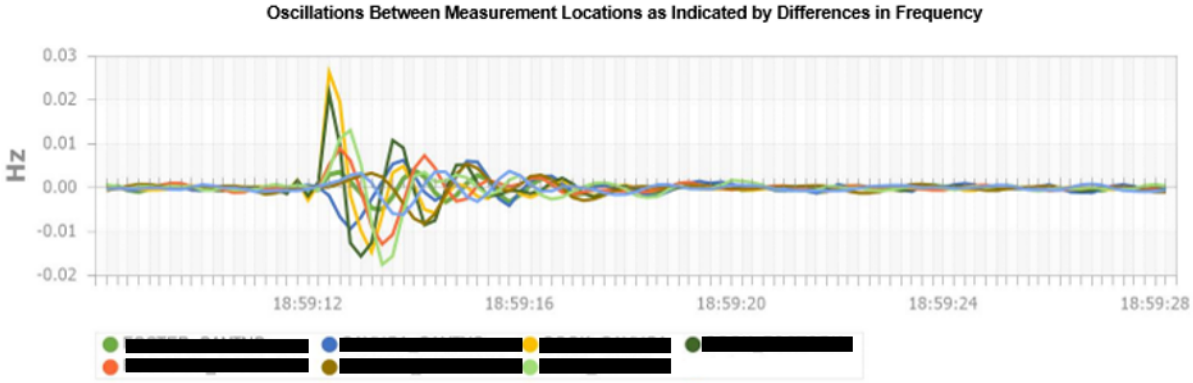

Figure 10. Ringdown Report

3.2 Wide-Area Phase-Angle Applications

The second group of ESAMS applications described here monitored phase angles within wide areas of the Eastern Interconnection. Knowing the differences in phase angles facilitates assessing the effects of power transfers on the overall condition of the grid.[22] Phase angles measured across wide areas can be monitored only by using synchrophasors. Conventional SCADA measurements are not time-stamped with sufficient precision to enable meaningful alignment of measurements made by different grid operators.

Poor situational awareness was a direct cause of the 2003 U.S.-Canada blackout. Figure 11 shows the differences in phase angles during the hour immediately before the blackout. The differences in phase angles between northern Ohio and the regions south of Ohio increased rapidly during that hour. Industry members and researchers have suggested that had neighboring grid operators been able to observe the rapid increase they might have been able to take actions to prevent the blackout from spreading beyond northern Ohio.

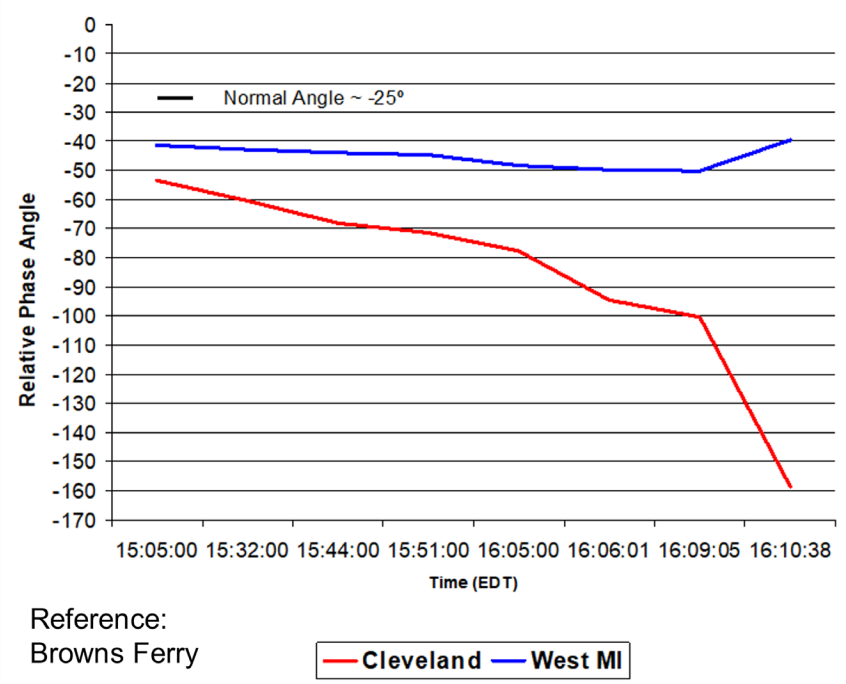

Figure 11. Cleveland Separation—Northeast U.S.–Canada Blackout August 14, 2003

Source: R. Cummings. 2005.

[22] See, for example, North American SynchoPhasor Initiative (NASPI) Control Room Solutions Task Team Paper, "Using Synchrophasor Data for Phase Angle Monitoring," NASPI-2016-TR-003 released 03/2016 https://www.naspi.org/node/351 [Last accessed 06/23/2022.], and NERC. Phase Angle Monitoring: Industry Experience Following the 2011 Pacific Southwest Outage, Recommendation 27, Technical Reference Document, June 2016. https://www.nerc.com/comm/PC/Synchronized%20Measurement%20Subcommittee/Phase%20Angle%20Monitoring%20Technical%20Reference%20Document%20-%20FINAL.pdf [Last accessed 06/26/2022.]

3.2.1 Phase Angles as a Measure of Power Transfers

Phase angles measure the amount of power flowing in one general direction over a given set of transmission lines. Monitoring phase angles is superior to the conventional method of monitoring individual transmission line voltages, because phase angles are an aggregated measure of the cumulative effect of power transfers over the many lines through which power is flowing.[23]

A change in phase angle indicates a change in either the amount of power that is flowing or the set of transmission lines conveying the flows. Both changes are affected by the dispatch of generators and the configuration of transmission lines available to transmit power between generation and load.

Rapid, large changes in phase angles indicate a sudden change in one or both of the factors noted above. In some instances, the changes are planned; in other cases they are not. Continuously monitoring phase angles within wide areas of the grid makes the sudden changes visible to grid operators in all parts of the interconnection.

As described, phase angles tend to change slowly for known reasons (e.g., because of scheduled changes in dispatch). Thus, the ranges within which the angles vary generally exhibit a regular pattern from hour to hour and day to day. Phase angles that persist for hours at values far outside the usual ranges indicate that grid operation differs significantly from recent history.

The wide-area phase-angle applications demonstrated in the ESAMS captured both rapid, large changes and large angles that persisted.

3.2.2 ESAMS's Three Wide-Area Phase-Angle Applications

The ESAMS demonstrated three complementary phase-angle applications. The first identifies rapid, large changes in phase angles. The second identifies hourly trends in phase angles that differ markedly from past trends. The third considers all phase-angle pairs simultaneously to identify unusual combinations of angles. Each application produced a daily summary report on the events it had identified. Figure 12 depicts the approximate locations of the PMUs and angle pairs used in the three applications.

[23] NERC. Phase Angle Monitoring: Industry Experience Following the 2011 Pacific Southwest Outage, Recommendation 27, Technical Reference Document. June 2016. https://www.nerc.com/comm/PC/Synchronized%20Measurement%20Subcommittee/Phase%20Angle%20Monitoring%20Technical%20Reference%20Document%20-%20FINAL.pdf [Last accessed 06/23/2022.]

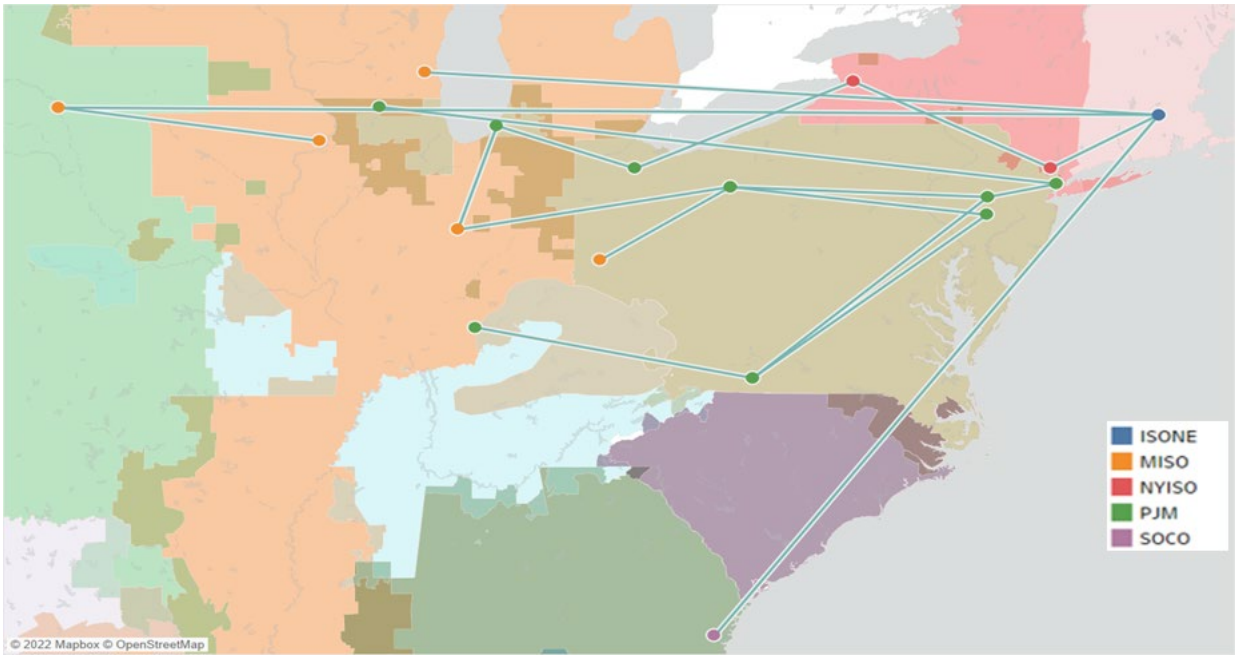

Figure 12. Locations of PMUs Used in Wide-Area Phase-Angle Applications

3.2.2.1 Rapid, Large Changes in Phase Angles

This phase-angle application runs at the end of each day to identify if and when a group of wide-area phase angles suddenly changed significantly compared to the angles observed during the rest of the day. For the demonstration, the size of the change in phase angle that would be called out was set at 20 standard deviations from the mean of the changes in phase angles observed during the entire day.[24] One can modify the application to adjust the size of change required (i.e., the number of standard deviations away from the mean) and the number of angle pairs that must simultaneously exhibit those changes.

Figure 13 shows an example report produced when a qualifying event was recorded. The top part of the report gives the date and time of the event and then lists the number of angle pairs that detected a rapid change. The next part of the report displays a map showing the locations of the angle pairs in red. The table below the map lists the angle pairs individually and reports the Z-scores in descending order of magnitude. The Z-score[25] indicates how far away (i.e., how much larger or smaller) a given measurement is from the mean of prior measurements. A measurement having a large Z-score is farther away from the mean than a measurement having a low Z-score. Note that the Z-score evaluates changes individually for each angle pair relative to past observations for just that angle pair. It is not a measure of the absolute value of a change in phase. The plot at the bottom of the page presents the information recorded by the angle pair for which the Z-score was highest.

[24] The changes in phase angles were measured by calculating the differences between the largest and smallest measurements observed in a 10-second window.
[25] https://www.statisticshowto.com/probability-and-statistics/z-score/

1) Disturbance at 08/20/2021 05:31 was detected by 4 angle pair(s)

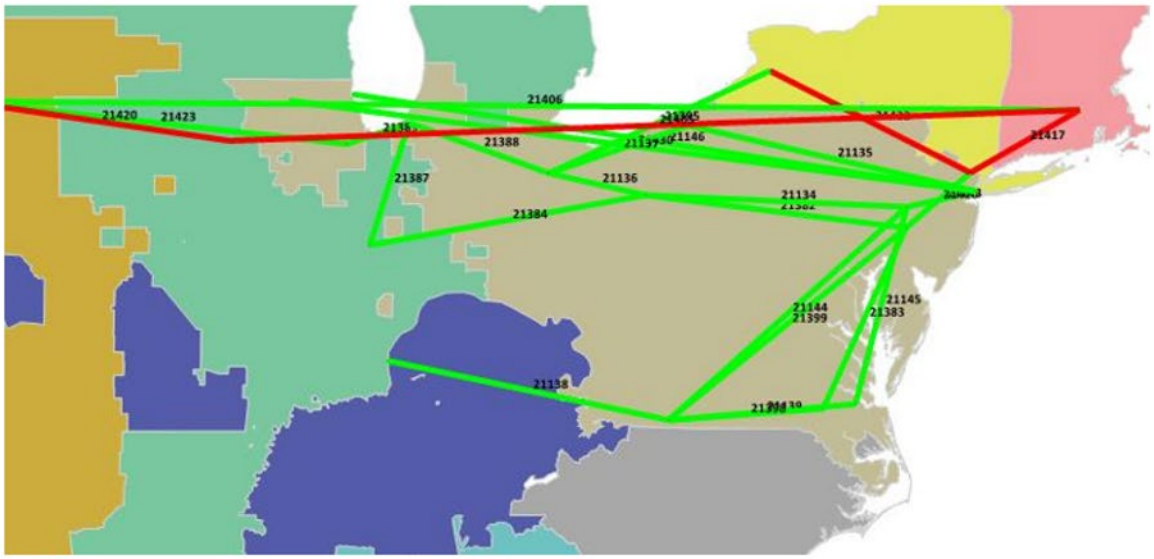

Angle Pairs showing disturbance event

ID	Angle Pair Name	Z-Score Before	Z-Score After	Z-Score Change	Time
21417	[redacted]	1.172	0.489	0.683	05:31
21420	[redacted]	0.774	0.155	0.619	
21405	[redacted]	-1.450	-1.102	0.348	
21422	[redacted]	-1.075	-1.360	0.285	

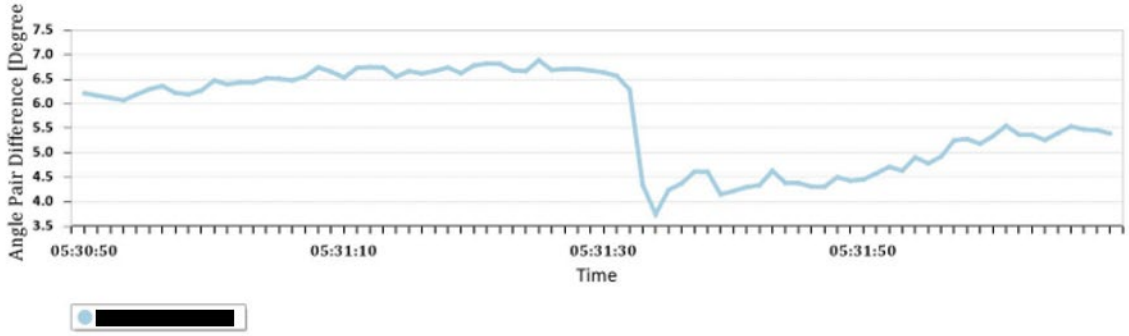

Figure 13. Report of Rapid, Large Change in Phase Angle

3.2.2.2 Very Large, Persistent Phase Angles

This phase-angle application also ran at the end of each day. It generated a report whenever a phase angle persisted for multiple hours at values that differed significantly from the average hourly value observed during the same period in the recent past. For the demonstration, the size of the phase angle difference was set at plus or minus 3 standard deviations from the mean; the number of hours the difference had to persist was set at 5; and the number of prior days against which the difference was measured was set at 10. All three values can be changed.

Figure 14 shows an example of the report produced when a qualifying event is recorded. The top of the report gives the date and time of the event and identifies the angle pair involved. Below that a map shows the angle pair in red. The plot at the bottom of the page shows the values that are 3 standard deviations above or below the hourly means in red and the measured values in blue.

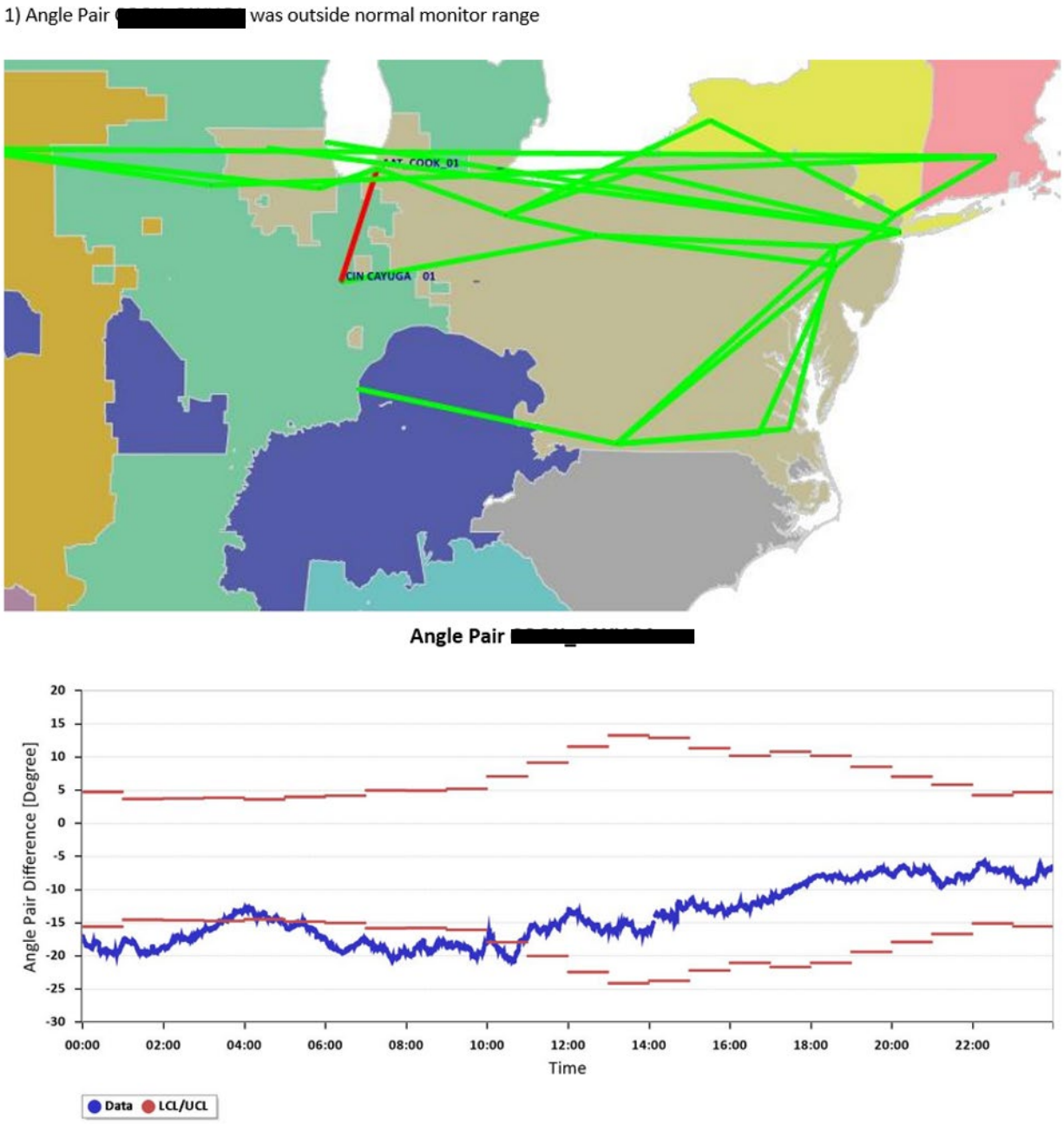

Figure 14. Report of Very Large, Persistent Phase Angle

3.2.2.3 Atypical Combinations of Phase Angles

Like the other applications described in this subsection, this ESAMS application also ran at the end of each day. It generated a report whenever it detected a combination of phase-angle measurements (both rapid changes and large values) that together differed significantly from past combinations.

The atypicality application is based on a powerful set of statistical algorithms that consider all phase-angle measurements simultaneously.[25] The application generates a score that reflects the extent to which a particular combination of values differs from past values. For the demonstration, the previous 14 days of operations were used to establish the baseline against which differences were evaluated. The event detection threshold was set so as to distinguish between low scores corresponding to ambient periods and higher scores corresponding to events.

Figure 15 shows an example of a report generated by the atypicality application. The top part of the report shows how the atypicality scores changed every minute of the day. The next part of the report identifies the angle pairs that were the most atypical by time of day and shows the atypicality scores. A subsequent page of the report plots the measurements for the angle pairs that contributed the most to the overall atypicality score. An example plot, Figure 16, shows how the observed behavior of a given angle pair immediately before, during, and after the atypicality (indicated by vertical dashed red lines) compares to the behaviors observed during the previous 30 days. The observed behavior is indicated in orange. The ranges of past behaviors are quantized over one-minute aggregations of time. Darker shading corresponds to more frequent observations of a given range in each time slice. In this example, the observed values did not differ significantly during the period identified as atypical compared to the periods immediately before or after it. On the other hand, none of the atypicality values had been observed routinely in the previous 30 days, as indicated by the absence of shading.

[25] B. Amidan, J. Follum, T. Yin, N. Betzsold. "FY18 Discovery Through Situational Awareness: Anomalies, Oscillations, and Classification," Pacific Northwest National Laboratory, PNNL-27812, Richland WA. 2018. doi:10.2172/1846595 and https://www.osti.gov/biblio/1846595 [Last accessed June 23, 2022.] and J. Follum, N. Betzsold, T. Yin, J. Buckheit. "Event Screening Methods for the Eastern Interconnection Situational Awareness and Monitoring System (ESAMS)," Pacific Northwest National Laboratory, PNNL-30137, Richland WA. 2020. https://www.osti.gov/biblio/1846589

Atypical Combinations of Rapid Step Changes and Large Angles

Statistically abnormal behavior observed for 5 instances:

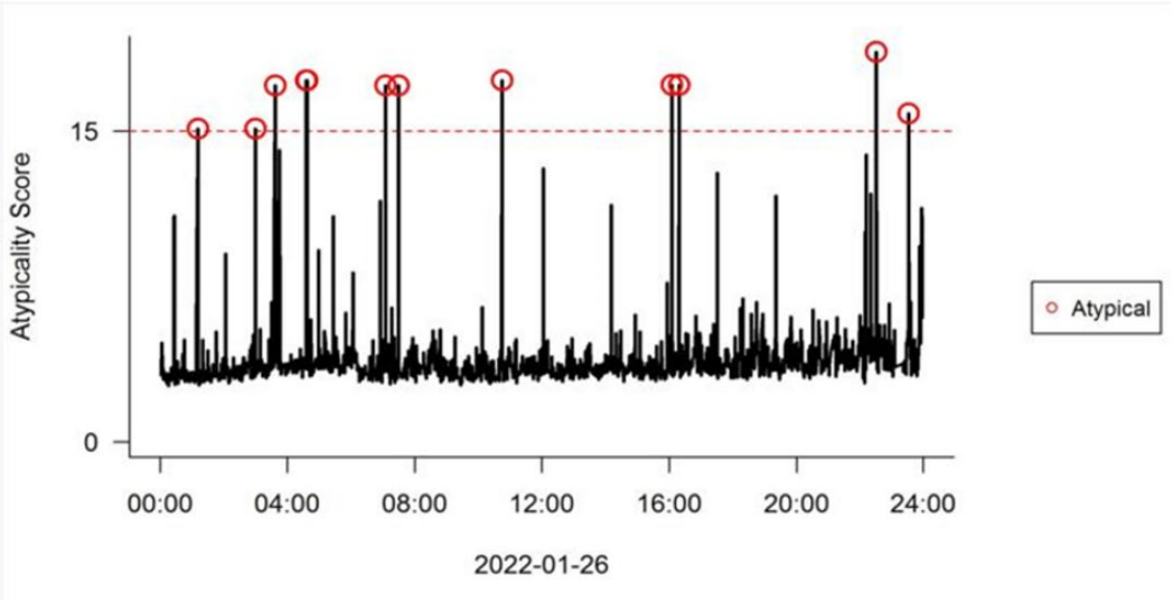

Time (EST)	Signal	Atypicality Score (Top 5)
01/26/2022 04:35	[redacted]	17
01/26/2022 10:45	[redacted]	17
01/26/2022 16:05	[redacted]	17
01/26/2022 16:19	[redacted]	17
01/26/2022 22:30	[redacted]	19

Figure 15. Atypicality Report

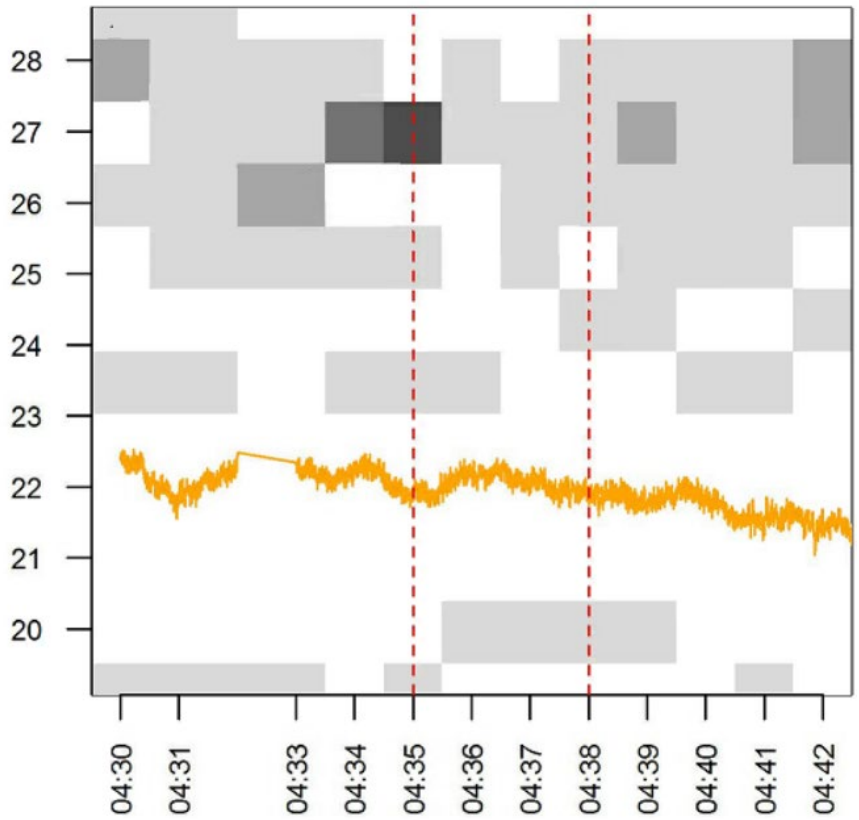

Figure 16. Atypicality Report—Detail

3.3 Data Quality Management

The applications in the ESAMS were supported by two groups of online data quality management processes that run continuously. The first group of processes, which is represented by items 1 through 5 in Figure 17, consists of standard quality checks consistent with those used to support commercially available software tools that utilize synchrophasor data. The second group (items 6 and 7 in Figure 15) consists of specialized data quality checks or data-handling procedures developed specifically to support the applications demonstrated in the ESAMS. The following two subsections describe how the ESAMS reported on both groups of data quality checks. Subsection 3.3.3 describes an offline review that led to a series of one-time manual adjustments needed to provide consistency among the various phase-naming conventions used by the Eastern Interconnection partners.

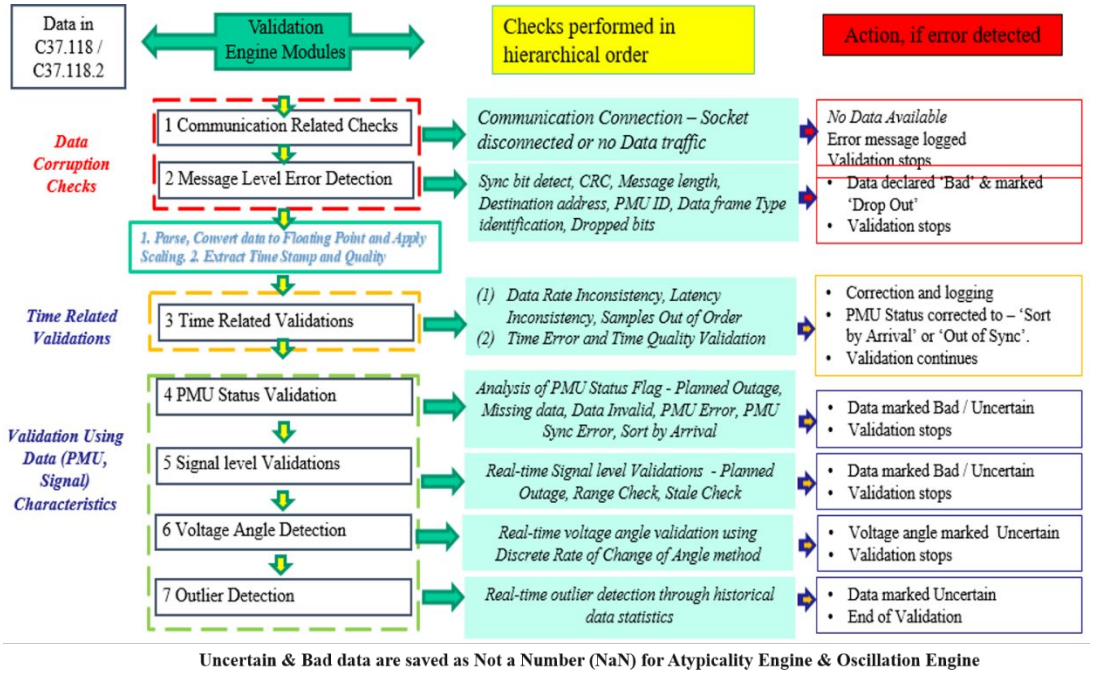

Figure 17. Online ESAMS Data Validation Processes

3.3.1 Standard Online Data-Checking Procedures

The ESAMS demonstration applied five closely related data-checking procedures, which are commercially available in the RTDMS, to all synchrophasor data before they were made available to any ESAMS application. Because the functions are common to many software tools that rely on synchrophasor data, they are listed here simply for completeness.[26]

- Communication-related checks, which confirmed that data were flowing into the RTDMS and no errors in data transfer were detected by the communication interfaces.

[26] Electric Power Group, RTDMS Server User Guide. August 2020.

- Message-level error detection, which confirmed that the message conformed with standard format and that the data the RTDMS was receiving contained no errors.
- Time-related validation checks, which confirmed that the data were being received in the correct order, as indicated by their individual time stamps.
- PMU status validation, which confirmed that the status flag sent with each measurement affirmed that the measurement was valid and synchronized.
- Signal-level validation, which confirmed that measurements fell within an expected range of feasible values.

3.3.2 Data Quality Procedures Developed for the ESAMS Project

The applications demonstrated in the ESAMS required the project team to develop two specialized procedures for managing online data quality (items 6 and 7 in Figure 17).

3.3.2.1 Validation of Raw Voltage Angle

Accurate measurement of voltage angle is critical for all ESAMS applications. Early testing confirmed the need to implement additional checks on voltage angle measurements to assure they were used consistently in the ESAMS applications.

After a review of the literature, the project team decided to implement the method developed by ISO New England, which relies on the discrete rate of change of angle.[27] The method compares the frequency measured and reported directly by all PMUs to the frequency calculated by examining the rate of change of the voltage angle that each PMU reported. If a given PMU's measurement of voltage angle was valid, the frequency calculated for that PMU should be nearly identical to those reported by all other PMUs. If the frequencies differed, the voltage angle measured by that PMU was flagged as suspect and not used in any application.

3.3.2.2 Detection of Outliers

Several ESAMS applications rely on the difference between phase angles measured by two separate PMUs. Although each measurement might appear valid because each is within a reasonable range of values, the difference between them would appear as an outlier if, in fact, one of the measurements was in error.

The method the project team developed for detecting outliers involved comparing the differences in phase angles to those recorded in the recent past. The method calculates the cumulative mean and standard deviation of differences in phase angles. If the difference between two measurements exceeds a user-specified number of standard deviations from the mean of combined measurements, then the angle difference is flagged as an outlier and not used in subsequent calculations.
For the ESAMS demonstration, the mean and standard deviation used to flag data were updated every

[27] Q. Zhang, X. Luo, E. Litvinov. "Automated PMU Data Quality Monitoring System," *2019 IEEE Power & Energy Society General Meeting*, August 4-8, 2019. Atlanta GA. DOI: 10.1109/PESGM40551.2019.8973633. [Last accessed 06/23/2022.]

second based on the rate at which the partners' synchrophasors provided data, which was 30 samples per second. That is, the mean and standard deviation calculated from the 30 samples received in one second were used to evaluate the 30 samples received in the next second. For the ESAMS demonstration, a sample was flagged as an outlier if it exceeded 5 standard deviations above or below that mean. Note: if a sample was flagged as an outlier, it was not used in calculating the mean and standard deviation used to evaluate the samples from the next second of data.

This method of detecting outliers worked well when there were few outliers (e.g., fewer than 5% of the samples), as shown in Figure 18. The method worked less well when there were many outliers, as shown in Figure 19.

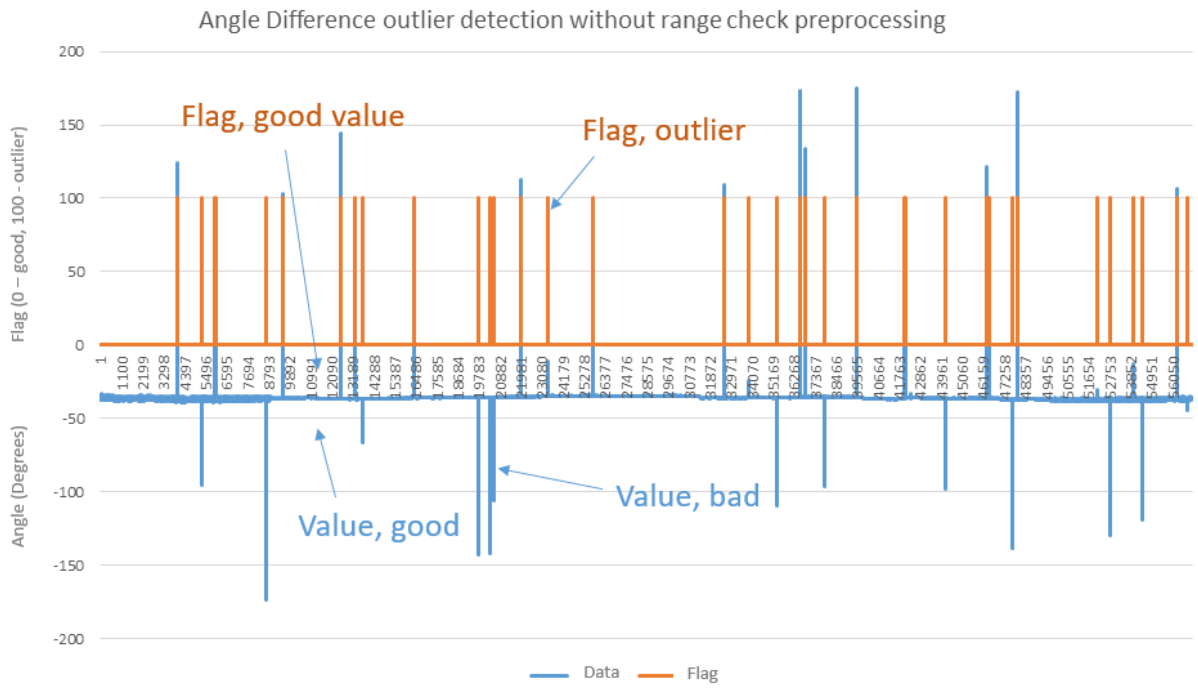

Figure 18. Outlier Detection for Sporadic Errors

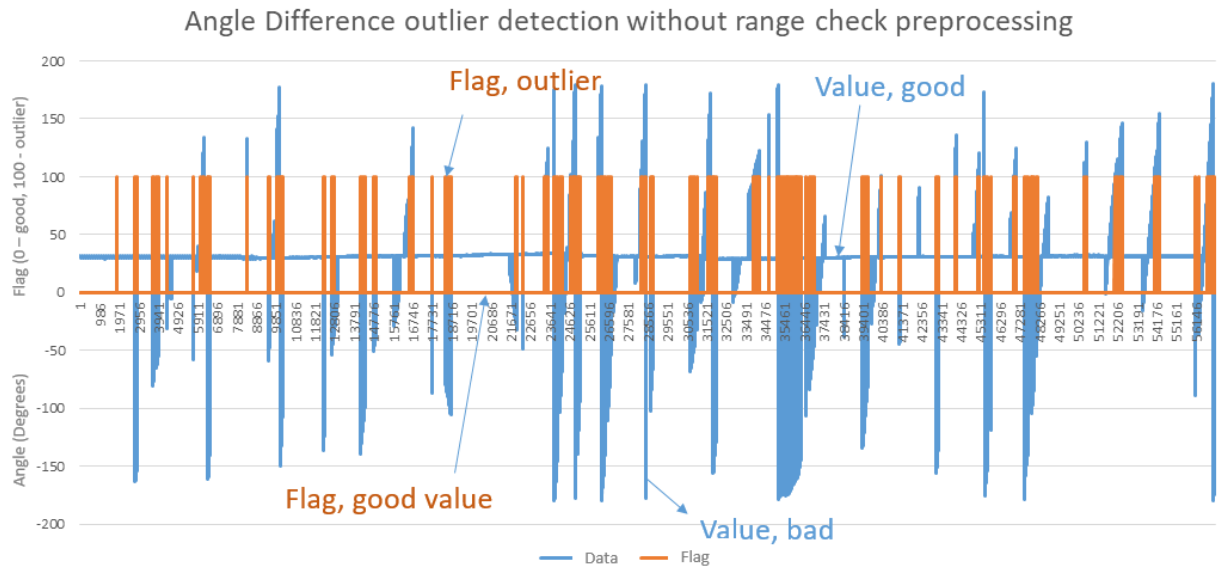

Figure 19. Outlier Detection for Many Errors

To address situations involving large numbers of outliers, the team implemented a range-checking function, shown in Figure 20. When the measurement of an angle pair exceeded stipulated high or low limits, the measurement was marked as uncertain. The uncertain measurements were not used in calculating cumulative mean and standard deviations for angle pairs. When the apparent out-of-range measurements were omitted, results of calculating the cumulative mean and standard deviation better reflected the true historical mean and standard deviation of angle pairs.

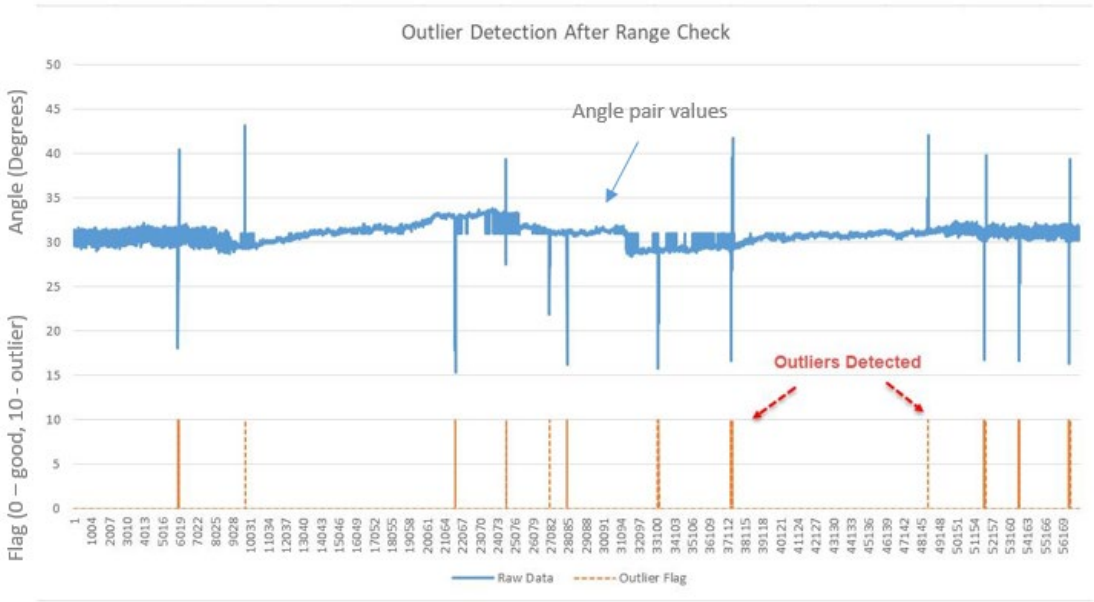

Figure 20. Outlier Detection after Range Check

3.3.3 Data Quality Reports

Each ESAMS daily report included two data quality reports at the PMU level. Each report summarized the data that were or were not used in the ESAMS based on PMU status flags. There were six types of status flags: Good Samples, Drop Error (for data dropout), Data Invalid, PMU Error, Synch Error, and Time Error.

Figure 21 presents an example of the first data quality report, called the data availability summary report. The report visually summarizes the parts of the day that data from each PMU fell into one of the six categories. In the example the identities of the PMU signals have been masked. The report shows that, on that day, the ESAMS was able to use about 55% of the data for the signal labeled PMU X, with 45% being unusable. More than 40% was unsuitable because of a drop error; less than 5% was unsuitable because the data were found to be invalid.

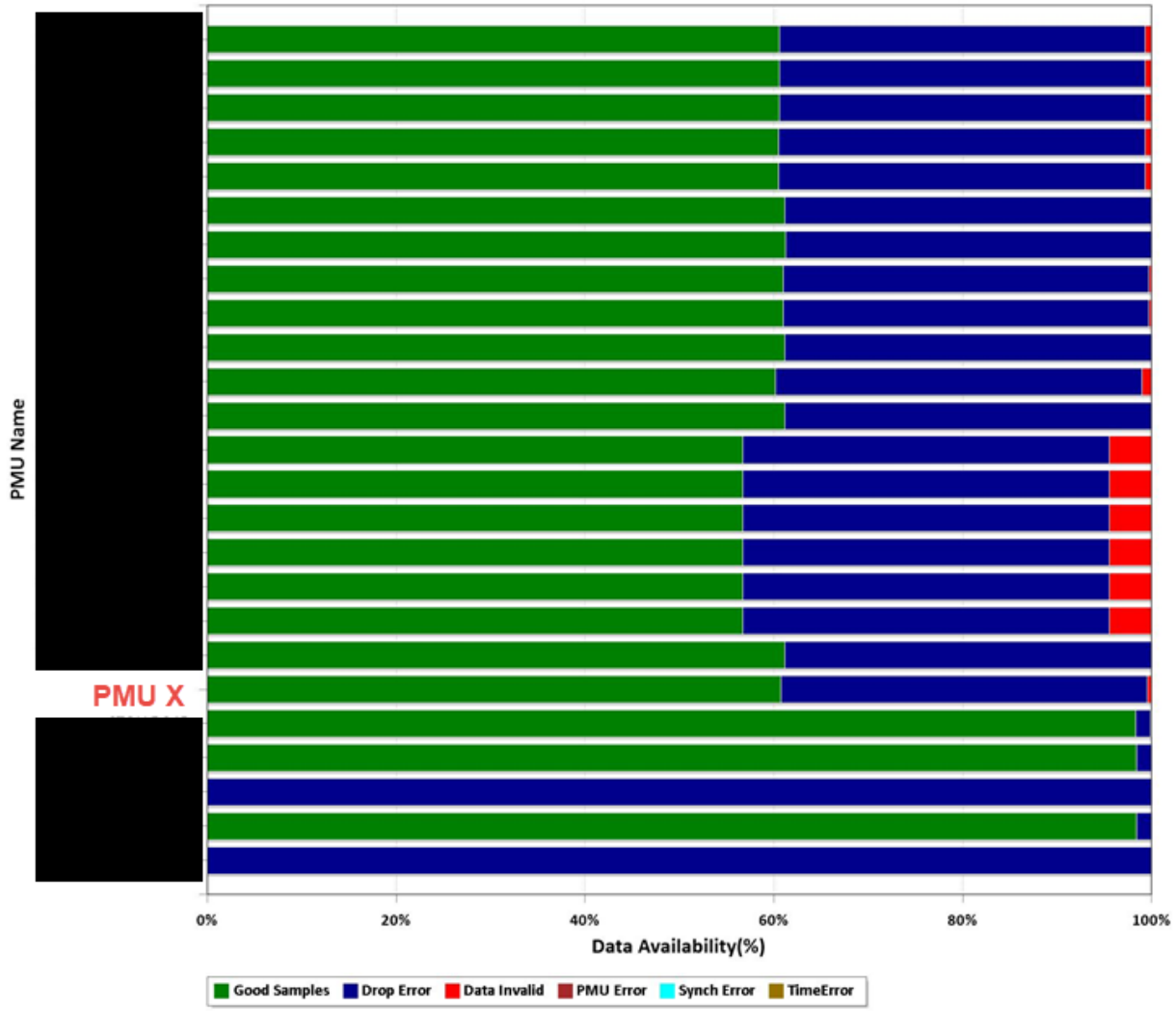

Figure 21. Summary Report on ESAMS Data Availability

Figure 22 shows an example of the second report, termed the data availability chronology report. The report visually summarizes the time of day when data fell into each category, formatting the information chronologically throughout the day. This report highlights only the data that the ESAMS could not use; good samples are indicated by the absence of color. This presentation format enables the viewer to identify data issues common to more than one PMU signal throughout the day.

In Figure 22, individual PMUs are identified by the numbers in the key. This example shows that on that day the data from all but three PMUs were unusable in the ESAMS because data were dropped, invalid, or both. The usable data from the other three PMUs were available throughout the day except for a drop error starting at 1 AM and lasting about 30 minutes. PMUs 9 through 12 and 14 through 16 show data drops at about this same time, suggesting a shared communication problem.

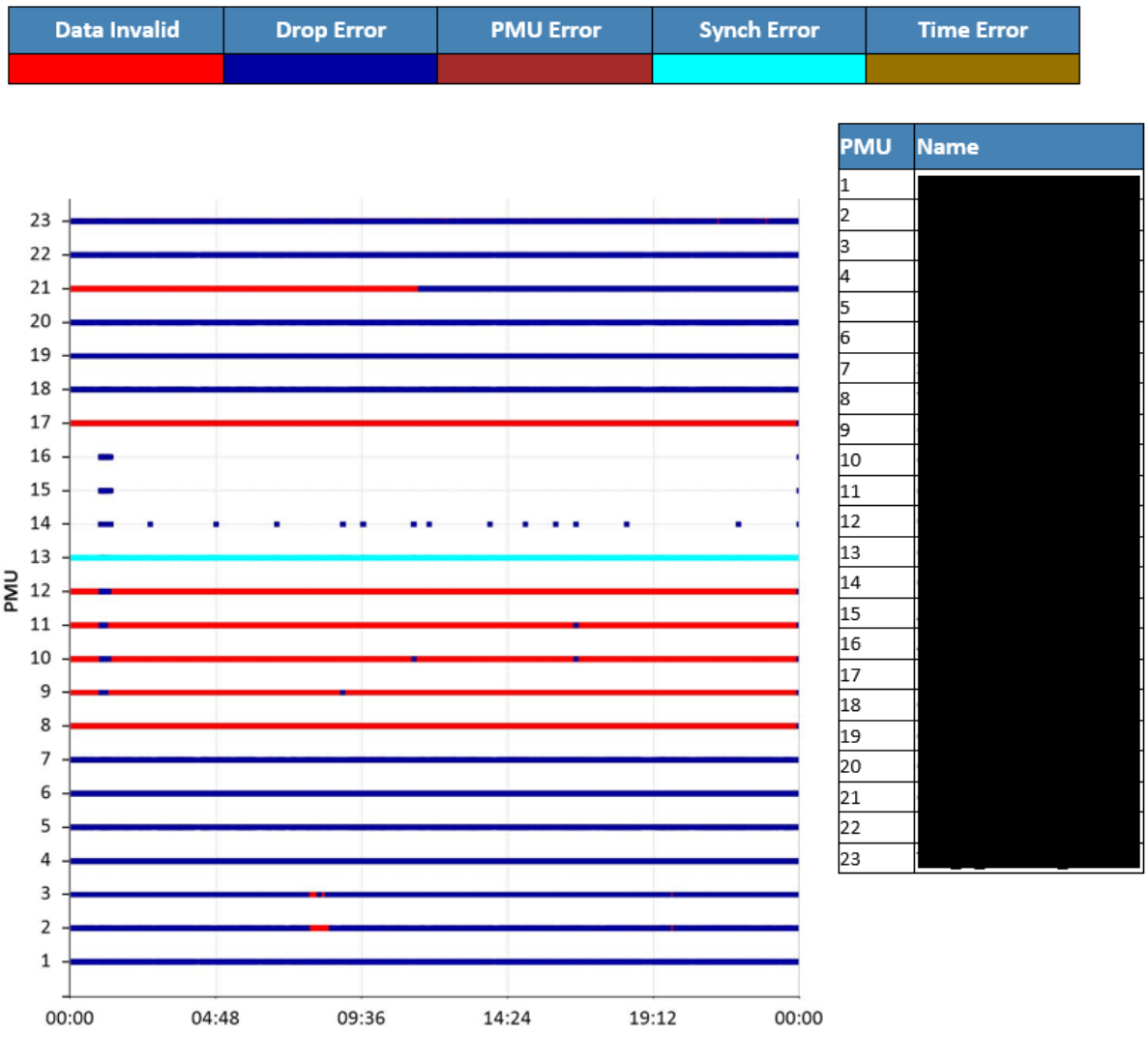

Figure 22. Chronology Report on ESAMS Data Availability

3.3.4 Offline Review of Data Consistency

In addition to the online procedures described above, the synchrophasor data that the Eastern Interconnection partners provided had to undergo an offline review in order to make sure the ESAMS could process and analyze the data consistently. The review was intended to identify the conventions each demonstration partner used to label each voltage phase. Each partner labeled the phases of the voltages that its synchrophasors measured using conventions that were internally consistent but that could (and did) differ from those their neighboring RCs used. In order to calculate the differences in phase-angle measurements received from different partners, the project team developed procedures for identifying the adjustments required to apply universal phase conventions throughout the interconnection.

The adjustments needed generally consisted of a fixed shift of 120 degrees. For example, if the phase angles from one partner's system (system 1) were based on phase A, while the phase angles from another partner's system (system 2) were based on phase B, applying a fixed 120-degree shift to the measurements from system 2 aligned them with those from system 1.

Additional differences in measurements called for other offsets to provide consistency among all systems in the Eastern Interconnection. One common offset involved accounting for the manner in which the power transducers (PTs) were connected. If voltage was measured from a PT connected line-to-line rather than line-to-neutral, an offset of 30 degrees was introduced to provide consistency.

The project team relied on information from PJM's SCADA-based state estimator (SE) to guide the review process and identify which adjustments had to be implemented. The procedure is outlined below.

1. Determine the bus that serves as the reference for all the angles produced by the SE.
2. Find a bus monitored by a PMU that is as physically close as possible to the SE reference bus. Assume that this bus is as electrically close as feasible to the SE reference bus. This bus is labeled PMUref.
3. If the SE also produces an estimate for the PMUref bus, use this estimate to apply an initial offset to the PMUref bus in order to align it exactly with the SE reference bus.
4. Obtain a SE snapshot from the EMS showing the angles estimated at each bus and the voltage at each bus.
5. Obtain a snapshot from all PMUs for the same time as the SE snapshot. Arrange the PMU data by bus name in a manner that facilitates comparison with the corresponding SE estimate for the same bus (e.g., on a spreadsheet).
6. Calculate the bus angle for each PMU by subtracting the angle of the PMUref bus from each measurement and then resolving the angle to within +/- 180 degrees.

7. Compare the angle of each PMU bus with that of the same bus in the SE set. The angles should be within 1 to 2 degrees. In comparisons done for the ESAMS, the measurements were almost all within 0.5 degrees.[28]
8. If, however, angle measurements differed by approximately +/- 120 degrees, implement the offset correction. All the measurements from a given Eastern Interconnection partner usually required the same offset during the ESAMS demonstration project.
9. Further investigate differences that were greater than 1 to 2 degrees but that did not match a 120-degree offset. Such differences might indicate incorrect wiring or equipment failure.

[28] This process , which involved manually comparing the names of/labels used to designate PMU signals with the names used in PJM's state estimator, was complicated and time-consuming. The names were rarely identical. Although many names could be matched, some proved impossible to match.

4. Findings from the ESAMS Demonstration

This section describes findings from the ESAMS demonstration that PJM hosted. The first subsection discusses findings from the applications related to oscillations. The second subsection describes findings from the applications related to wide-area phase angles. The third subsection presents findings from the applications used to manage data quality.

Each subsection begins by reviewing what the applications revealed during the demonstration. When perusing the findings, remember that the number of synchrophasors available to the applications expanded over time in response to requests from the demonstration partners. See Section 2.[29] Therefore, findings for some of the applications span the entire demonstration period from June 2021 through the end of March 2022, while findings for others incorporate fewer data.

Before discussing findings, the authors wish to clarify their use of the term "event." As a tool for providing wide-area situational awareness, the ESAMS was designed to detect the times when grid operating conditions might warrant examination. Accordingly, the term "events" describes the measurements collected. The authors seek to neither imply nor conclude that the events represented conditions that warranted increased operator scrutiny. A key element of the demonstration was the demonstration partners' after-the-fact reviews of and comments on events the ESAM detected.

4.1 Findings from Oscillation Applications

The ESAMS demonstrated two oscillation-related applications. The first was designed to detect and identify the RC source locations of forced oscillation events and, upon detection, to disseminate notifications and preliminary analyses in real time. Overall findings regarding forced oscillations will be discussed first, then findings on forced oscillations visible to multiple RCs. Subsection 4.1.1 also discusses the real-time notifications that were enabled during the last phase of the demonstration.

The second application, which utilized mode meters, was not designed to detect specific events. Its purpose was to continuously monitor and assess the ambient oscillatory behavior of the Eastern Interconnection.[30] This ongoing information was essential to providing context for and understanding of the forced oscillations detected in real time.

[29] When the first phase of the demonstration began in June 2021, the applications were run using synchrophasor data from the four ISO/RTOs that had participated in the Eastern Interconnection Baselining projects (ISO-NE, MISO, NYISO, and PJM). During the second phase, which began in September 2021, the coverage area for the oscillation detection and source location applications was expanded to include synchrophasors in Southern, SPP, and TVA. For the third phase, which began in January 2022, the project team added real-time notifications of forced oscillations.

[30] A third ESAMS application related to oscillations—ringdown analysis—is an offline method for further corroborating the estimated mode frequencies and damping ratios relayed by the mode meters. Ringdown analysis relies on information collected immediately following discrete grid events, such as the unplanned loss of a generator. Although data from ringdown events were collected, they were not analyzed for the demonstration.

4.1.1 Detection and Source Identification of Forced Oscillations

The discussions that follow are based on ESAMS observations made between October 1, 2021, and March 31, 2022, the period during which the applications incorporated synchrophasor data from all seven demonstration partners.[31]

During this period, the ESAMS detected 65 forced oscillation events having peak-to-peak amplitudes greater than 2 MW or MVAr.[32] See Table 2. To date, those data represent the most comprehensive body of information regarding forced oscillations in the Eastern Interconnection. First, this subsection describes the primary characteristics of the events the ESAMS detected, with the goal of laying the groundwork for future studies. The focus then turns to those events that are of greatest interest for supporting interconnection reliability–forced oscillations that produce effects that can be observed at multiple locations throughout the Eastern Interconnection, including locations distant from the source.

Each month the ESAMS detected, on average, between 10 and 15 forced oscillation events having peak-to-peak amplitudes greater than 2 MW or MVAr. Most of the forced oscillations recorded during the demonstration were small scale. Peak-to-peak amplitudes of only 5 of the 65 events exceeded 10 MW or MVAr.[33]

From the standpoint of supporting interconnection-wide reliability, the most important forced oscillations are those that create effects visible at locations distant from the source. Those events are termed wide area to distinguish them from events seen by only one RC, which are termed local. If a wide-area event is of sufficient magnitude, it may call for RCs throughout the Eastern Interconnection to communicate with one another.[34]

About two-thirds of the forced oscillations the ESAMS captured were classified as wide-area events. That is, events that were observable in more than one RC region. This finding is not surprising given that the ESAMS was designed specifically to detect events that would be seen throughout broad regions of the interconnection.[35] The highest observed peak-to-peak amplitude of most oscillations was less than 10 MW or 10 MVAr. Hence, most events registered below the threshold established for sending near-

[31] As discussed in Section 2, synchrophasors from Southern, SPP, and TVA were enabled in the ESAMS starting October 1, 2021.
[32] Most of the forced oscillations the ESAMS detected were detected using the MW signal. This fact reflects the design of the ESAMS, which emphasizes forced oscillations that can be observed throughout wide areas of the Eastern Interconnection. MVAr signals, by their nature, tend to remain close to their source.
[33] Note that the ESAMS detected forced oscillations by monitoring sparsely distributed synchrophasor measurements. Measurements taken at the source of a forced oscillation may have had amplitudes higher than 10 MW or MVAr.
[34] NERC notes, "This coordination is important even when the source is readily apparent and the oscillation is not large enough to threaten reliability within the RC/TOP footprint from which it is originating." For further discussion, see Section 4.2 in Synchronized Measurement Working Group. "Recommended Oscillation Analysis for Monitoring and Mitigation Reference Document," NERC. November 2021. https://www.nerc.com/comm/RSTC_Reliability_Guidelines/Oscillation_Analysis_for_Monitoring_And_Mitigation_TRD.pdf. [Last accessed 06/24/2022.]
[35] The leadership of the NERC Synchronized Measurement Working Group contacted the project team to learn whether the ESAMS had recorded a forced oscillation within the territory of one RC that was not seen by adjacent RCs. After reviewing the records, the project team concluded that the ESAMS had not detected the event (consistent with its focus on detecting only those events that can be observed by multiple RCs).

time notifications. Still, the analysis of those events, documented in daily reports, confirmed that they could be observed in regions both adjacent to and more distant from the area identified as containing the source of the forced oscillation.

Table 2. Forced Oscillations Recorded from October 2021 to March 2022

Forced Oscillation Frequency (Hz)	Number of Events (> 2 MW/MVAr)	Largest Amplitude (Peak-to-Peak)	Observability – Number of RC regions (> 2 MW/MVAr)
0.1	1	2.6 MVAr	1 RC
0.17	4	25 MW	4 RCs (all 4 events)
0.2	2	8 MW	2 RCs (both events)
0.24	1	7 MW	5 RCs
0.31	2	6 MW	4 RCs (both events)
0.34	1	5 MW	2 RCs
0.38	1	5 MW	5 RCs
0.39	1	5 MW	1 RC
0.44	1	4 MW	1 RC
0.45	1	10 MVAr	1 RC
0.55	2	3 MW	1 RC
0.57	1	9 MW	4 RCs
0.64	1	17 MW	3 RCs
0.72	27	10 MW	> 1 RCs (all 27 events)
0.83	4	7 MW	2 RCs (3 of 4 events)
1.13, 1.17, 1.18	3	9 MW	1 RC
1.43	9	3 MW	1 RC
1.44	1	8 MW	1 RC
1.67	1	2 MW	1 RC
1.72	1	4 MW	1 RC
	Total = 65		**Total (>1) = 43**

Table 3 lists the maximum amplitudes of a subset of forced oscillations that were reviewed by the project team in detail. The results show that it is relatively common for oscillations at low frequencies to become widespread with amplitudes greater than 2 MW in multiple regions. This result conforms with expectations because the system's natural modes of oscillation are typically found at these low frequencies.

Table 3. Maximum Amplitudes by RC Regions for Forced

		Max Amplitude (MW)						
Date	**Frequency (Hz)**	**ISNE**	**MISO**	**NYIS**	**PJM**	**SOCO**	**SPP**	**TVA**
12/8/21	0.17	16.7	NA**	NA	11.9	24.6*	5	NA
2/11/22	0.24	7.1	NA	NA	3.7	4.8	3.4	2.8
2/17/22	0.38	4.7	NA	NA	2.3	2.3	3.4	2.2
2/23/22	0.33	5.1	NA	1.8	2.4	0.8	1.9	0.3
3/1/22	0.64	3.4	NA	NA	1.6	16.9	12.3	0.9
3/21/22	0.72	2.8	5.1	0.1	10.1	2.7	2.1	1.9

*Further investigation revealed oscillations up to 85 MW in SOCO.

**NA indicates that measurements were not available for the region during the event.

The forced oscillations that are of greatest concern for power system reliability are those that occur at frequencies close to one of the two dominant natural oscillatory modes of the Eastern Interconnection. A forced oscillation at one of those frequencies, when its source is at one end of the mode-shape or when system damping is low, may resonate with and thereby become amplified by the natural mode as the oscillation propagates through the interconnection. As discussed in subsection 4.1.2, the frequencies of the two dominant natural modes range from 0.17 to 0.21 Hz for the NE-S mode and generally from 0.20 to 0.24 Hz for the NE-MW mode. During the four months of the demonstration - when synchrophasors from all seven demonstration partners were incorporated - the ESAMS detected seven forced oscillation events within the ranges of the two modes.

The most significant of the seven forced oscillations occurred on December 8, 2021. On that day, the ESAMS detected four separate forced oscillations at the same frequency within five hours. One, which is the focus of this discussion, was the largest forced oscillation detected during the demonstration.[36] The peak-to-peak amplitude the ESAMS reported was comparatively low at the measurement locations closest to the source (25 MW). However, the peak-to-peak amplitude was nearly as high at the opposite end of the interconnection (17 MW). In fact, the event was observable throughout the Eastern Interconnection.

The ESAMS daily report for all four events initially identified SOCO as the likely source region. However, the ESAMS also reported that confidence in that assessment was low. By reviewing additional synchrophasor measurements not available to the ESAMS, Southern staff concluded that the source was located in their neighbor's territory. This conclusion is consistent with the low confidence the ESAMS had assigned to its identification of the source region and highlighted the importance of having good observability of the tie-lines between regions.[37]

One of Southern's local synchrophasors that was not available in the ESAMS further showed that the magnitude of the oscillation was more than three times larger than what the ESAMS had observed

[36] Although this magnitude would have called for a real-time notification, it took place in December 2021, before real-time notifications were enabled (in January 2022).

[37] The project team found that the ESAMS confidence scoring routinely assigned low confidence to its identification of RC source locations. Appendix A describes the project team's initial ideas for improving the usefulness of the confidence scoring logic and criteria.

(almost 85 MW peak-to-peak). Again, this finding is consistent with the fact that measurements for the ESAMS are collected from locations that are sparsely located across the interconnection. Measurements made closer to a source can be expected to be greater.

Recognizing that the frequency of the December 8, 2021, event approximated that of the NE-S mode, the project team compared the forced oscillation's shape (its amplitude and relative phasing at various points in the system) with the NE-S mode's shape estimated in November 2021. As displayed on Figure 23, the shapes are almost identical in terms of the coherent groups of signals that oscillate against one another. This analysis supports the conclusion that the effects of this forced oscillation were transmitted across the interconnection by exciting the NE-S mode.

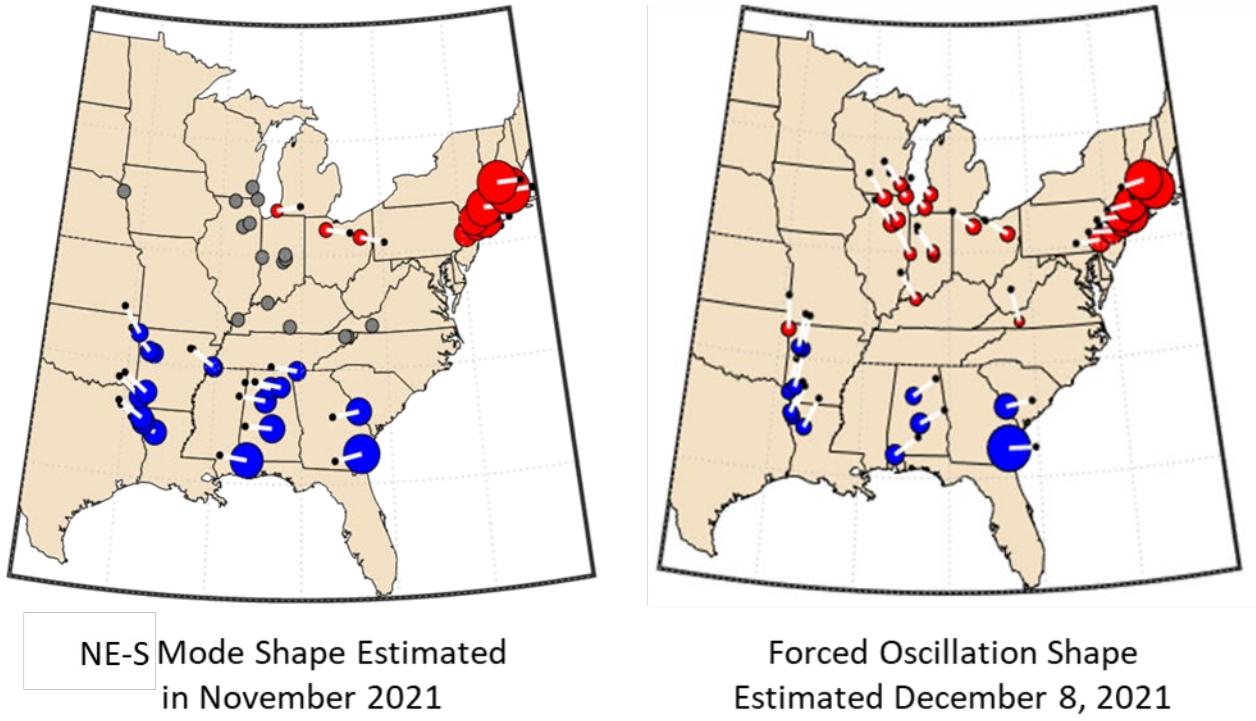

Figure 23. Shape of NE-S mode as of November 2021 and shape of forced oscillation December 8, 2021

The project team's final observation on wide-area forced oscillations is that some occur with surprising regularity. For example, the ESAMS detected 27 forced oscillations at a single frequency (0.72 Hz) in regions both adjacent to and distant from the source. Although the highest recorded amplitudes generally were less than 10 MW/MVAr, the ESAMS recorded many instances when amplitudes exceeded 10 MW/MVAr. When the project team followed up with staff in the region identified as containing the source, they were informed that the forced oscillation was caused by a load (not a generator) exhibiting unusual behavior that had been recognized for a long time.

Real-time notification of the detection and RC source location of forced oscillations was enabled in January 2022 and functioned until the end of the demonstration. After discussions with the demonstration partners, the project team set the threshold for oscillation amplitude that would trigger a notification considerably higher than that used to identify events for the daily report. Unlike the daily report, which included all forced oscillations greater than 2 MW/MVAr, real-time notifications were sent only for forced oscillations that exceeded 10 MW/MVAr. In addition, the ESAMS was configured to confirm the oscillation by observing it for one minute before sending this notification.

A real-time notification included preliminary supporting pages that described the forced oscillation. The same information was made part of the following day's daily report, which might contain additional/refined information from further observation of the oscillation. The notifications were sent to staff who had been pre-selected with each demonstration partner.

The ESAMS detected two qualifying events during the final two months of the demonstration. All the demonstration partners received the two notifications.

4.1.2 Baselining Natural Oscillatory Modes

Mode meters monitored the natural oscillatory modes of the Eastern Interconnection continuously during the final four months of the demonstration. The first mode meter monitored the NE-MW mode; the second monitored the NE-S mode. Both meters yielded important new and reinforcing insights into the oscillatory behavior of the Eastern Interconnection as a whole. Those insights add to knowledge gained through previous studies and establish a new baseline for future studies to build on.

To clarify the ESAMS's contribution, the NERC's previous study of oscillatory modes in the Eastern Interconnection was based on recordings of seven disturbances.[38] The mode meters associated with the ESAMS were installed after several months of continuous monitoring identified which locations provided the greatest visibility for each mode. The meter settings were tuned to focus narrowly on each mode. Once set up, each meter produced approximately 800,000 estimates of its mode's damping ratio and frequency.[39]

As discussed in Section 3.1.1, the damping ratio is the most important indicator of the potential consequences of oscillatory modes on the reliability of power systems. Poorly damped modes greatly increase the chances that a disturbance could trigger an undamped oscillation and cause a cascading blackout. Figure 24 shows the distributions of the estimated damping ratios for the two modes monitored in the ESAMS. The distributions confirm that both modes were well damped, meaning that their ratios were rarely less than 10% and generally more than 15%.

[38] NERC. Interconnection Oscillation Analysis, Reliability Assessment. July 2019. https://www.nerc.com/comm/PC/SMSResourcesDocuments/Interconnection_Oscillation_Analysis.pdf [Last accessed 06/24/2022.]

[39] J. Follum, N. Nayak, J. Eto. "Online Tracking of Two Dominant Inter-Area Modes of Oscillation in the Eastern Interconnection," *Hawaii International Conference on System Sciences (HICSS)*. 2023.

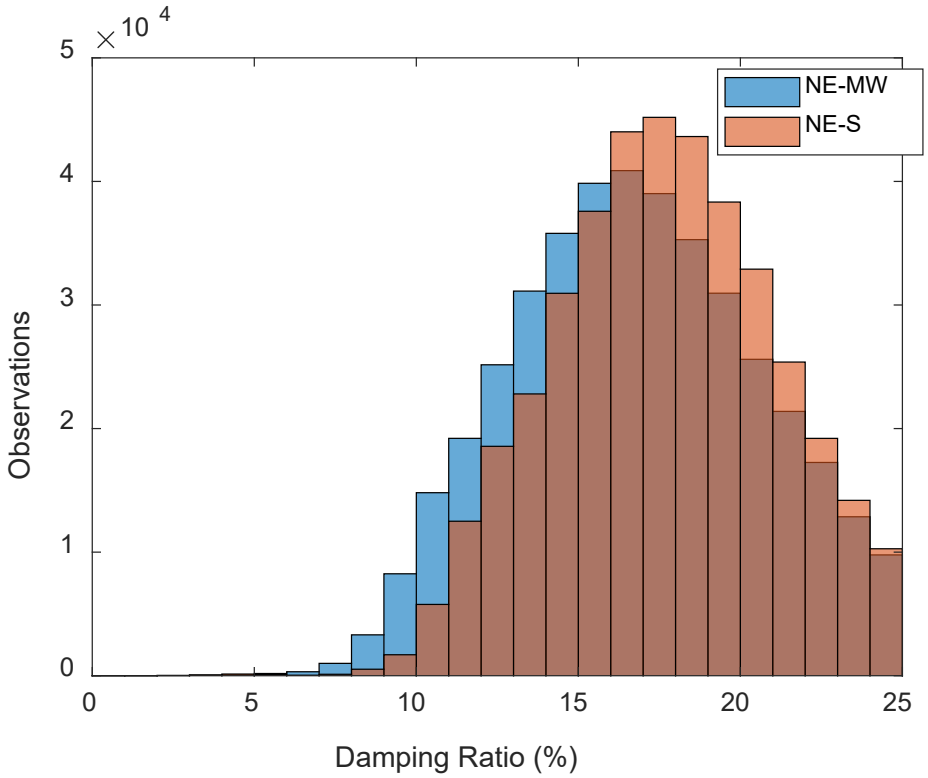

Figure 24. Damping Ratios for NE-MW and NE-S Modes

Figure 25 shows the means of the values estimated for the frequencies and damping ratios of the two modes during one week. The ESAMS's continuous monitoring documented an expected, although previously unobserved, aspect of the natural oscillatory behavior of the Eastern Interconnection: The frequency and damping ratios of both modes followed a consistent diurnal cycle. Mode frequencies were highest during the night and lowest during the day. Damping ratios were highest during the day and lowest during the night.

Interestingly, this is the opposite of the pattern observed in the Western Interconnection, where heavy power flow during the day leads to lower damping ratios. Still, it seems logical that system damping might be lowest during the middle of the night, when fewer generators are online (and hence fewer are available to contribute to system damping). Similarly, it is reasonable that frequency would be higher at night given the system's lower inertia when fewer generators are online.

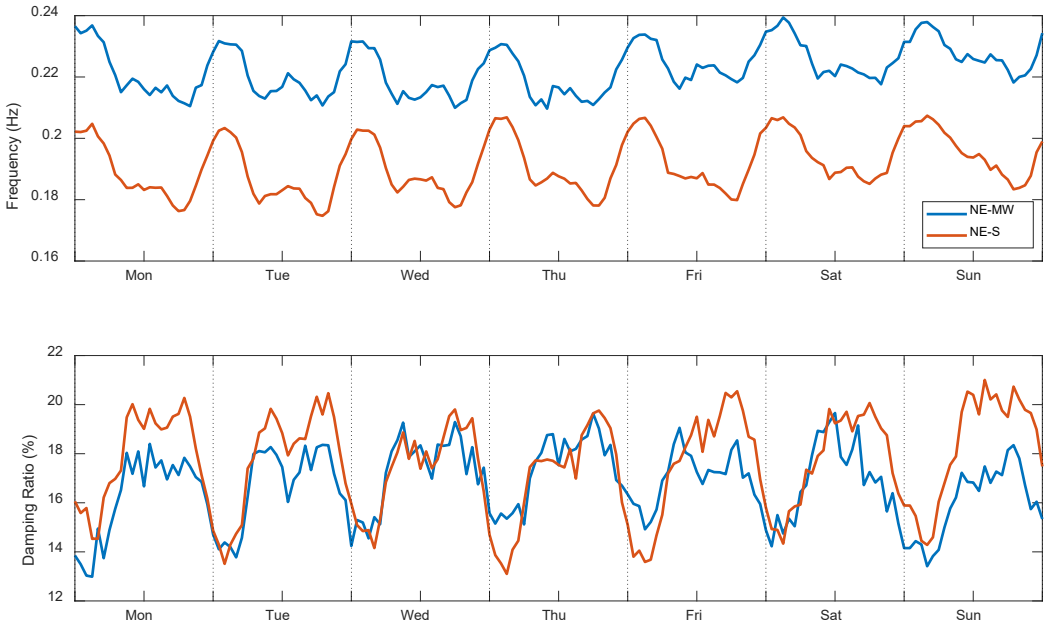

Figure 25. Frequencies and Damping Ratios of NE-MW and NE-S Modes during One Week

Figure 26 shows that the frequency of the NE-S mode generally ranged within a bandwidth between 0.17 and 0.21 Hz. The frequency of the NE-MW mode generally ranged between 0.20 and 0.24 Hz. At some times, the modes were observed having the same frequency, about 0.20/0.21 Hz.

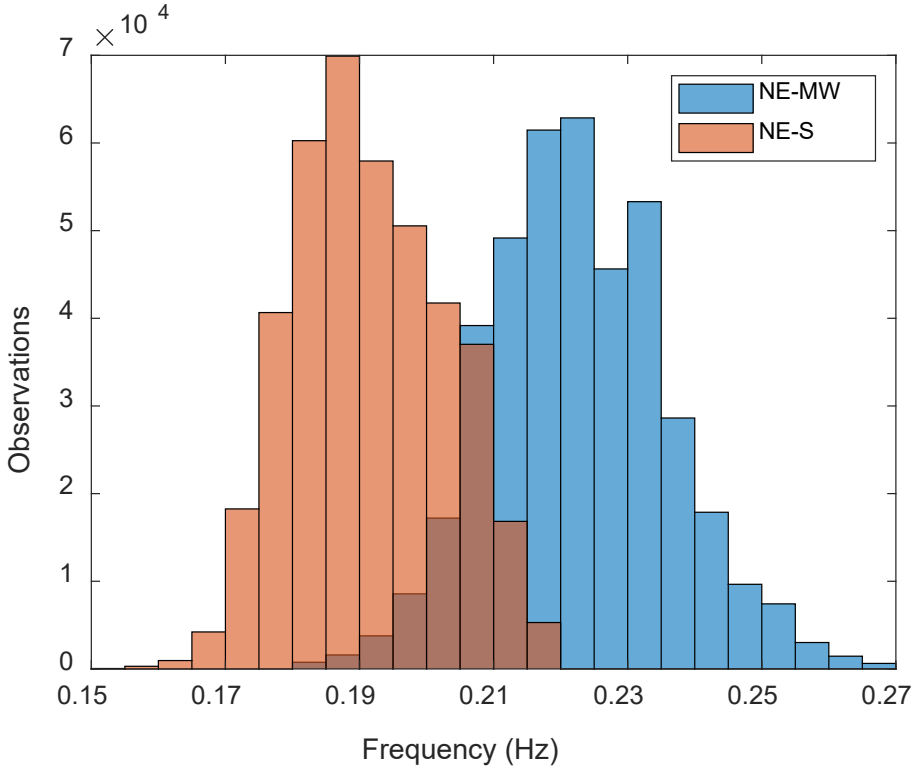

Figure 26. Frequencies of NE-MW and NE-S Modes

Figure 27 shows that the overlaps in modal frequencies can occur at the same time, which begs the question of whether the estimation algorithms can differentiate between the two modes. The answer lies with the previous analysis of each mode's observability in voltage angle pairs, to which the natural oscillation baselining application contributed. Generally speaking, synchrophasor pairs that span the two "ends" of each mode will tend to provide the best observability of the shape of each mode. By tracking each synchrophasor pair separately, each mode can be observed and its properties measured continuously and separately from the other even though the estimated frequencies may at times be identical.

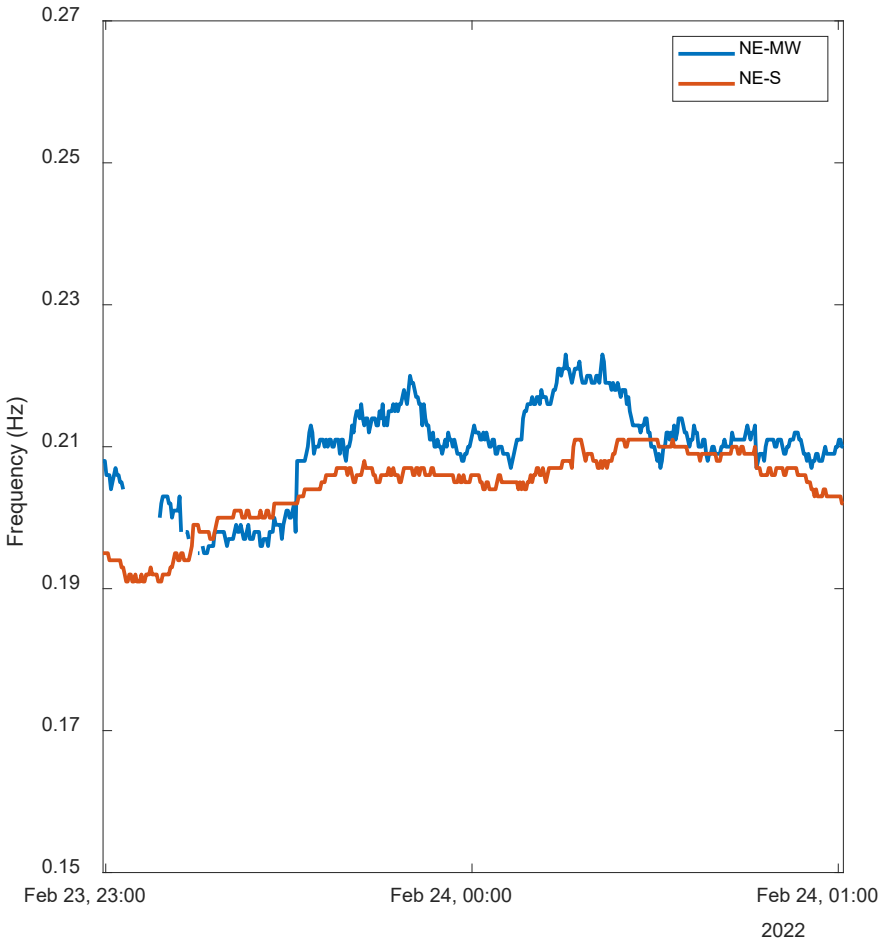

Figure 27. Estimates of Mode Frequencies for February 24, 2022

As well as continually monitoring each mode's frequency and damping ratio, the ESAMS was able to collect wide-area measurements to support offline analysis of mode shapes. The information the ESAMS collected for the NE-MW mode produced estimates of its shape that confirmed earlier

estimates.[40] The mode shapes estimated using the information the ESAMS collected for the NE-S mode, however, differed significantly from earlier characterizations of this mode's shape. Additional research is required to understand the basis for and significance of those differences.[41]

4.2 Findings from Wide-Area Phase-Angle Applications

The ESAMS demonstrated three wide-area phase-angle applications, all of which received data from 19 wide-area phase-angle pairs from 23 synchrophasors spread throughout ISO-NE, MISO, NYISO, and PJM. The applications were designed to detect: (1) rapid changes in phase angles for multiple phase-angle pairs; (2) large phase angles that persisted for many hours; and (3) unusual or atypical combinations of phase-angle measurements compared to all the measurements taken at the same time.

4.2.1 Rapid, Large Changes in Multiple Phase-Angle Pairs

This ESAMS application is triggered by rapid changes in phase angles that are significantly larger than others seen on a given day and that are detected simultaneously by more than one phase-angle pair. For the demonstration, the application was set to trigger based on rapid, large changes that were detected simultaneously by three or more pairs of phase angles. The application was designed and its settings established to capture sudden changes in power flows that affected a wide area of the Eastern Interconnection (i.e., beyond what operators could observe within their own regions using conventional monitoring systems).

Figure 28 summarizes the events detected during the demonstration.[42] The date within the month when an event was detected is indicated along the X-axis. The number of separate events detected on a given day is indicated on the Y-axis. Each event displays a number that indicates the number of angle pairs that contributed to the event's identification. Deeper colors highlight events that were identified by many angle pairs. On July 21, 2021, for example, the application detected a rapid change in phase angles that was seen simultaneously by 14 angle pairs.

The project team consulted the demonstration partners whose synchrophasors were involved in some of the larger events during which many angle pairs demonstrated rapid, large changes. Table 4 summarizes findings for four such events involving at least eight angle pairs each. The partners reported that all four events could be traced to routine actions that had been recorded in their operating logs.

The follow-up with partners confirmed that local events, such as the four studied, can be observed outside the boundaries of the region within which they originated. Because they affect power flows beyond the regional boundaries, wide-area phase angles can capture the aggregate effect of changes in

[40] NERC. Interconnection Oscillation Analysis, Reliability Assessment. July 2019. https://www.nerc.com/comm/PC/SMSResourcesDocuments/Interconnection_Oscillation_Analysis.pdf [Last accessed 06/24/2022.]

[41] J. Follum, N. Nayak, J. Eto. "Online Tracking of Two Dominant Inter-Area Modes of Oscillation in the Eastern Interconnection," *Hawaii International Conference on System Sciences (HICSS).* 2023.

[42] The results shown for June 2021 are based only on events detected on or after June 24. Before that time the detection threshold was set so low that many qualifying events were detected each day. On June 24 the threshold was raised to reduce that number.

power flows. It is also clear that, currently, interpretation of the operational significance or reliability implications of sudden large changes in power flows must rely on supplemental information available to local grid operators.

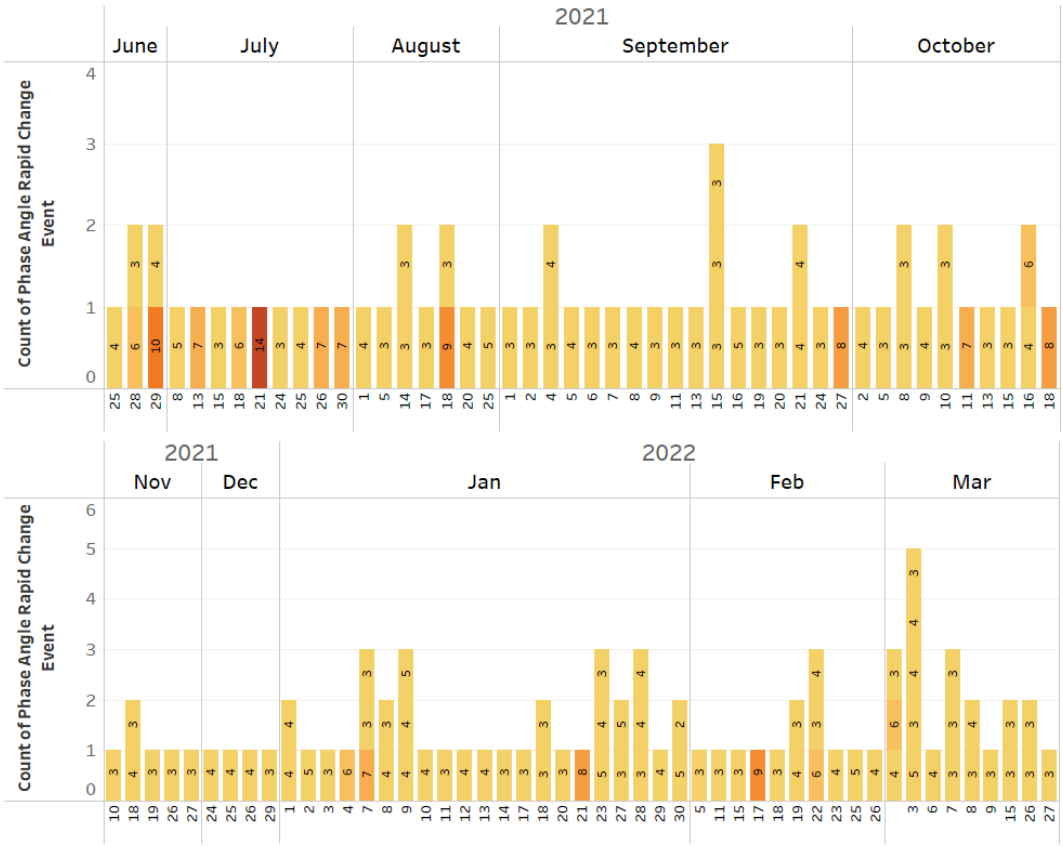

Figure 28. Rapid Changes in Wide-Area Phase Angles

Table 4. Summary of Review of Four Wide-Area Phase-Angle Events

Index	Event Detection	Number of Participating	Initiated By	Event Description
1	6/29/2021 3:10:00 PM	10	[redacted] BAN	Large change in clockwise circulation;
2	7/21/2021 6:26:00 PM	14	[redacted] Circuit Breaker I/S	[redacted] RNS5 I/S;
3	8/18/2021 11:36:00 AM	9	[redacted] PAR Moves	PAR: L33-L34 [redacted] [redacted] Details: Tapping 125 south to 0.;
4	10/18/2021 10:30:00 AM	8	[redacted] Simultaneous Activation of Reserve	1200MW's at [redacted]

4.2.2 Large, Persistent Phase Angles

This ESAMS application is triggered by observations of phase angles having hourly averages that persist for 5 or more hours at values that are significantly different from hourly averages recorded during the previous 10 days. The application was designed and its settings established to identify unusual (in the sense of not having been observed recently), persistent changes in power flows that might warrant further investigation. The application was focused on those persistent changes that could be seen by multiple phase-angle pairs because, as with the previous application, multiple pairs indicate persisting changes in power flows that affect a wide area of the Eastern Interconnection (i.e., beyond what operators can observe from within their own region using conventional monitoring systems).

Figure 29 summarizes the events this application captured. The date on which a persistent event was identified is displayed on the X-axis. The number of events detected on a given day is indicated on the Y-axis. On November 26, 2021, for example, the application detected events from four angle pairs. The various colors indicate which angle pair was involved. The figure indicates, for example, that events detected by the pink angle pair were observed on multiple days in June and September and once in both October and November.

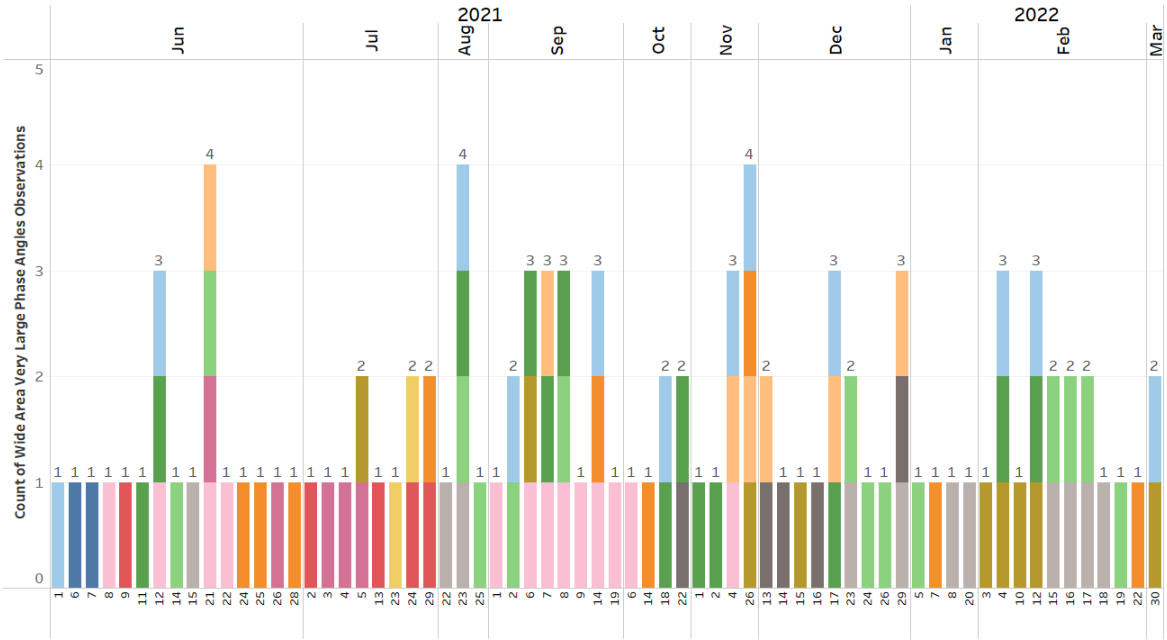

Figure 29. Large, Persistent Phase Angles

Figure 30 shows in blue the measurements collected on November 26, 2021, from four angle pairs. The ranges in angles, which were established from previous measurements, are shown in red. All four angle pairs persisted outside those ranges during the same hours of the day.

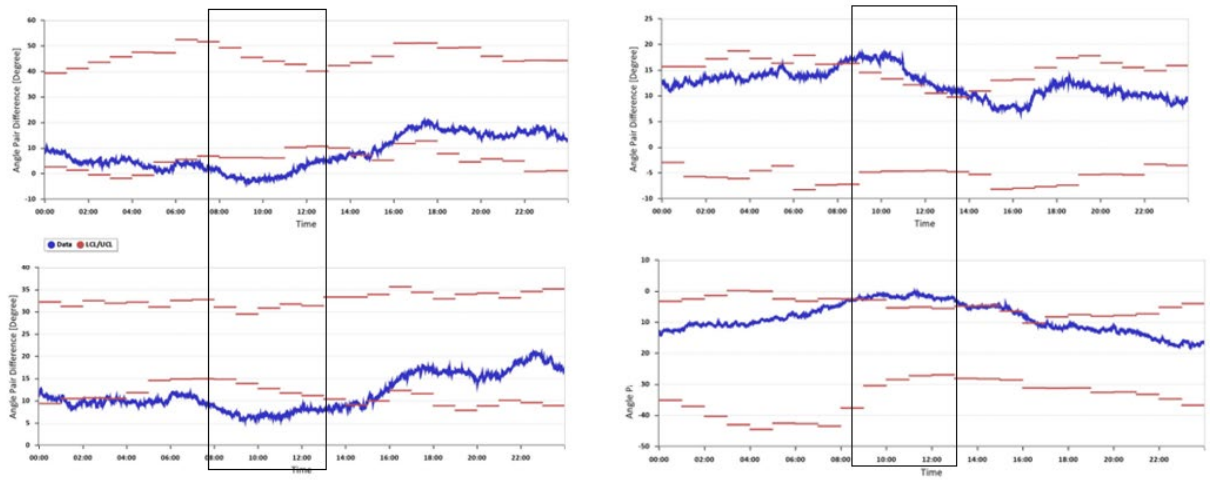

Figure 30. Four Angle Pairs Showing Large, Persistent Values—November 26, 2021

The project team asked those demonstration partners whose signals contributed to the measurements to review their operating logs for the identified hours on the affected day. The feedback received was that no unusual or noteworthy operating circumstances occurred that day. In other words, although the application correctly identified a period when multiple phase-angle pairs persisted at values that differed statistically from values collected in the recent past, the baseline established and the thresholds used to trigger the application were overly sensitive. The settings led to identifying "false positives." Going forward, it may be necessary to establish the hourly baselines based on a period longer than the previous 10 operating days in order to identify appropriate baselines and thresholds.

The information our demonstration partners reported highlights that this and the previous application are in the early stages of development. Currently, supplemental information is required to interpret and assess the significance of phase-angle information that is compared only to recent operating conditions. In this instance, final conclusions required that grid operators review results.

When discussing results from the phase-angle applications, one demonstration partner made an even finer point: Although phase angles are measures, crudely speaking, of system stress, they alone cannot characterize the reliability implications of stress—instead, they must be evaluated within a framework that establishes when stress is acceptable and when it is not. Historical records alone cannot establish that framework unless truly stressed conditions are found within those records. When considering the reliability of the interconnection, it is fortunate that the historical records rarely display such truly stressed conditions. The lack of historical records of true stress throughout the demonstration period proved unfortunate for our applications, however.

Barring such historical records, a model-based framework may be the preferred alternative for evaluating large, persistent phase angles. In other words, applying contingency analysis to a multi-region area could establish meaningful thresholds against which to assess phase-angle information.

Finally, in reviewing the events the application identified, the project team identified three unexpected and initially concerning issues. First, in some locations the phase-angle differences within a relatively short distance were much larger than expected. The phase-angle difference between two directly connected points depends on the power flow and the impedance of lines between the points. In this case, either the impedance or the loading had to be higher than reasonably expected for the given lines. Second, the observed phase angles occasionally exceeded a ± 180° range, which was unexpected and not accounted for by the software and displays. Third, on a few occasions a monitored phase angle made a large change very rapidly, on the order of 90° in a few hours. This occurrence indicated a very large change in power flow or a change in line configuration, situations that had not been observed before.

Appendix B describes the project team's investigation into phase-angle differences, which found that large changes in phase-angle differences are consistent both in theory and given the nature of the monitoring used to support the ESAMS.

4.2.3 Atypical Combinations of Phase Angles

This ESAMS application was designed to take a broad view in identifying measurements that, when viewed individually, might not appear unusual, but when viewed in conjunction with all other recent measurements would stand out as very unusual or atypical. The application is driven by a complex set of statistical algorithms that compare the measurement of each phase-angle pair to measurements recorded during the previous 14 days (see Section 3.2.2.3). The application then combines all the comparisons into a dimensionless atypicality score. The project team selected a detection threshold (15) that would yield a significant number of events for evaluating the application.

During the 9-month demonstration period, the atypicality application identified more than 700 events. Figure 31 presents a histogram of the atypicality scores that were assigned. The project team reviewed the findings by examining both the highest scores and the signals providing measurements that were identified routinely as significant contributors to the overall score.

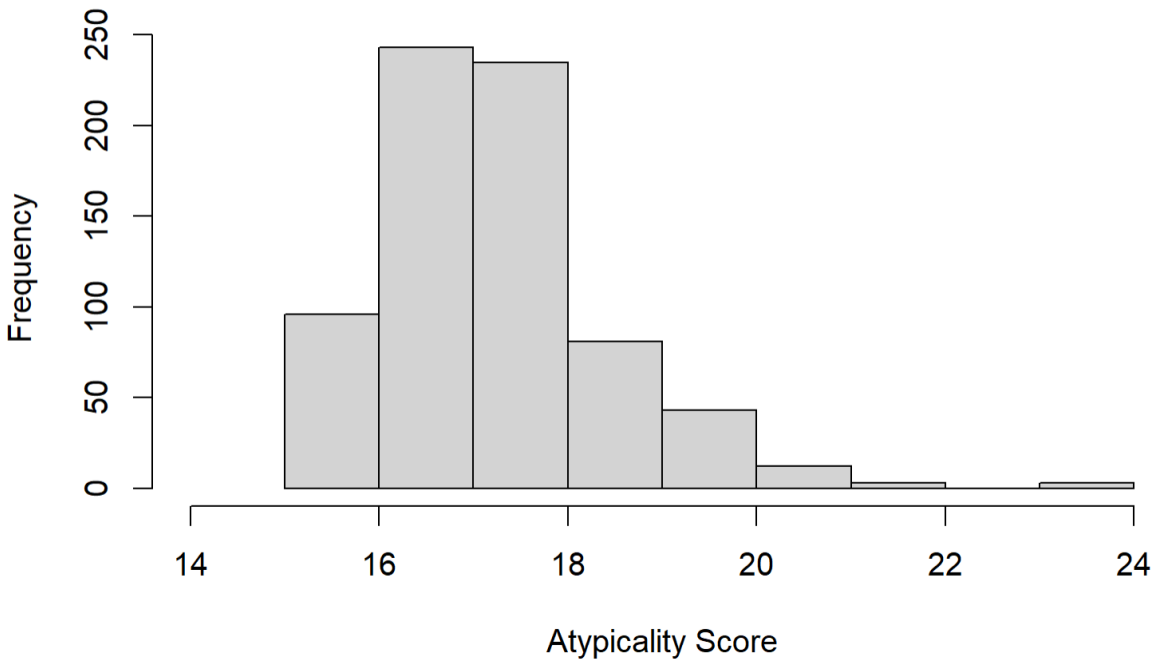

Figure 31. Histogram of Atypicality Scores

The atypicality scores recorded on August 20, 2021, were among the highest recorded during the demonstration. On that day, the atypicality application identified three separate events having scores that exceeded 23. Figure 32 contains plots for the three signals that contributed the most to the final atypicality score for one of the events. The figure reveals that the high atypicality score was due largely to data quality issues that affected all three signals. The first plot shows that although the signal values fell generally within the range of values observed in the recent past, the vertical discontinuities (jumps) in values indicated a data quality issue. The second plot shows that the signal values were also highly variable, both well in excess of and well below values observed in the recent past. The third plot shows that the signal values were consistently and dramatically lower than those observed in the recent past.

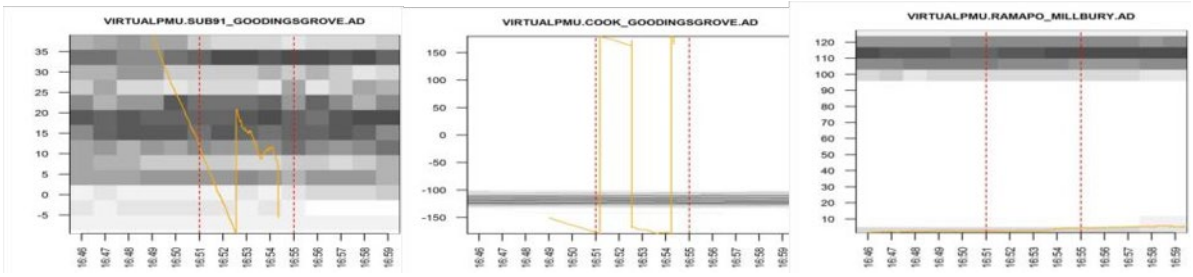

Figure 32. Event Plots from Atypicality Report—August 20, 2021

Figure 33 ranks the signals that routinely were the greatest contributors to atypicality scores greater than 15. The first signal was the largest contributor to nearly half of the events having atypicality scores of 15 or more (300 out of 700 total). A review of the higher-ranked signals revealed that the periods the

application selected often experienced data quality problems that had not been flagged and removed by the ESAMS filters before the application was run.

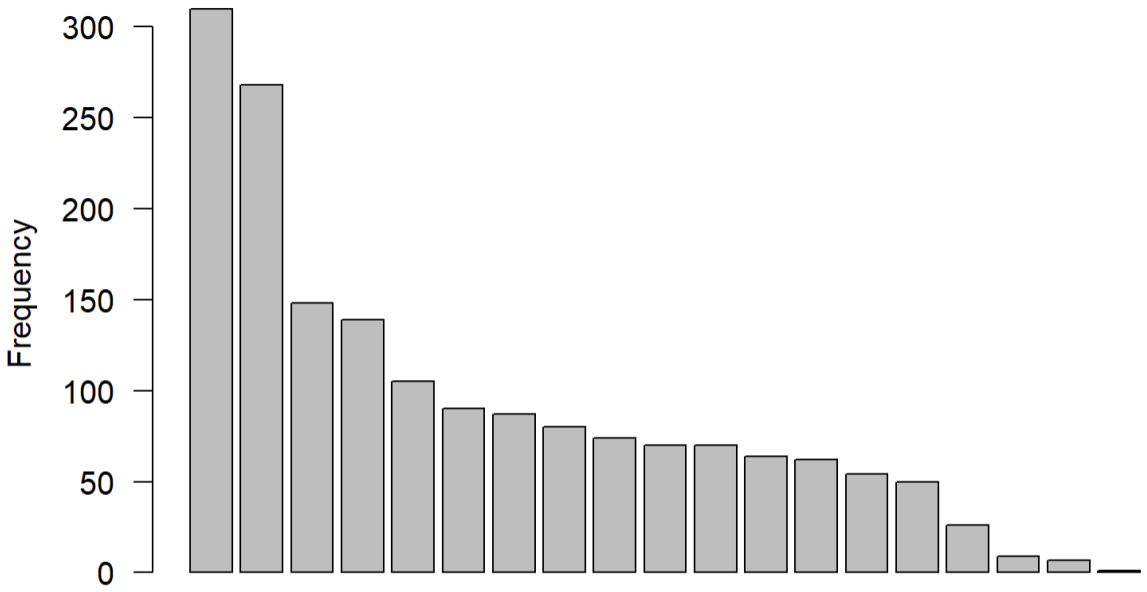

Figure 33. Signals that Contributed Most to Atypicality Scores Greater than 15

Despite the large number of non-events the atypicality application identified (i.e., those due to data quality issues), the application successfully identified some atypicalities that could be traced to system events. For example, the application identified an event on October 18, 2021, that one of the demonstration partners subsequently confirmed reflected a generator trip. See Figure 34.

It was reassuring that events identified by the atypicality application were consistent with (and thus corroborated) findings from other ESAMS wide-area phase-angle applications. For example, Figure 30 showed an instance when four angle pairs persisted at values larger those observed in the recent past. The atypicality application assigned that event a score of 17, thereby flagging it for review.
The application generally succeeded adequately in identifying smaller deviations from steady-state operations, such as operator-directed line switching. Although those findings were reassuring, manual processes usually were required to confirm system events and identify corroborating findings from other ESAMS applications.

Following early reviews of atypicality events, the team implemented methods to identify and classify such events automatically. Unfortunately, during the demonstration period, the team was unable to develop a method that was sufficiently robust. Further, the team recognizes that even given robust identification of event types, significant offline work would be required to ~~r~~eview or post-process findings from the application to provide operators with actionable information.

The two most important next steps for improving the atypicality application are (1) to improve the screening of input signals to remove those affected by data quality issues, and (2) to develop robust

automated methods that can recognize and distinguish between routine system operations such as line switching and unusual patterns that may warrant further scrutiny and possibly operator response/action.

Statistically abnormal behavior observed by following angle pair(s):

Time (EDT)	Signal (Top 4)	Atypicality Score
10/18/2021 10:30	[redacted]	17.926

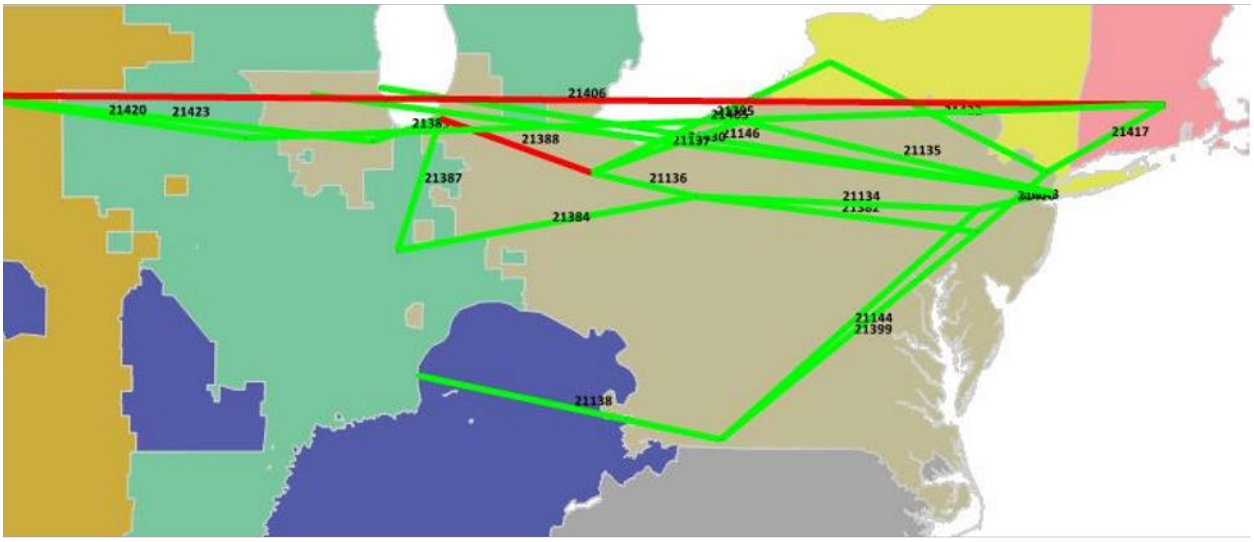

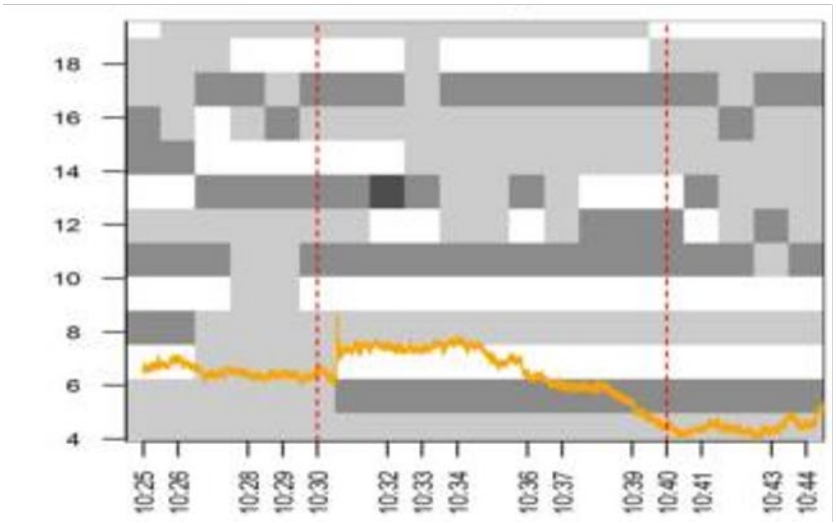

Figure 34. Atypicality Report for Event Detected on October 18, 2021

4.3 Real-Time Data Availability, Quality, and Consistency

All the applications demonstrated in the ESAMS rely on extensive processes for assessing, filtering, and remediating data quality. The processes run continuously to prepare synchrophasor data for use in the applications. Some of the processes are common to many synchrophasor-based applications; others were developed specifically to support the applications the project demonstrated. This subsection reviews the findings derived from running the quality control processes throughout the 9 months of the demonstration period (June 2021–March 2022).

Figure 35 graphically summarizes the quantity and quality of synchrophasor data used in the ESAMS during the demonstration, separated by source (the seven demonstration partners). The width of each column is scaled to indicate the relative number of signals that source provided. For example, PJM provided about five times the number of signals as did MISO. The actual number of signals each source provided is shown in parentheses. Although PJM made signals available to the applications 95% of the time (whether or not their quality made them usable), for 5% of the time some of the signals were not available to the ESAMS, as discussed below. See also Table 1.

The top of the figure shows the dates during which signals from a source were incorporated into the ESAMS. As noted in Section 2, PJM, MISO, NYISO, and ISO-NE provided signals during the entire demonstration period. Southern, SPP, and TVA provided signals for the final 6 months of the demonstration. Each column in Figure 35 designates the composite percentage of signals that were flagged as either usable in the applications (good) or not usable for one of five reasons (data dropout, data invalid, PMU error, GPS out of synch, or time error).[43] The first source, for example, provided usable signals 74% of the time. The percent of usable signals ranged from 67% to 98%.

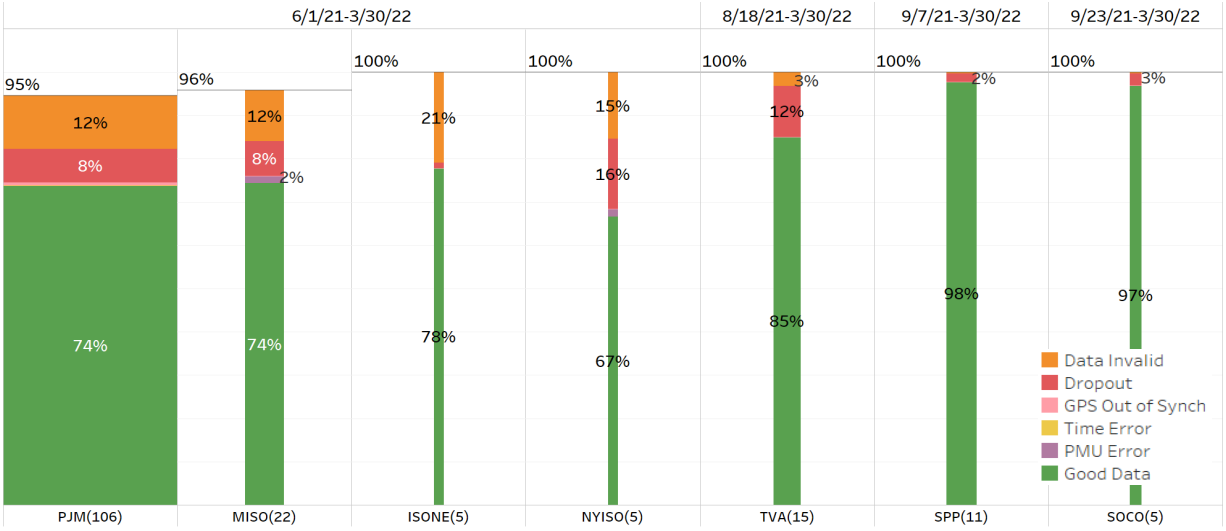

Figure 35. ESAMS Data Availability and Quality by Source

[43] The error codes are introduced in subsection 3.3.3.

The following two figures summarize daily availability and quality of individual signals.[44] Each row, which represents an individual PMU, comprises daily summaries of data quality following the conventions used for the overall summaries presented in Figure 35 (i.e., the same color coding). The daily summaries are shown in chronological order from the beginning of the demonstration period.

Figure 36 shows the daily summaries for five PMUs in ISO-NE. The figure shows that almost all of the PMUs had some, albeit small, data quality issues every day. In the most extreme instance, the ESAMS never received usable data from the first PMU.[45] For most of each day, the data from that PMU were flagged as invalid, and when not flagged as invalid, were flagged as dropped out. Either the PDC or the PMU may flag data as invalid. Data dropout usually results from the time synchronization process or a communication failure. The figure shows instances when data were flagged as invalid for more than one PMU on the same days. This situation suggests there may have been a shared reason the data were flagged as invalid, in this case perhaps because the PMUs were located in the same substation.

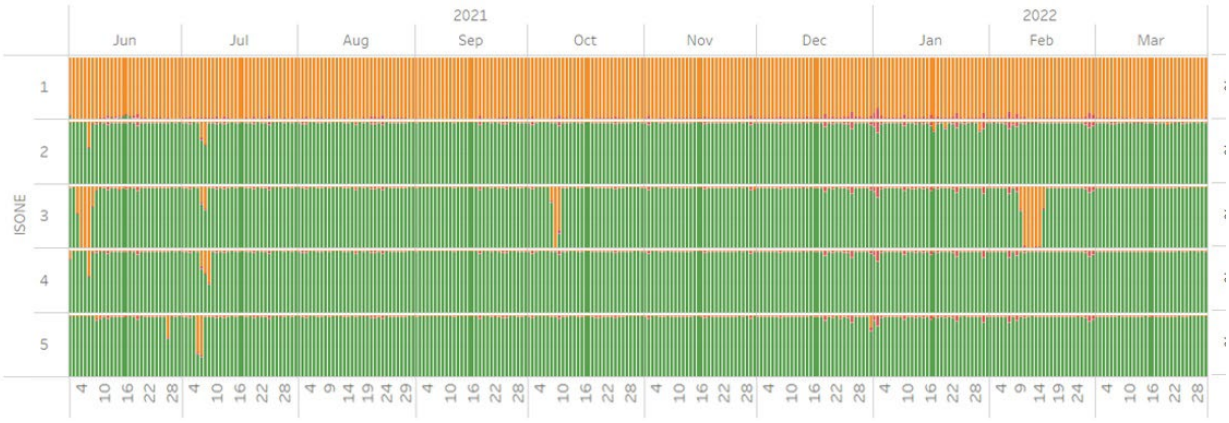

Figure 36. Daily Data Availability and Quality for Five PMUs in ISO-NE

Figure 37 shows the daily summaries for 10 PMUs in MISO. The figure indicates that PMUs 16, 17, and 18 were not integrated into the ESAMS until early September 2021, and that the ESAMS stopped receiving signals from PMU 18 starting in early February 2022.

As with the PMUs described above, some PMUs depicted in Figure 37 show similar patterns. The percentages of invalid data for PMUs 12 and 13 tracked each other's variations through mid-June, at which point the data from both PMUs became invalid for entire days. This situation lasted until mid-July, when PMU 12 began sending useable data for at least parts of days. For the rest of the demonstration, PMU 13 continued to send the ESAMS unusable data.

[44] Appendix C contains the daily summaries for all the signals used in the ESAMS.
[45] After the demonstration, the project team learned that the substation where this PMU was located underwent a major rebuild during the demonstration period; hence, this signal was out of service.

Another apparently shared, although unverified, cause began to affect data quality from PMUs 14 through 17 and 19 and 20 during the last month of the demonstration. Data dropouts from those units made data unusable for many or all the hours of many days in March 2022.

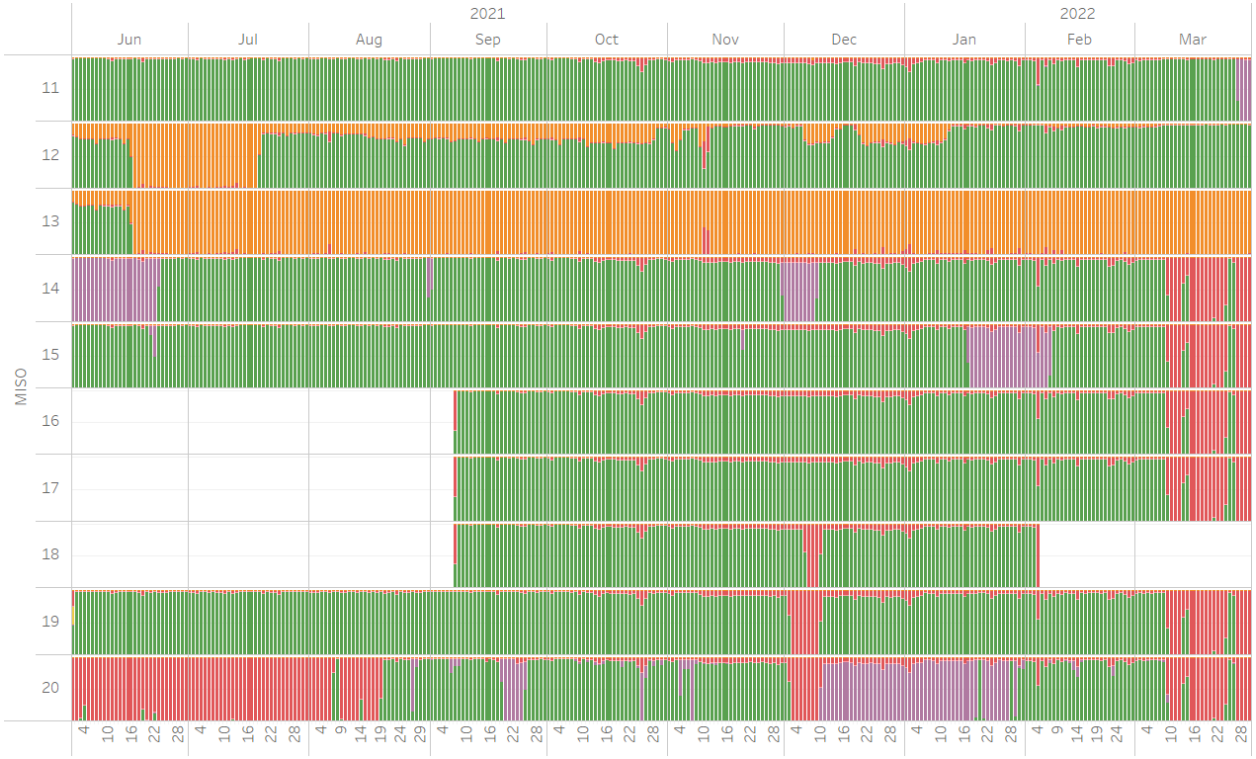

Figure 37. Daily Data Availability and Quality for 10 PMUs in MISO

In summary, the ESAMS data-handling and filtering procedures confirmed that overall data availability and quality generally exceeded 70%, but every synchrophasor experienced data issues at one time or another. The ability to maintain high data availability and quality clearly represents a developing practice among the demonstration partners.

In conclusion, it is important to account for the limits on data availability and quality when developing synchrophasor applications. For example, the confidence assessment for locating sources of forced oscillations factored data availability directly into its calculations, as described in Appendix A.

The ESAMS applications generally ignored data that were identified as suspect. By simply not processing suspect data, the applications assured that validated data would underlie the wealth of new information produced regarding the characteristics and behavior of the Eastern Interconnection.

5. Summary of Project Accomplishments

The ESAMS demonstration project represented an important step toward realizing the capabilities of synchrophasors in providing wide-area situational awareness in the Eastern Interconnection. The project demonstrated the feasibility of collecting and integrating synchrophasor measurements continuously from throughout the interconnection to produce a heretofore unavailable visibility of grid phenomena that affect the Interconnection as a whole. More importantly, the project demonstrated that the synchrophasor systems currently operating in the Eastern Interconnection are capable of supporting real-time notification of an important grid phenomenon, forced oscillations.

This ESAMS demonstration was timely because grid operators in the Eastern Interconnection know that forced oscillations occur frequently and, more importantly, that some warrant real-time communication and coordination among RCs. The ESAMS project demonstrated a method for supporting such communications via a robust and standardized analysis of interconnection-wide events, which can be produced and delivered to RCs in real time.

The ESAMS demonstration project also confirmed the usefulness of tracking and analyzing interconnection-wide grid phenomena going forward, not solely through one-time studies. For example, the analysis of the data collected during the 9-month demonstration not only confirmed previous findings regarding the two dominant natural oscillatory modes of the Eastern Interconnection, it also extended them in several ways. First, the data analysis greatly improved characterization of the shapes of two modes, which in turn increases understanding of how forced oscillations at those frequencies will propagate and be observable in the interconnection. Second, the analysis identified heretofore unrecognized diurnal patterns in the two modes' frequencies and damping ratios. Damping ratios were found to be consistently high, indicating that the grid is very stable. Third, the data analysis demonstrated that patterns in modes' frequencies could be monitored and distinguished consistently even though the frequencies overlapped from time to time.

The ESAMS demonstration project also laid the groundwork for potentially developing a means of directly monitoring interconnection-wide grid stress, based in part on synchrophasor data. The project confirmed that using synchrophasors to monitor phase angles is a viable means of observing the effects of grid events or actions on power flows throughout broad regions of the grid. This finding is significant because it means that grid operators adjacent to and distant from the location of an event or action can notice it without needing to communicate with the RC of the region where the event or action is taking place. Although future applications are promising, significant additional work will be required to pair information from synchrophasor data with broader regional analyses (e.g., contingency analysis that considers multiple operating areas simultaneously) in order to convert the information into guidance that grid operators will find useful.

Finally, the ESAMS demonstration project confirmed the maturation of synchrophasor-based monitoring systems in the Eastern Interconnection. The project produced and shared daily reports on

the availability and quality of data received from the demonstration partners. During the project, ESAMS application algorithms were hardened to detect and correct for initially anomalous signals caused by what are now well-understood features of synchrophasor measurements. In addition, the project team performed independent investigations that documented the need for interconnection-wide coordination regarding the conventions used for naming signals. Independent investigations also confirmed the validity of large phase-angle measurements that, in the past, would have been discounted or deemed spurious.

At the institutional level, the ESAMS project prompted the demonstration partners and project team to engage in regular discussions, information-sharing, and learning about synchrophasor technologies, applications, and systems. ESAMS project findings were shared widely with industry audiences in the NERC's Synchronized Measurement Working Group and at meetings of the North American Synchrophasor Initiative.

In summary, the ESAMS demonstration project confirmed the promise of synchrophasors to offer real-time, wide-area situational awareness of grid performance. Although much work remains to be done to integrate and incorporate that awareness into daily operations, an important next step has been taken.

6. References

Amidan, B., J. Follum, T. Yin, N. Betzsold. "FY18 Discovery Through Situational Awareness: Anomalies, Oscillations, and Classification," Pacific Northwest National Laboratory, PNNL-27812, Richland WA. 2018. doi:10.2172/1846595 and https://www.osti.gov/biblio/1846595

Cummings, R. "Blackout Dynamics and Phasor Measurements." NERC Operating Committee. June. 2005.

Eastern Interconnect Data Sharing Network's Electric Information network. https://eidsn.org/.

Electric Power Group, RTDMS Server User Guide. August 2020.

Follum, J., N. Nayak, J. Eto. "Online Tracking of Two Dominant Inter-Area Modes of Oscillation in the Eastern Interconnection," Hawaii International Conference on System Sciences (HICSS). 2023.

Follum, J., J. Eto. "Confidence Metrics for Regional Forced Oscillation Source Localization," The 2022 International Conference on Smart Grid Synchronized Measurements and Analytics (SGSMA), May 24-26, 2022. Split, Croatia.

Follum, J., N. Betzsold, T. Yin, J. Buckheit. "Event Screening Methods for the Eastern Interconnection Situational Awareness and Monitoring System (ESAMS)," Pacific Northwest National Laboratory, PNNL-30137, Richland WA. 2020. https://www.osti.gov/biblio/1846589

Follum, J., S. Maslennikov, E. Farantatos. IEEE/NASPI Oscillation Source Location Contest, NASPI Work Group Virtual Meeting and Vendor Show, October 5-7, 2021. PNNL-SA-167027. https://www.naspi.org/sites/default/files/2021-10/D3S8_01_follum_pnnl_20211007.pdf

Follum, J. "Statistical Evaluation of New Estimators used in Forced Oscillation Source Localization," Hawaii International Conference on System Sciences (HICSS-53). January 7-10, 2020. doi: http://hdl.handle.net/10125/64111.

Follum, J., T. Yin, B. Amidan. "A New Spectral Estimator for Identifying Dominant Modes and Detecting Events in Power Systems," 2018 Probabilistic Methods Applied to Power Systems (PMAPS) Conference, June 24-28, 2018, pp. 1-6. Boise, ID. Available online: https://doi.org/10.1109/PMAPS.2018.8440203.

Follum, J., F. Tuffner and U. Agrawal, "Applications of a new nonparametric estimator of ambient power system spectra for measurements containing forced oscillations," 2017 IEEE Power & Energy Society General Meeting, 2017, pp. 1-5, doi: 10.1109/PESGM.2017.

Maslennikov, S., E. Litvinov. "ISO New England Experience in Locating the Source of Oscillations Online," in IEEE Transactions on Power Systems, vol. 36, no. 1, pp. 495-503. January 2021. DOI: 10.1109/TPWRS.2020.3006625

North American Electric Reliability Corporation (NERC). Recommended Oscillation Analysis for Monitoring and Mitigation Reference Document. Synchronized Measurement Working Group. November 2021 https://www.nerc.com/comm/RSTC_Reliability_Guidelines/Oscillation_Analysis_for_Monitoring_And_Mitigation_TRD.pdf

NERC. Eastern Interconnection Oscillation Disturbance: January 11, 2019, Forced Oscillation Event. December 2019. https://www.nerc.com/pa/rrm/ea/Documents/January_11_Oscillation_Event_Report.pdf

NERC. Interconnection Oscillation Analysis, Reliability Assessment. July 2019. https://www.nerc.com/comm/PC/SMSResourcesDocuments/Interconnection_Oscillation_Analysis.pdf

NERC. Phase Angle Monitoring: Industry Experience Following the 2011 Pacific Southwest Outage, Recommendation 27, Technical Reference Document. June 2016. https://www.nerc.com/comm/PC/Synchronized%20Measurement%20Subcommittee/Phase%20Angle%20Monitoring%20Technical%20Reference%20Document%20-%20FINAL.pdf

North American SynchoPhasor Initiative (NASPI) Control Room Solutions Task Team Paper, "Using Synchrophasor Data for Phase Angle Monitoring," NASPI-2016-TR-003 released 03/2016 https://www.naspi.org/node/351

Oak Ridge National Laboratory. Advancement of Synchrophasor Technology in Projects Funded by the American Recovery and Reinvestment Act of 2009. March 2016. https://www.energy.gov/sites/prod/files/2016/03/f30/Advancement%20of%20Sychrophasor%20Technology%20Report%20March%202016.pdf

Synchronized Measurement Working Group. Recommended Oscillation Analysis for Monitoring and Mitigation Reference Document, NERC. November 2021. https://www.nerc.com/comm/RSTC_Reliability_Guidelines/Oscillation_Analysis_for_Monitoring_And_Mitigation_TRD.pdf

Trudnowski, D., J. Pierre, N. Zhou, J. Hauer, M. Parashar. "Performance of Three Mode-Meter Block-Processing Algorithms for Automated Dynamic Stability Assessment," IEEE Transactions on Power Systems, vol. 23, no. 2, pp. 680-690. May 2008. DOI: 10.1109/TPWRS.2008.919415.

U.S.-Canada Power System Outage Task Force. Final Report on the August 14, 2003, Blackout in the United States and Canada: Causes and Recommendations. April 2004. https://www.energy.gov/sites/default/files/oeprod/DocumentsandMedia/BlackoutFinal-Web.pdf

Western Systems Coordinating Council. Disturbance Report for the Power System Outage that Occurred on the Western Interconnection August 10, 1996, at 1548 PAST. October 1996.

Zhang, Q., X. Luo, E. Litvinov. “Automated PMU Data Quality Monitoring System,” 2019 IEEE Power & Energy Society General Meeting, August 4-8, 2019. Atlanta GA. DOI: 10.1109/PESGM40551.2019.8973633.

Appendix A. Confidence Scores for Forced Oscillation Source Locations

The ESAMS uses the dissipating energy flow method to identify the RC region where the source of a forced oscillation is located.[46, 47] The energy flows between two regions are calculated using phasor measurement unit (PMU) measurements from tie-lines. Because not all tie-lines are monitored by PMUs, and some PMUs may be unavailable because of issues such as communication failures, the ESAMS ends up gaining limited observability of the system. This limited observability may lead to erroneous results when locating sources of forced oscillation. Such incorrect source information may lead to inappropriate actions/inactions from reliability coordinators (RCs) and erode confidence in the ESAMS's performance.

Calculating Confidence Scores

To address the issue of fallible results, the project team developed confidence scores for the ESAMS's identification of the sources of forced oscillations. A score was calculated based on data availability, network flows, and robustness of the findings. To provide simplicity, the final scores conveyed in notification emails sent to RCs bore one of three values: Low, Medium, or High. A low score might indicate that the actual source of a forced oscillation was located outside the area the ESAMS identified, and neighboring RCs should investigate within their areas as well. The logic behind the confidence scores assigned during the demonstration project considered the five metrics described below.

Data Availability	(M1) System data availability (percentage of synchrophasors available on network tie-lines)
	(M2) Source region data availability (percentage of synchrophasors available on tie-lines within the identified source region)
Network Flows	(M3) Import from other regions (number of areas from which the identified source region is importing oscillation energy)
	(M4) Other regions showing net export (number of areas other than the identified source region showing net energy export)
Robustness of Finding	(M5) Percentage of synchrophasors on tie-lines within the identified source region (removed in order of energy flow) that would have to be unavailable to change the results of the source localization

Each metric (M1) through (M5) was mapped to a discrete value: {0, 1, -1}; the confidence score is the sum of those values. The confidence score could range from -5 to 5. In the ESAMS deployment, a score of 2 translated to Medium confidence in source localization; a higher or lower score implied High or

[46] S. Maslennikov, B. Wang, E. Litvinov. "Locating the source of sustained oscillations by using PMU measurements," *IEEE PES General Meeting*, pp. 1-5, 2017. doi: 10.1109/PESGM.2017.8274006.
[47] J. Follum. "Statistical Evaluation of New Estimators used in Forced Oscillation Source Localization," *Hawaii International Conference on System Sciences (HICSS-53)*, January 7-10, 2020. doi: http://hdl.handle.net/10125/64111

Low confidence, respectively. The project team decided to make the connection between numeric values and qualitative scores somewhat conservative, intending to recalibrate the scoring method after the demonstration period. Follum and Eto provide further details.[48]

Suggested improvements

During the demonstration project, the partner RCs were able to validate ESAMS findings even for some events assigned low confidence scores. This outcome shows that the current scoring scheme errs on the conservative side and that the way qualitative confidence scores were assigned to numeric confidence values needs to be recalibrated. Other suggested improvements for future ESAMS deployments are described below.

Modify the source identification logic for leaf nodes: In the ESAMS, the region showing the largest net export of oscillation energy is identified as the likely source of a forced oscillation. Consider the example network configuration shown in Figure A-1. The arrows represent tie-lines, and edge weights correspond to normalized energy flows on the lines. Although a forced oscillation may have originated within region A, imperfect observability means that PMU measurements did not capture all the energy flowing out of the region. In the example network, region B appears to have a greater energy export than does A and would be chosen as the likely source region. The figure also shows that because A is a terminal or leaf node, it can import energy from/export energy to B only. The energy export from A to B indicates an oscillation originated within region A. In such cases, the logic behind identifying the source region may be modified as follows: *If region B, which shows the highest oscillation energy export, is connected to a leaf region? A in the network, and energy is exported from region A to B, then the likely source of the forced oscillation is either region A or B*.

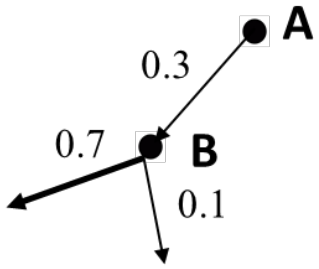

Figure A-1. Dissipating energy flow at the interface between regions A and B in an imperfectly observable network.

This way of modifying the logic behind source location prompts RCs in both region A and B to take appropriate actions to quickly identify the origin of the forced oscillation. In the Eastern Interconnection, the Florida Reliability Coordinating Council forms a leaf region.

[48] J. Follum, J. Eto. "Confidence metrics for Forced Oscillation Source Localization," *International Conference on Smart Grid Synchronized Measurements and Analytics (SGSMA), 2022* (accepted).

Composite metric for data availability: Currently, data availability for the entire system and for an identified source region are considered separate metrics. When overall system data availability is low, however, a larger percentage of the energy export from regions having better visibility may be captured, erroneously indicating them as the likely source. Figure A-2 illustrates a simple example. On the left, both the system and identified source region (D) provide 100% data availability. On the right, system data availability is 57%, whereas data availability for the identified source region (B) is 80%.

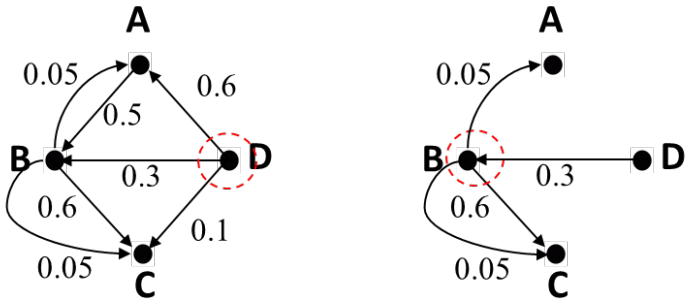

Figure A-2. Effect of data availability on identification of source region.

The schematic on the left illustrates that when the system provides 100% observability, region D clearly has the highest energy export and is the source of the forced oscillation. The schematic on the right represents a case in which data availability is low for the system but relatively high for region B. A larger percentage of the energy export from B is captured, giving it the appearance of producing more energy export than the actual source region, which is D. In such a case, the results of the source identification will be incorrect.

To avoid such misinterpretations, the project team formed a composite metric for data availability:

System Data Availability	Source Region Data Availability	Data Availability Metric
High	High	1
High	Low	0
Low	High	-1
Low	Low	-1

Assigning weights to tie-lines: At present, the PMUs at every tie-line are treated with equal weight in developing the confidence score for a source localization. Some PMUs, however, are located more centrally within a network and thus are more critical to capturing energy flow information that, if lost, will severely impact source localization. Conversely, losing some PMU availability or capturing flow information on tie-lines, say, on the network periphery, may not affect source identification. Therefore, when computing system data availability, it may help to differentiate tie-lines according to how central they are to a network (e.g., betweenness centrality).

Note that although the confidence scoring scheme certainly can be improved, good data availability and wide-area observability are key to accurately identifying the source of a forced oscillation. Therefore, increasing tie-line observability in the ESAMS would improve its ability to locate sources and provide RCs with better wide-area situational awareness. Exact information such as the number of tie-lines between areas and how many tie-lines PMUs are not currently monitoring also would support better estimates of the proportion of network flow the ESAMS is capturing, thereby informing any strategy for recalibrating confidence scoring.

Appendix B. Investigation into Phase-Angle Measurements

Introduction

One ESAMS application monitors the angles between selected stations and reports when an angle exceeds statistical norms. The function continuously computes statistics on the angle, including the average and standard deviation (sd). It computes the norm for each hour and the sd of the signal during that hour based on a trailing time period, usually 10 days. The application establishes a range around the norm within which the signal should be found, usually 3 sd from the norm. If the signal is outside that range for more than 5 hours in a day, the ESAMS adds the occurrence to the daily report.

The Issues

Most of the reports generated during the demonstration project required no investigation because they seemed reasonable. Three issues arose from time to time that were unexpected and warranted further investigation.

1. In some locations the phase angle was much larger than expected within a relatively short distance. The phase angle between two points depends directly on the power flow and the impedance of the lines between the points. To produce an exceptionally large angle, either the impedance or the loading would have to be higher than would be expected for the given lines.

2. The phase angle occasionally exceeded a ± 180° range, which was not only unexpected but also not accounted for by the software and displays. See Figure B-1.

3. On a few occasions, the monitored phase angle made a large change very rapidly, on the order of 90° in a few hours. This occurrence would indicate a large change in power flow or a change in line configuration, neither of which had been observed before. See Figure B-2.

Although the above results could be legitimate, they also could be caused by bad measurements or an error in processing. Confirming the results required obtaining the measurement data that the analysis was based on as well as data from the EMS.

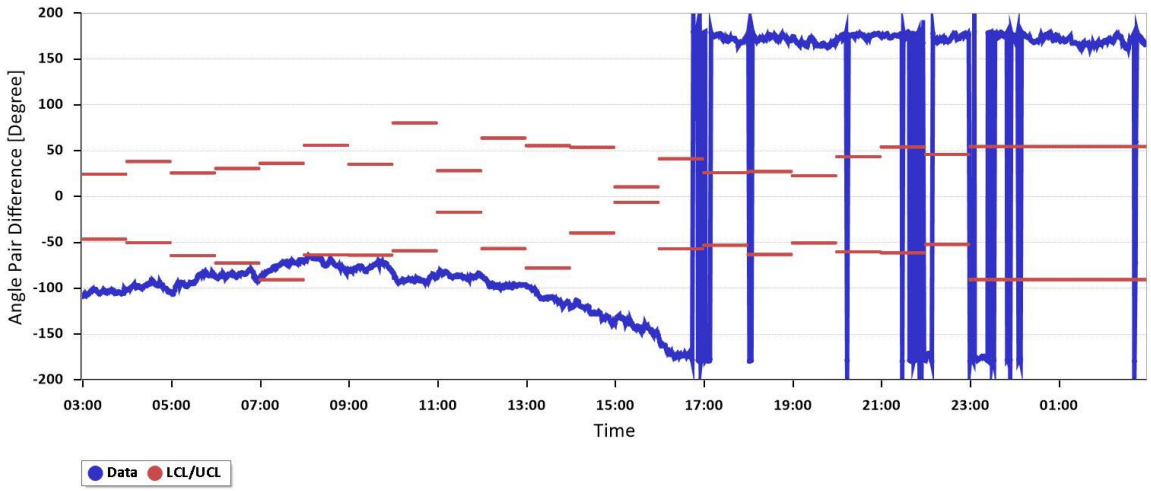

Figure B-1. Based on the Standard Algorithm, the Phase Angle Exceeds -180° and Wraps Around to +180°

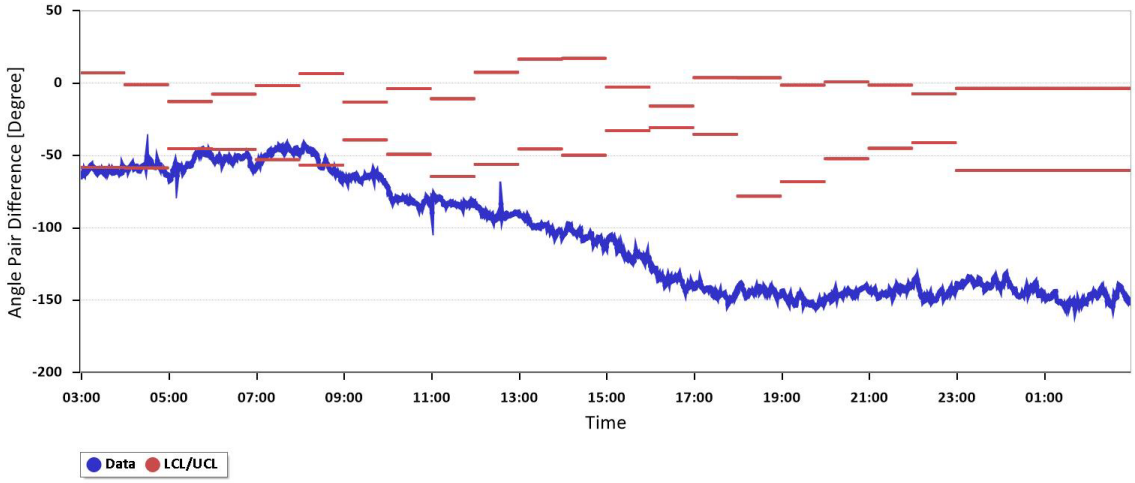

Figure B-2. A Phase Angle Dropping Rapidly (within 9 Hours) from -50° to -150°

Analysis

The project team used the well-known power flow equation to compute the phase angle and the line impedance between busses:

$$P_{ab} = \frac{V_a V_b}{X_{ab}} \sin(\delta_b - \delta_a)$$

where V is the voltage, δ is the phase angle at busses a and b at each end of the line, and X is the line reactance. Although a PMU usually does not report power flows, the EMS gathers extensive information on power flows. The line impedances are found in both the system model used for state estimation (SE) and the EMS. Therefore, the project team used the angles computed by the SE to validate the angles measured by the PMU. The SE computes the angle at each bus relative to a reference bus. Phasor data were used to make a direct comparison. Team members took a snapshot of phasor values for the same time as the SE solution and calculated the angle at each bus relative to the same reference bus. This comparison validated the phasor angles.

In most cases the angles computed from the two measurement systems were within ± 1°. In several cases, however, they were off by ± 120°, indicating that the phase selected as A-phase at a given PMU in one station differed from the A-phase used at the PMUs in other stations. This problem, which had been observed before, reflects the fact that each utility selects its own A-phase, which then is used throughout its territory. A utility's selection may differ, however, from the A-phase another utility uses. Consequently, a ± 120° offset in phase is needed to compare phase angles within a multi-utility system. The team identified three different choices of A-phase in the northern half of the Eastern Interconnect. Applying the offset resolved the issue surrounding large angles.

A PMU computes the phase angle of a signal based on a cosine function at nominal frequency synchronized to UTC time. The ac signal takes a sinusoid shape that repeats indefinitely every $2\pi f_0$ sec, so the PMU resolves the measurement to a value within $\pm\pi$ relative to the synchronized cosine. The angle is relative to the cosine synchronized in UTC time, so all the measured synchrophasor values have time as their common reference. Normally the difference in angles between busses is simply that difference, but because the angles rotate in response to frequency offset, the angle the PMU reports passes through the $\pm\pi$ boundary, creating a large jump in the angle difference. Thus, algorithms for calculating relative angle must check whether the angle crosses the $\pm\pi$ boundary and, if so, must adjust the calculation as needed. In addition, if the angle between two substations is > 180° it cannot be resolved as the difference between the two angles. The solution requires finding an appropriate intermediate bus (or busses) between the substations that has an angle difference < 180° and that therefore can be resolved. Prior to the demonstration project, team members had not seen a situation where the angle between stations exceeded 180°.

Phase angles were analyzed using the 1-minute averages of relative phase angles from records in the Real Time Dynamics Monitoring System (RTDMS). A relative angle is the angle of a bus that is calculated

relative to the angle of another bus. A centrally located bus is chosen as the reference bus, and its angle is the reference angle. The relative angles of all other busses are calculated relative to this reference. The reference bus must be within ± 180° of all the other busses to resolve the angles as described above. Because they are determined largely by the power flows, the angles between busses change relatively slowly (except during faults or other disturbances). Because they are fairly constant over short periods, the relative angles can be averaged, whereas the time-based angles cannot be averaged because of the angle rotation. The RTDMS calculates the relative angles for samples every 30 seconds, which makes them all precisely time aligned. The system averages those instantaneous angles at 1-second intervals and then, for this analysis, averaged them throughout 1 minute. Those averaged angles then can be considered representative of that location. For this study 10 days of 1-minute averages were used to compare relative phase angles.
Cases in which a phase angle seemed to exceed ± 180° called for confirming that the signals used in calculating the angles were reasonably accurate. Because no measurements were available for validating the angles directly, the angles were compared with those measured nearby. Angles in a system roughly track together, changing as power flows change. The team plotted several signals from each region to see whether the angles tracked each other and seemed reasonable.

Figure B-3 plots the phase angles in the New England and New York City area. The plot shows a few spikes, which represent missing data samples. Figure B-4 plots the phase angles in the Western New York to Ohio area. A reversal in power flow is indicated between the first and second three days, when the yellow and blue traces switch positions. The angle change is small, however, because the stations are close together. Figure B-5 plots phase angles from East Nebraska to the Chicago area. Although the plot spans two regions, only one measurement was collected at the western side (shown in grey). That signal shows a large divergence as well as significant reversals in power flow on January 2 and 7, 2022.

The 10-day plots show that the signals within each area tracked well but also showed some dispersion. The dispersion was largely E-W; the west end is positive for the most part and the east end all negative. When a couple of representative signals from each area were plotted together (Figure B-6), the angle across the extremes was about 205°. This finding confirmed that an angle within the system was > ± 180°. The plot also shows that the angle could differ greatly in areas between load clusters, such as in large urban areas. This result probably reflects the presence of lighter transmission connections between service areas.

In addition to discovering that angles within a system could exceed ± 180°, the project team also observed places where angle swings exceeded 23° per hour. Sometimes the swings could exceed 100° in several hours. As noted above, the swings occurred between large urban areas, likely indicating a significant change in inter-area power transfers (i.e., exchange schedules) for economic reasons or to accommodate changes in output from renewable generation sources.

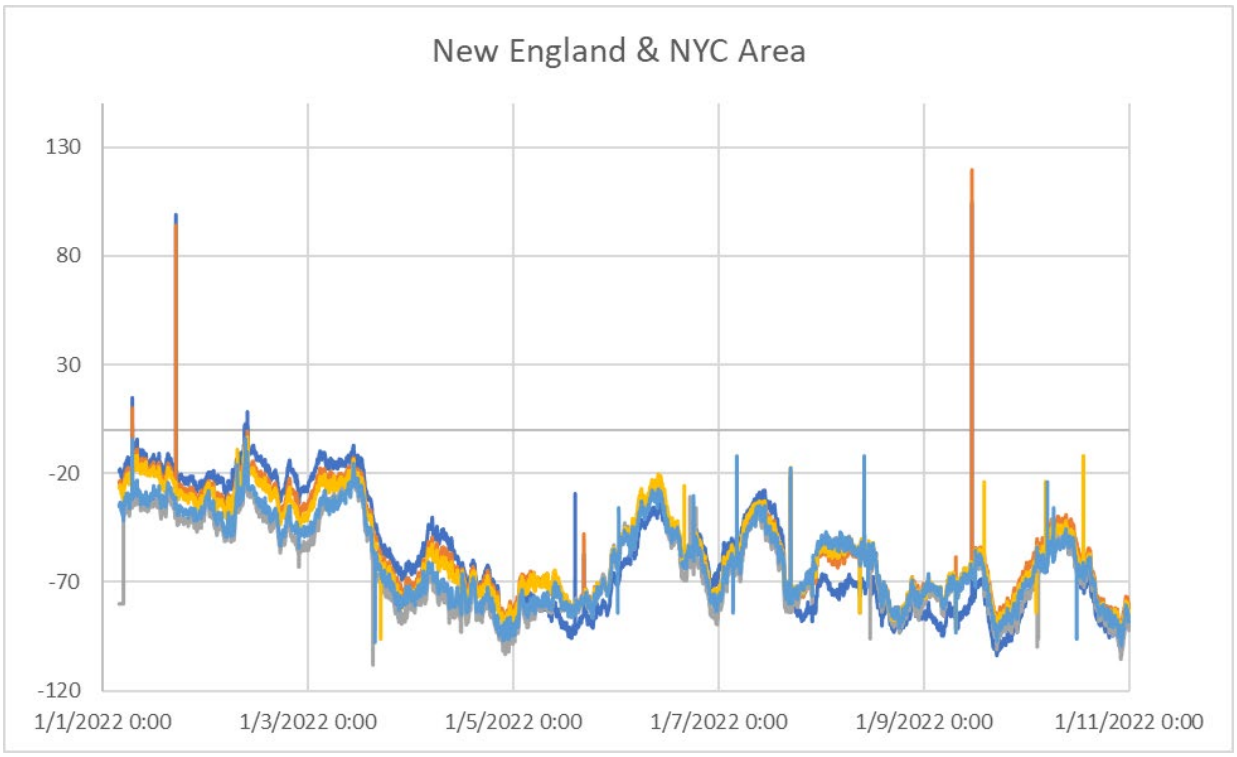

Figure B-3. Phase Angles in the New England and New York City Area

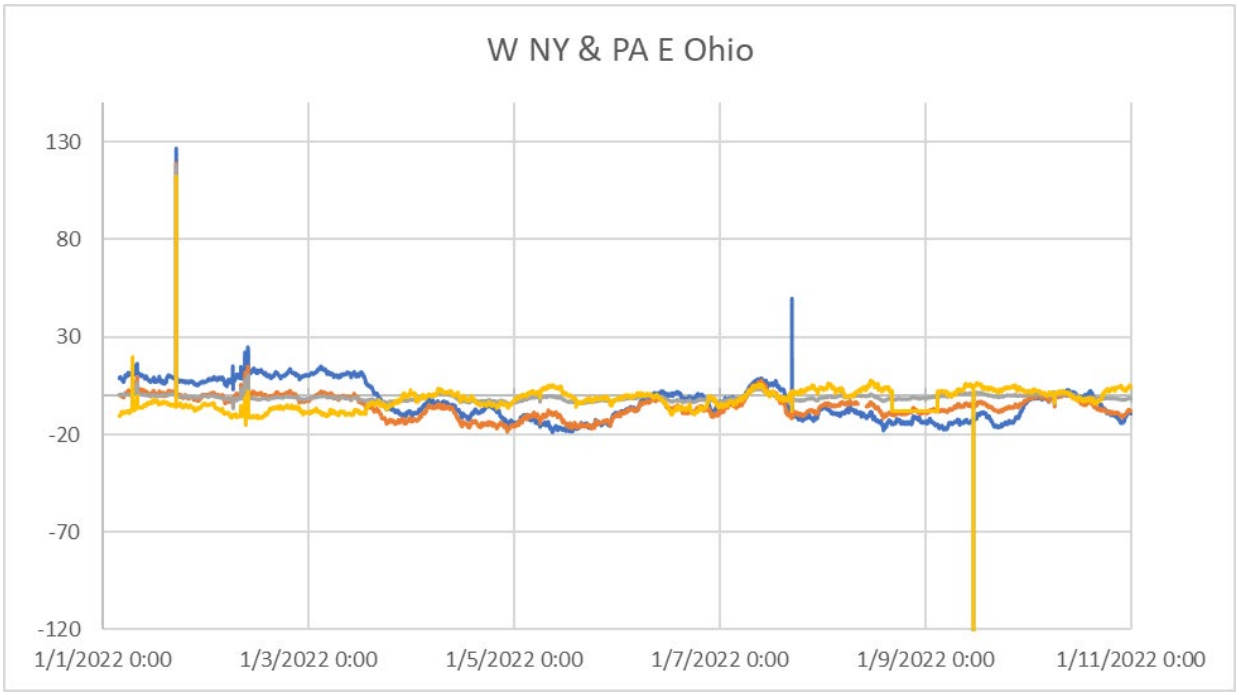

Figure B-4. Phase Angles in the Western New York to Ohio Area

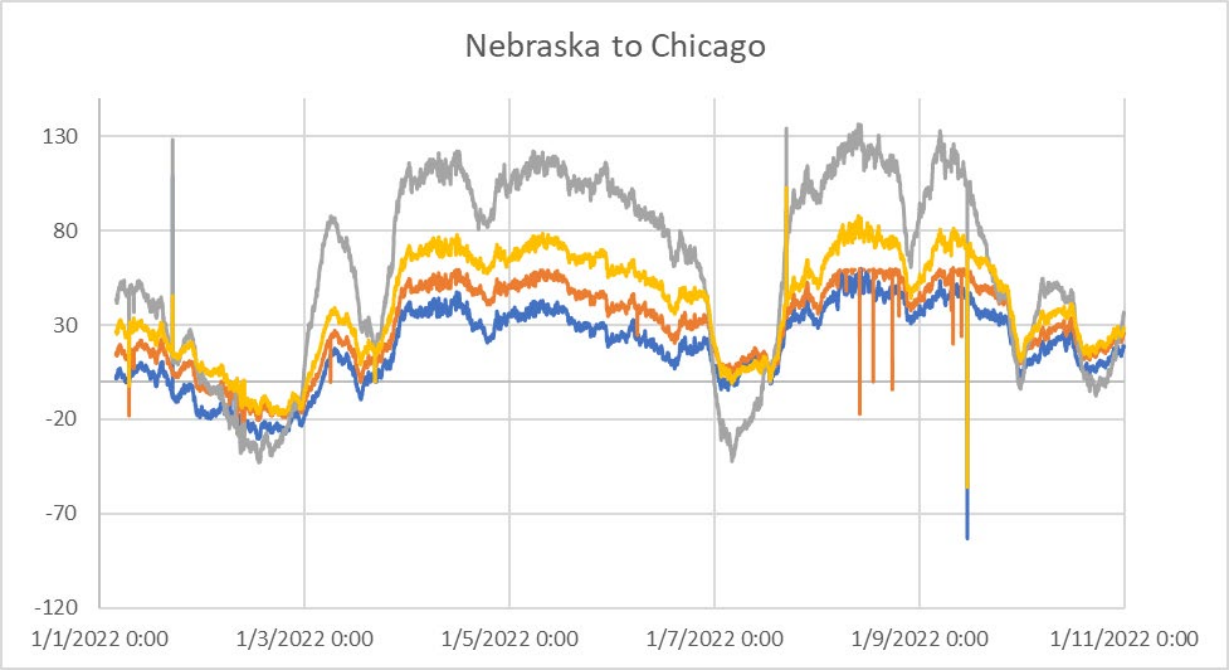

Figure B-5. Phase Angles from East Nebraska to the Chicago Area

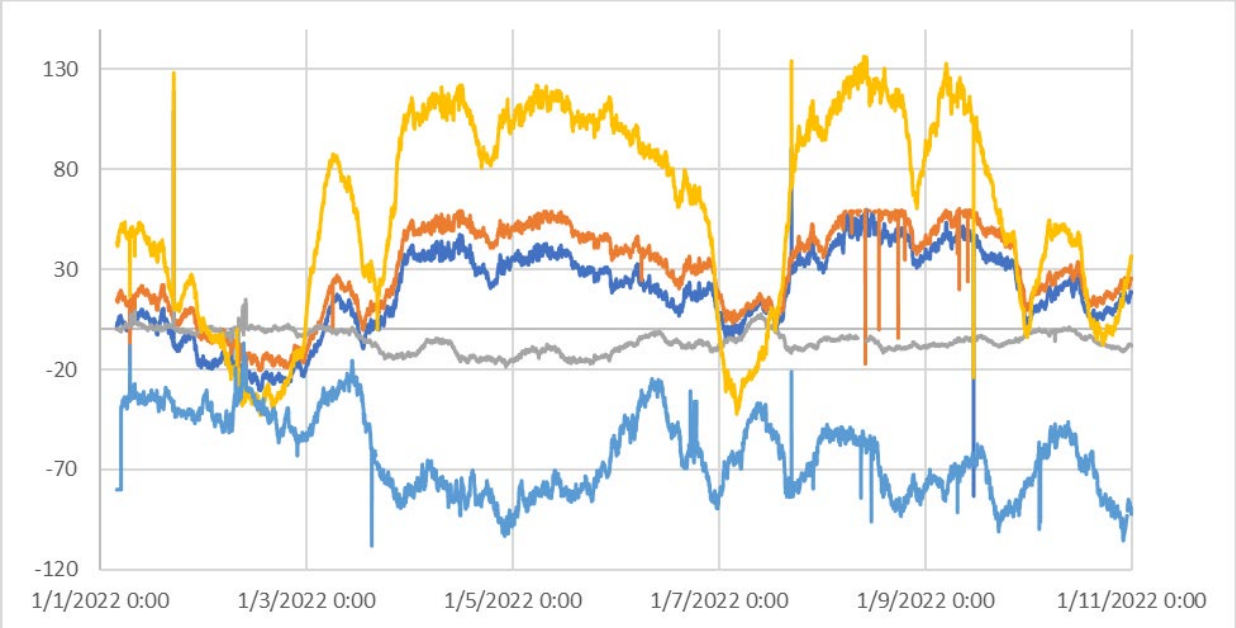

Figure B-6. Phase Angles from East Nebraska to the New England Area

Conclusions

The analyses described in this appendix indicate that when measurements are collected from various utilities, one must consider the details of the measurement system each utility uses. The magnitudes and angles each PMU measures must be validated against known references and preferably the system itself through state estimation. Errors in measurement of both voltage and current were documented in this and other studies.

This study confirms the established fact that angles within large systems can exceed 180°. In fact, given reactive support, an angle can be arbitrarily large. Large angles must be resolved from the time-based measurements to a reference bus. It is impossible to resolve PMU (time-based) angle differences > ± 180° without referring to topology and information on power flows. After the measured angles are resolved to a common bus, however, angle differences from bus to bus can be determined by simple subtraction. A good approach is to resolve angles to a bus in the center of a system and test using state estimation to confirm that all angles from that bus are well within ± 180°. For a large, connected area that forms a somewhat square shape such as the Eastern Interconnection, that approach probably would work. The entire length of a very long area, however, may contain no central point that is within ± 180°. In such a case, an additional reference bus is needed to span the area.

This study also revealed that very large angle changes can occur in a relatively short time. Those changes probably reflect changes in generation among service areas, which could create large changes across weaker connecting links. In order to create useful system alarms, a monitoring function is needed to account for this type of swing.

Appendix C. Availability and Quality of Synchrophasor Data

The plots that follow summarize the daily availability and quality of signals received from the project's demonstration partners, ISO-NE, MISO, NYISO, PJM, SOCO, SPP, and TVA. The plots are color-coded to indicate whether data were good or ruled unusable because of one or more flaws. The coding conventions follow those introduced in Section 4.3.

ISONE

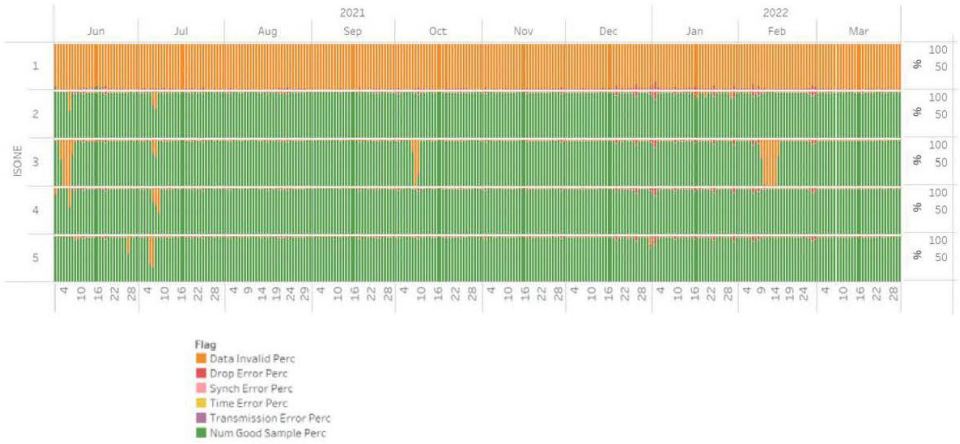
2021
2022
Jun
Jul
Aug
Sep
Oct
Nov
Dec
Jan
Feb
Mar
ISONE
Flag
Data Invalid Perc
Drop Error Perc
Synch Error Perc
Time Error Perc
Transmission Error Perc
Num Good Sample Perc

MISO


2021
2022
Jun
Jul
Aug
Sep
Oct
Nov
Dec
Jan
Feb
Mar
MISO
Flag
Data Invalid Perc
Drop Error Perc
Synch Error Perc
Time Error Perc
Transmission Error Perc
Num Good Sample Perc


MISO
2021
2022
Jun
Jul
Aug
Sep
Oct
Nov
Dec
Jan
Feb
Mar
MISO
11
12
13
14
15
16
17
18
19
20
%
100
50
Flag
Data Invalid Perc
Drop Error Perc
Synch Error Perc
Time Error Perc
Transmission Error Perc
Num Good Sample Perc

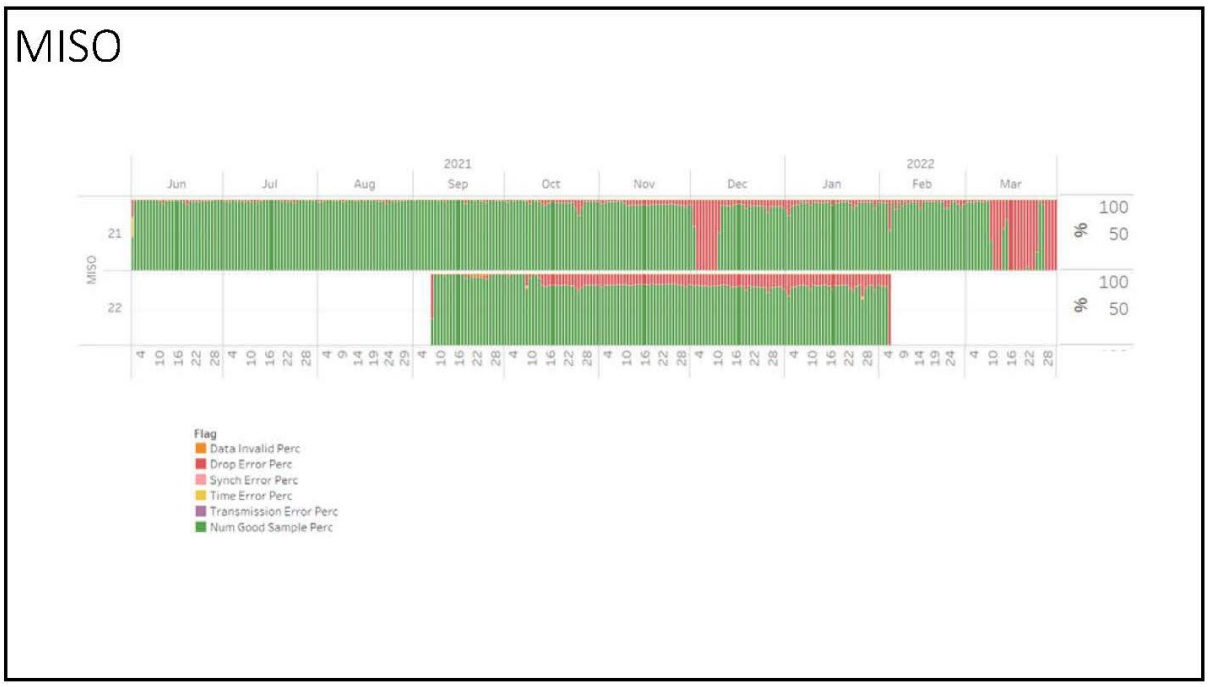
MISO
2021
2022
Jun
Jul
Aug
Sep
Oct
Nov
Dec
Jan
Feb
Mar
MISO
21
22
%
100
50
Flag
Data Invalid Perc
Drop Error Perc
Synch Error Perc
Time Error Perc
Transmission Error Perc
Num Good Sample Perc

NYISO

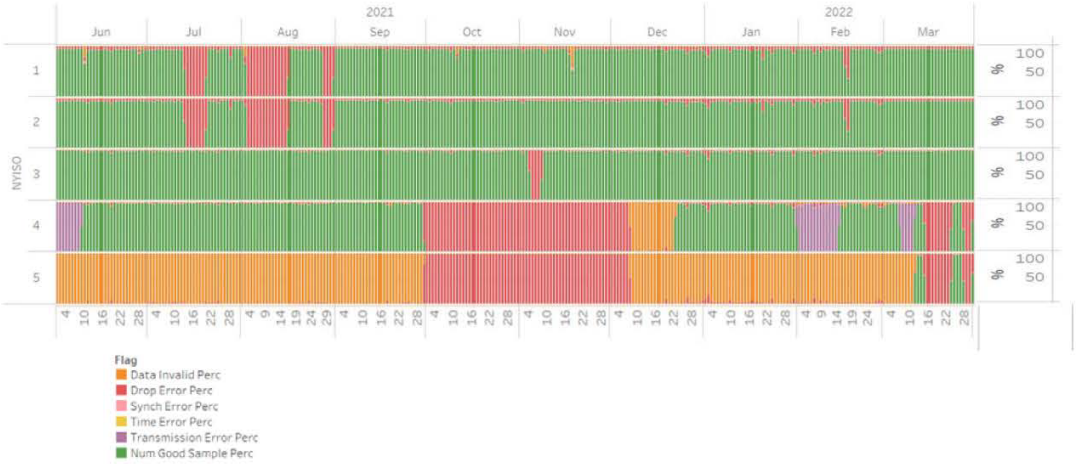
2021
2022
Jun
Jul
Aug
Sep
Oct
Nov
Dec
Jan
Feb
Mar
NYISO
1
2
3
4
5
% 100 50
Flag
Data Invalid Perc
Drop Error Perc
Synch Error Perc
Time Error Perc
Transmission Error Perc
Num Good Sample Perc

PJM


2021
2022
Jun
Jul
Aug
Sep
Oct
Nov
Dec
Jan
Feb
Mar
PJM
1
2
3
4
5
6
7
8
9
10
% 100 50
Flag
Data Invalid Perc
Drop Error Perc
Synch Error Perc
Time Error Perc
Transmission Error Perc
Num Good Sample Perc


PJM
2021
2022
Jun
Jul
Aug
Sep
Oct
Nov
Dec
Jan
Feb
Mar
PJM
11
12
13
14
15
16
17
18
19
20
Flag
Data Invalid Perc
Drop Error Perc
Synch Error Perc
Time Error Perc
Transmission Error Perc
Num Good Sample Perc
100
50
%

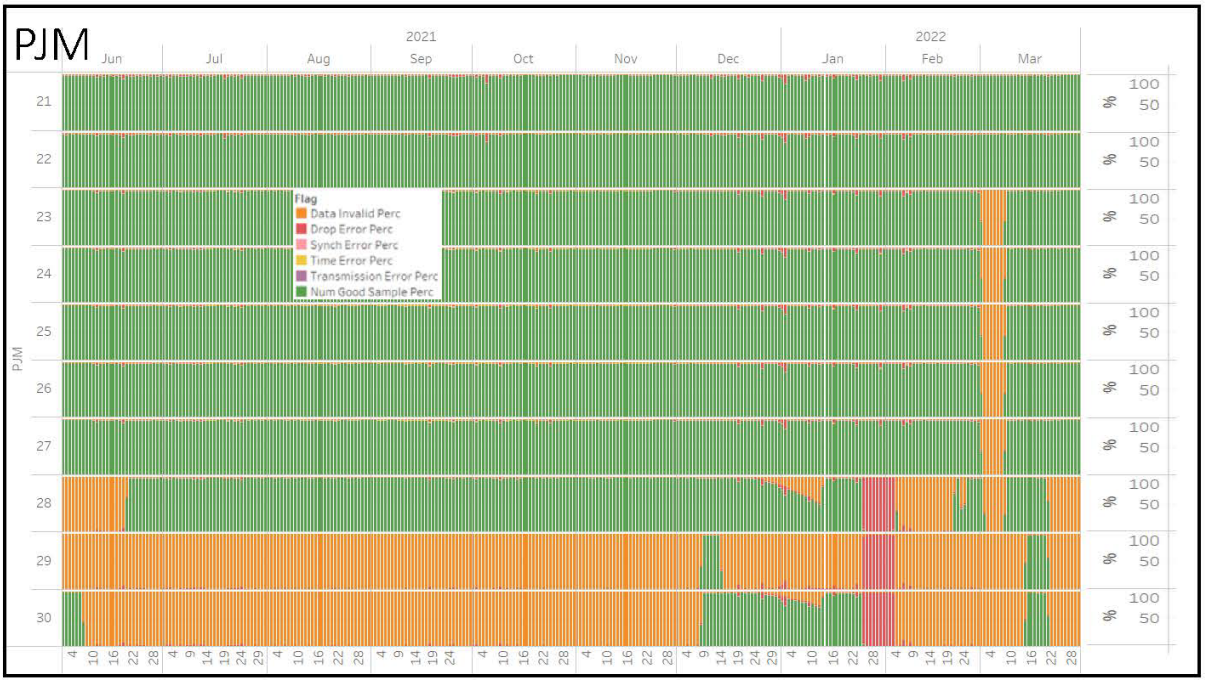
PJM
2021
2022
Jun
Jul
Aug
Sep
Oct
Nov
Dec
Jan
Feb
Mar
PJM
21
22
23
24
25
26
27
28
29
30
Flag
Data Invalid Perc
Drop Error Perc
Synch Error Perc
Time Error Perc
Transmission Error Perc
Num Good Sample Perc
100
50
%

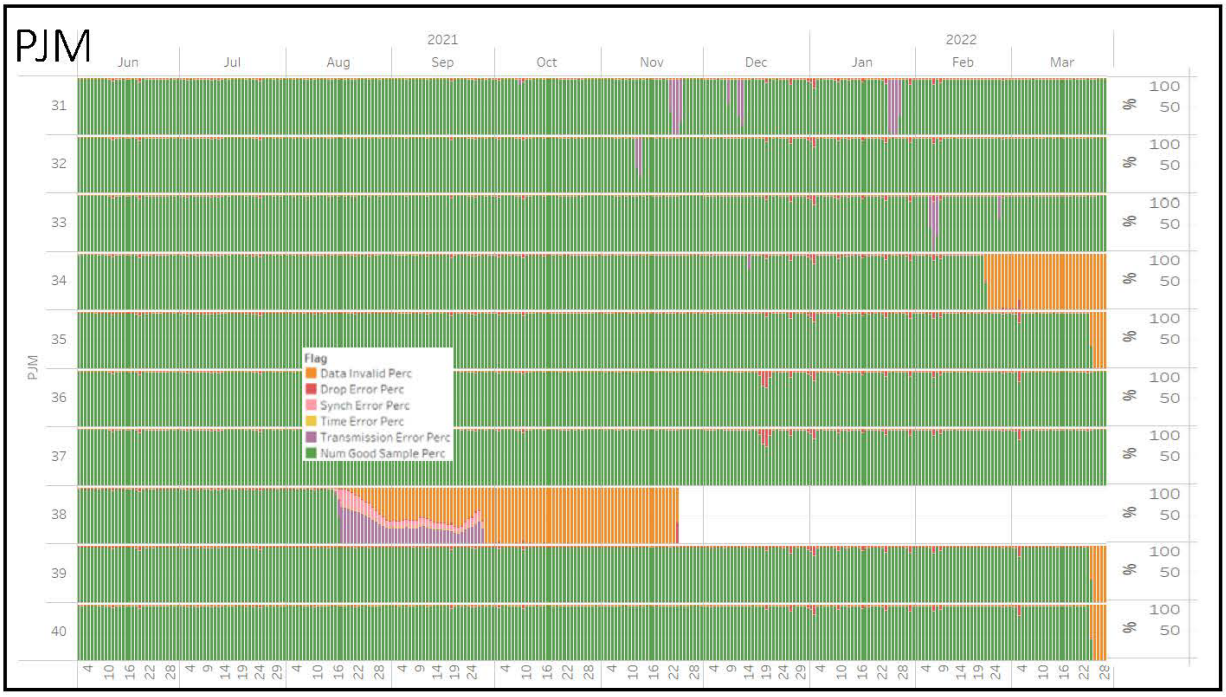
PJM
2021
2022
Jun
Jul
Aug
Sep
Oct
Nov
Dec
Jan
Feb
Mar
PJM
31
32
33
34
35
36
37
38
39
40
%
100
50
Flag
Data Invalid Perc
Drop Error Perc
Synch Error Perc
Time Error Perc
Transmission Error Perc
Num Good Sample Perc

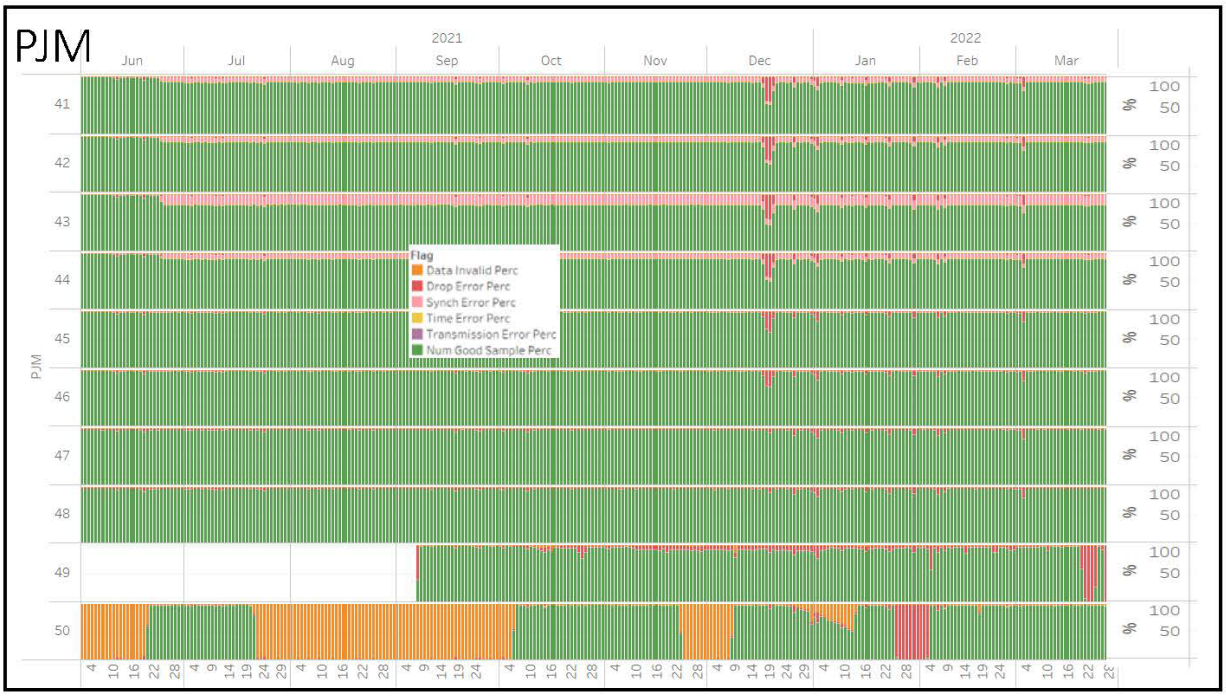
PJM
2021
2022
Jun
Jul
Aug
Sep
Oct
Nov
Dec
Jan
Feb
Mar
PJM
41
42
43
44
45
46
47
48
49
50
%
100
50
Flag
Data Invalid Perc
Drop Error Perc
Synch Error Perc
Time Error Perc
Transmission Error Perc
Num Good Sample Perc

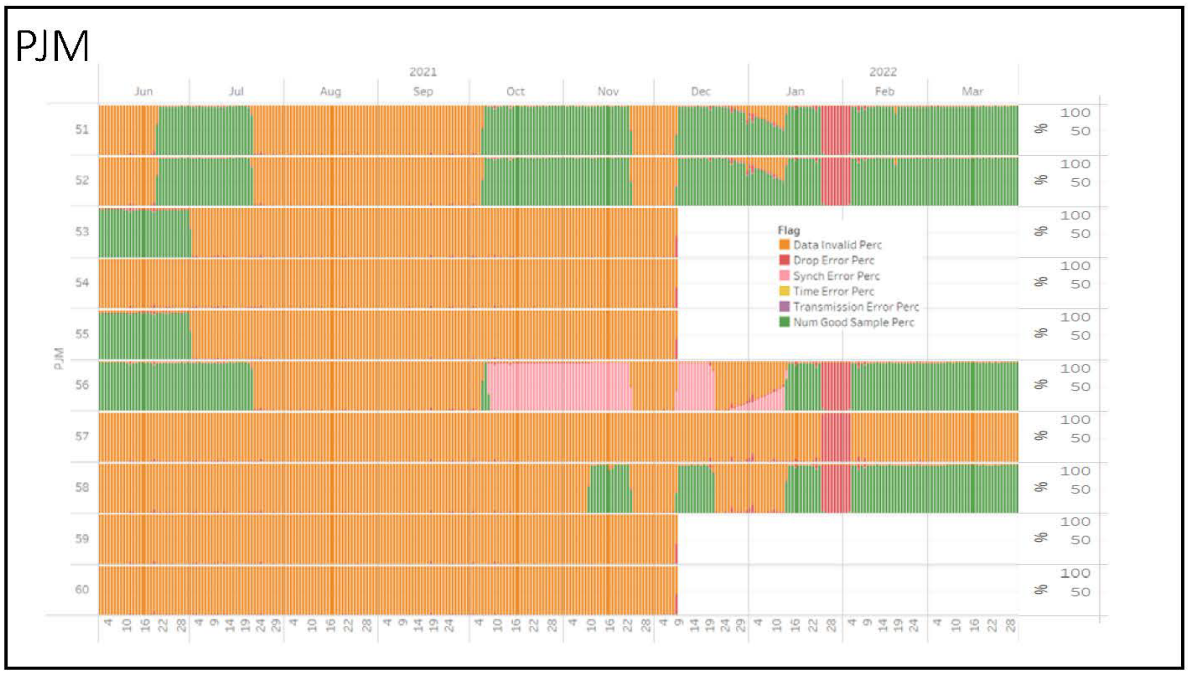
PJM
2021
2022
Jun
Jul
Aug
Sep
Oct
Nov
Dec
Jan
Feb
Mar
PJM
51
52
53
54
55
56
57
58
59
60
%
100
50
Flag
Data Invalid Perc
Drop Error Perc
Synch Error Perc
Time Error Perc
Transmission Error Perc
Num Good Sample Perc


PJM
2021
2022
Jun
Jul
Aug
Sep
Oct
Nov
Dec
Jan
Feb
Mar
PJM
61
62
63
64
65
66
67
68
69
70
%
100
50
Flag
Data Invalid Perc
Drop Error Perc
Synch Error Perc
Time Error Perc
Transmission Error Perc
Num Good Sample Perc

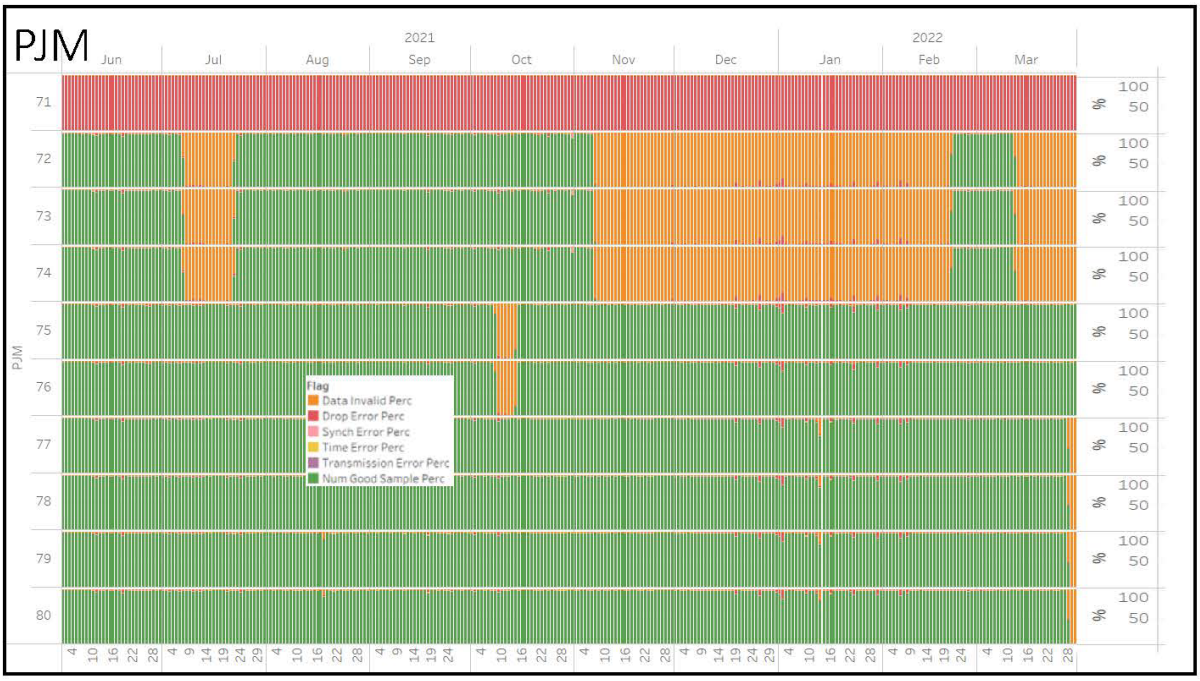
PJM
2021
2022
Jun
Jul
Aug
Sep
Oct
Nov
Dec
Jan
Feb
Mar
PJM
71
72
73
74
75
76
77
78
79
80
%
100
50
Flag
Data Invalid Perc
Drop Error Perc
Synch Error Perc
Time Error Perc
Transmission Error Perc
Num Good Sample Perc


PJM
2021
2022
Jun
Jul
Aug
Sep
Oct
Nov
Dec
Jan
Feb
Mar
PJM
81
82
83
84
85
86
87
88
89
90
%
100
50
Flag
Data Invalid Perc
Drop Error Perc
Synch Error Perc
Time Error Perc
Transmission Error Perc
Num Good Sample Perc

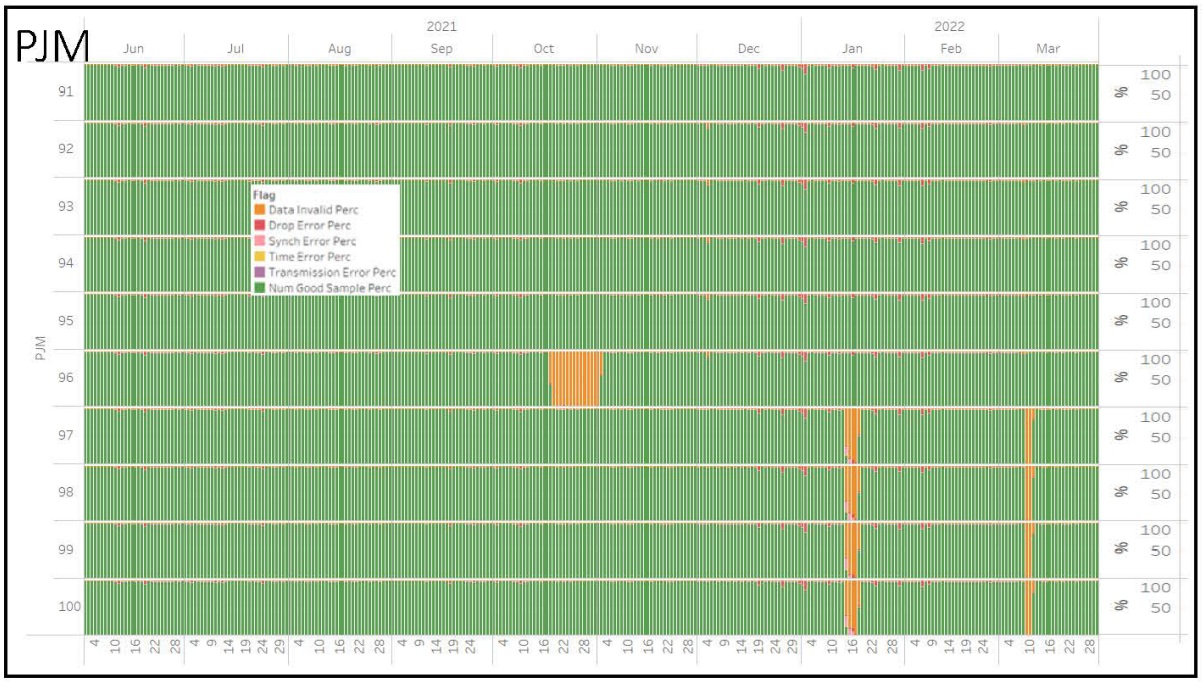
PJM
2021
2022
Jun
Jul
Aug
Sep
Oct
Nov
Dec
Jan
Feb
Mar
PJM
91
92
93
94
95
96
97
98
99
100
Flag
Data Invalid Perc
Drop Error Perc
Synch Error Perc
Time Error Perc
Transmission Error Perc
Num Good Sample Perc
%
100
50

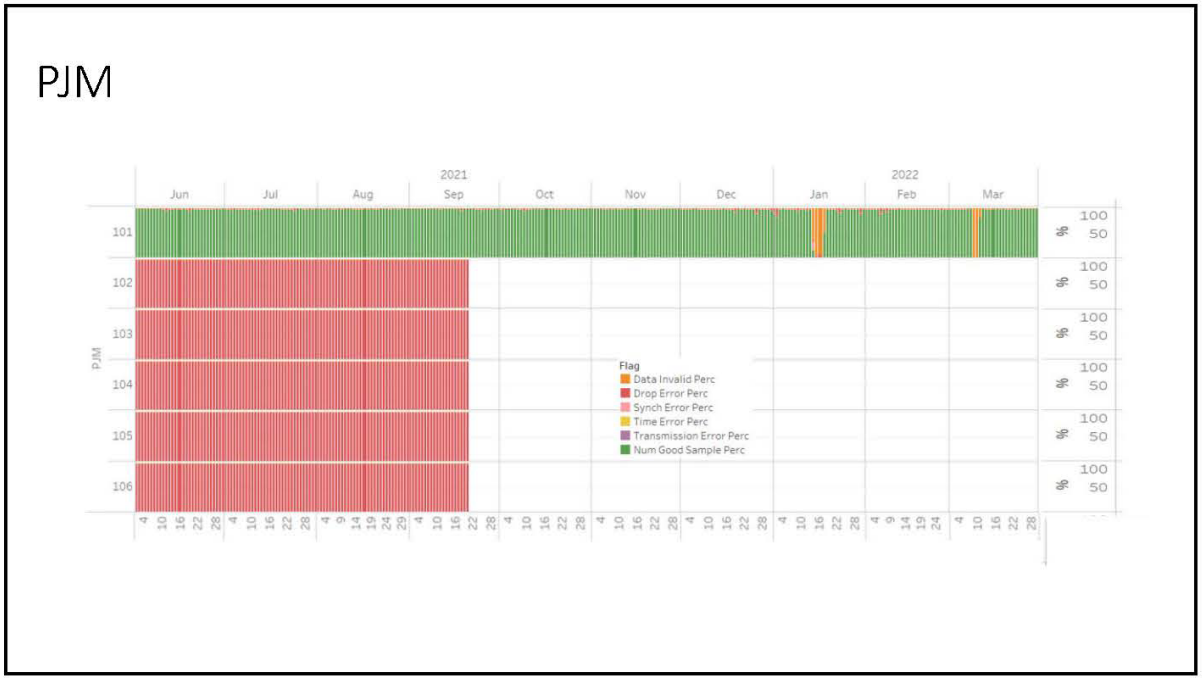
PJM
2021
2022
Jun
Jul
Aug
Sep
Oct
Nov
Dec
Jan
Feb
Mar
PJM
101
102
103
104
105
106
Flag
Data Invalid Perc
Drop Error Perc
Synch Error Perc
Time Error Perc
Transmission Error Perc
Num Good Sample Perc
%
100
50

SOCO


2021
2022
Jun
Jul
Aug
Sep
Oct
Nov
Dec
Jan
Feb
Mar
SOCO
1
2
3
4
5
Flag
Data Invalid Perc
Drop Error Perc
Synch Error Perc
Time Error Perc
Transmission Error Perc
Num Good Sample Perc
%
100
50

SPP


2021
2022
Jun
Jul
Aug
Sep
Oct
Nov
Dec
Jan
Feb
Mar
SPP
1
2
3
4
5
6
7
8
9
10
Flag
Data Invalid Perc
Drop Error Perc
Synch Error Perc
Time Error Perc
Transmission Error Perc
Num Good Sample Perc
%
100
50

SPP

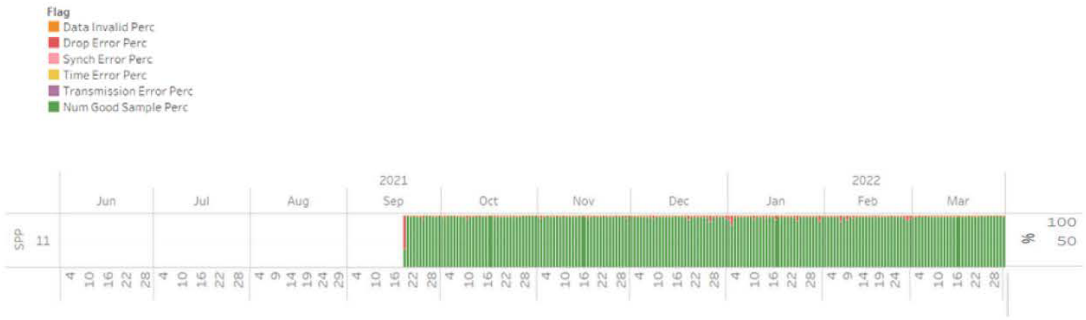
Flag
Data Invalid Perc
Drop Error Perc
Synch Error Perc
Time Error Perc
Transmission Error Perc
Num Good Sample Perc
2021
2022
Jun
Jul
Aug
Sep
Oct
Nov
Dec
Jan
Feb
Mar
SPP
11
%
100
50

TVA


2021
2022
Jun
Jul
Aug
Sep
Oct
Nov
Dec
Jan
Feb
Mar
TVA
1
2
3
4
5
6
7
8
9
10
Flag
Data Invalid Perc
Drop Error Perc
Synch Error Perc
Time Error Perc
Transmission Error Perc
Num Good Sample Perc
%
100
50

TVA


2021
2022
Jun
Jul
Aug
Sep
Oct
Nov
Dec
Jan
Feb
Mar
TVA
11
12
13
14
15
Flag
Data Invalid Perc
Drop Error Perc
Synch Error Perc
Time Error Perc
Transmission Error Perc
Num Good Sample Perc
%
100
50